1 2 9 0

UNIVERSIDADE D
COIMBRA

Vítor André Clímaco Vieira Borralho Paiva

Fluxos do Grupo de Renormalização de Modelos Matriciais de Gravidade Quântica 2d

Dissertação no âmbito do mestrado em Física, ramo de Física Nuclear e de Partículas, orientada pelo Professor Doutor Orlando Oliveira e pelo Doutor António D. Pereira, e apresentada ao Departamento de Física da Faculdade de Ciências e Tecnologia da Universidade de Coimbra.

Setembro de 2022

Faculty of Sciences and Technology
University of Coimbra

Renormalization Group Flows of Matrix Models of 2D Quantum Gravity

Vítor André Clímaco Vieira Borralho Paiva

A thesis written in fulfilment of the requirements for the Physics MSc Program,
Supervised by Prof. Dr. Orlando Oliveira and Dr. António D. Pereira.

September 2022

Abstract

The search for a complete quantum theory of gravitation has been pursued for years. Gravity in two dimensions becomes simpler. This triggered a large body of work, spreading over distinct approaches from continuum to discrete frameworks. It is expected that a comprehension of the lower dimensional formulation will inspire the attempts to formulate quantum gravity in higher dimensions. In this thesis, we focus on optimizing the application of the Functional Renormalization Group to Matrix Models of two-dimensional gravity.

We begin by briefly contextualizing the problem of quantizing the gravitational interaction. Two-dimensional quantum gravity is reviewed from the viewpoint of Polyakov's summation over continuum worldsheet histories - Liouville Gravity - and also from the viewpoint of the summation over discretized random surfaces - Matrix Models - and the equivalence between both frameworks is established. The concept of critical exponents is introduced, together with the results taken as benchmark for the remainder of the thesis. Then, the Renormalization Group approach to Quantum Field Theory is briefly reviewed. A detailed account of the Functional Renormalization Group and its applicability to the study of large scale phenomena and, in particular, the Asymptotically Safe Gravity hypothesis is given. Then, the implementation of the Functional Renormalization Group formalism to Matrix Models is presented, focusing on Hermitian Matrix Models. An optimization of the results of the 2013 article by Eichhorn and Koslowski is worked out. Stability of the results with respect to three quantities, namely the size of the effective action's truncation, the choice of regulator and the projection scheme, is evaluated. A projection scheme, different from the original one, is found to reproduce the original results, opening up the possibility of developing more general schemes. We introduce a new regulator that is able to solve a problem of the original article. The results with the new regulator are found to be stable for increasing truncation order, allowing us to postulate its asymptotic large-truncation behaviour.

Keywords: *Quantum Gravity, Two-Dimensional Quantum Gravity, Liouville Gravity, Matrix Models, Renormalization Group Flow, Functional Renormalization Group, Asymptotic Safety.*

Resumo

Uma teoria quântica completa da interação gravítica tem sido objeto de investigação há largos anos. A duas dimensões, a interação gravítica torna-se mais simples. Tal originou um repertório considerável de abordagens, tanto contínuas como discretas, à gravidade bidimensional. É esperado que a compreensão destas formulações bidimensionais possa inspirar as tentativas de formulação de teorias quânticas da gravidade a maiores dimensões. Nesta tese, focamo-nos na optimização da aplicação do Grupo de Renormalização Funcional a Modelos Matriciais de gravidade bidimensional.

Começamos por contextualizar o problema da quantização da interação gravítica. A gravidade bidimensional é revista do ponto de vista da soma contínua de Polyakov - Gravidade de Liouville - bem como do ponto de vista da soma sobre superfícies aleatórias discretizadas - Modelos Matriciais - e a equivalência entre as duas abordagens é estabelecida. É introduzido o conceito de expoentes críticos juntamente com os resultados utilizados como ponto de referência para o restante trabalho. De seguida, a interpretação da Teoria Quântica de Campos sob o ponto de vista do Grupo de Renormalização é brevemente revista. O Grupo de Renormalização Funcional é apresentado em detalhe, bem como a sua aplicabilidade no estudo de fenómenos físicos a largas escalas e, em particular, no estudo da hipótese da Gravidade Assimptoticamente Segura. Posteriormente, o formalismo do Grupo de Renormalização Funcional é aplicado aos Modelos Matriciais, com foco particular no Modelo Matricial Hermítico. O objetivo principal prende-se com a optimização dos resultados do artigo de 2013, de Eichhorn e Koslowski. A estabilidade dos resultados é avaliada relativamente a três quantidades: o tamanho da truncação da acção efectiva, a escolha de regularizador e o esquema de projecção. Os resultados originais são reproduzidos utilizando um esquema de projecção distinto do original, abrindo a porta à possibilidade de se considerarem esquemas de projecção mais genéricos. Introduzimos, ainda, um novo regularizador que resolve uma dificuldade do artigo original. Os resultados com o novo regularizador demonstram-se estáveis para ordens de truncação crescentes, permitindo-nos conjecturar o seu comportamento assimptótico para grandes truncações.

Palavras-Chave: *Gravidade Quântica, Gravidade Quântica Bidimensional, Gravidade de Liouville, Modelos Matriciais, Fluxo do Grupo de Renormalização, Grupo de Renormalização Funcional, Segurança Assimptótica*

Agradecimentos

Começo por agradecer aos meus orientadores. Ao Professor Doutor Orlando Oliveira, com o qual tive o prazer de realizar o meu primeiro projecto de investigação, e que, sabendo do meu interesse em fazer um projecto de tese na área da Gravitação Quântica, me ajudou rapidamente a encontrar um orientador nessa mesma área. Ao Doutor António D. Pereira, um agradecimento pela ajuda na construção desta tese e pelo conhecimento que me transmitiu nesta área, outrora um completo um mistério para mim e hoje... ainda misteriosa, mas (um pouco) menos desconhecida.

O projecto de investigação em que participei acabou por decorrer ao longo dos primeiros meses da tese. Nesse sentido, devo um agradecimento particular ao Doutor Paulo Silva, sem a grande ajuda do qual teria sido impossível conciliar esse projecto com o desenvolvimento da tese.

Um grandíssimo agradecimento aos meus amigos e amigas. Aos de Leiria, que trago desde criança. Reza a lenda que Leiria não existe, pelo que fica a dúvida se estas pessoas serão reais. Aos que fiz em Coimbra ao longo dos anos do curso. Em particular, aos membros da Tasca, os Gonçalos. Sem a vossa ajuda, o curso teria sido mais difícil e, sem a vossa presença, mais chato, porque Física não é só Física. Às amigas e amigos com quem partilhei a casa PM62 nos últimos dois anos, que são mais do que simples colegas de casa.

Um agradecimento enorme à Luísa, minha namorada, por tentar sempre ouvir com interesse as minhas dúvidas e divagações e, em particular, pela motivação incondicional e coragem para fazer esta tese, mesmo nos meus momentos de maior dificuldade ou menor confiança - ou especialmente nesses momentos.

Por último, um agradecimento gigante à minha família. Ao meu irmão e, em especial, à minha mãe e ao meu pai, que sempre me motivaram e ajudaram ao longo do meu percurso académico, e sem os quais esta tese não existiria, nem eu poderia ter feito este curso, nem tampouco saberia que este era o curso que queria estudar.

Contents

List of Figures

List of Tables

Acronyms

GR General Relativity

2D Two-Dimensional

4D Four-Dimensional

QG Quantum Gravity

2DQG Two-Dimensional Quantum Gravity

MM Matrix Models

CFT(s) Conformal Field Theory(ies)

QFT(s) Quantum Field Theory(ies)

SM Standard Model

IR Infrared

UV Ultraviolet

RG Renormalization Group

FRG Functional Renormalization Group

NGFP(s) Non-Gaussian Fixed Point(s)

Conventions

Throughout the thesis, the following convention is employed:

- Einstein's repeated index summation notation is assumed unless stated otherwise.

1 Introduction

The twentieth century saw the rise of three remarkable theories: Quantum Mechanics[1], Special Relativity[2] and General Relativity[3]. Quantum Mechanics made it possible to describe physics at very small scales, beyond those accessible with Classical Mechanics. On the other hand, Special Relativity altered the understanding of Classical Mechanics at very high velocities. General Relativity changed the view on the gravitational interaction, upgrading its Newtonian description.

Modern particle physics is grounded on three fundamental interactions: electromagnetism, the weak force and the strong force. The Standard Model[4], based on quantum theoretical methods (Quantum Field Theory) merging the principles of Quantum Mechanics and Special Relativity, achieves a valid description of microscopic phenomena with high accuracy within these three interactions. However, the Standard Model cannot be a complete theory as it does not include the fourth interaction: gravitation. A major goal would be to take the next step, that is, to merge the principles of Quantum Field Theory with those of General Relativity in order to build a theory of Quantum Gravity. After decades of research[5][6][7], such a theory has not yet been found. Conceptual and technical issues arise when one attempts to apply the same procedure used in the construction of the Standard Model. Furthermore, there is a lack of empirical evidence of quantum gravitational effects that could guide the construction of a theory of Quantum Gravity. Gravity is a weak interaction, making the experiments probing quantum gravitational phenomena extremely difficult, if not impossible, to realize. For example, the transition rate of spontaneous emission of a graviton[8] - the gravitational *quantum* - by a hydrogen atom is suppressed by a factor of 10^{47} when compared to the same process for a photon.

Frequently, theories become simpler in lower dimensions. That is the case with General Relativity[9][10]. In particular, General Relativity is topological in two dimensions[11] - it has no dynamical local degrees of freedom. However, being closely related to Liouville Field Theory[12], a possible quantum theoretical framework for two-dimensional gravity is provided[13], serving as a toy model of higher-dimensional gravity. Furthermore, two-dimensional quantum gravity is found to be equivalently described by a discrete formalism - Matrix Models[14] - in which the problem of quantizing gravity is treated as the problem of summing over random surfaces, discretized with appropriate polygonal structures. The equivalence between the continuum and discrete approaches can be shown, for example, by evaluating their large scale behaviour. In particular, a set of quantities known as the critical exponents are shown to depend on the type of matter under consideration[15]. Therefore, they help determine which Matrix Model (which restrictions to the matrices' properties) describes which type of matter.

Statistical Mechanics is a suitable tool to study large scale physics. In the 1970's, Quantum Field Theory and Statistical Mechanics were merged[16], giving rise to the Renormalization Group[17] approach to Quantum Field Theory. Different frameworks exist within the Renormalization Group approach. The Functional Renormalization Group[18] is one of them. It has an underlying exact functional differential equation, the Wetterich equation[19], allowing for a continuous evaluation of the system's scale evolution. Therefore, it can, in principle, be applied to Matrix Models in order to study their large scale behaviour.

Our goal is to apply the Functional Renormalization Group to Matrix Models[20]. In particular, we extract their critical exponents, making use of the Wetterich equation. Although it is an exact equation, its practical implementation requires some approximations. The exact values of the critical exponents are known from other methods to solve Matrix Models. Herein, we optimize the procedure set in the original article[20], aiming to reproduce those exact values.

The outline of this thesis goes as follows.

Section [2] makes a brief contextualization of the problem of building a theory of the quantum gravitational field. A few approaches are mentioned, pointing out their distinct conceptual frameworks, successes and unresolved problems.

Section [3] shifts the attention to the quantization of two-dimensional gravity, treating it both in the continuum - Liouville Gravity - and in the discrete approach - Matrix Models. The relationship between the two approaches is presented. Relevant quantities to the remainder of the thesis, such as the critical exponents, are extracted.

Section [4] briefly walks through the ideas behind the Renormalization Group approach to Quantum Field Theory. A close look is taken into the Functional Renormalization Group and its underlying functional differential equation is derived in detail. The strict relation between the Functional Renormalization Group and Asymptotic Safety is pointed out.

Section [5] describes the application of the Functional Renormalization Group to Matrix Models. Critical exponents are extracted in this setting and compared to known exact values. As the Wetterich equation can only be solved approximately, several spurious quantities that the critical exponents would not depend on (were the equation solved exactly) are introduced. Stability with respect to these quantities is tested, working toward an optimization of the procedure.

2 The Quantization of Gravity

Merging General Relativity and Quantum Mechanics is key in unfolding a fuller comprehension of space and time. To that end, many distinct approaches have been tried over the years. This is partly due to a lack of empirical evidence to guide the way for a theoretical construction but also due to conceptual difficulties in the application of formerly successful frameworks. This chapter is devoted to a brief overview of the rationale behind some of the first attempts to solve the problem of the quantization of gravity, pointing out their successes and unresolved problems. Namely, we discuss: the perturbative approach to the path integral; the canonical quantization of gravity developed in the 60's; the asymptotic safety scenario hypothesized in the late 70's. At the end of this chapter, it is the hope of the writer that the motivation behind the work developed in this thesis becomes clearer.

2.1 Perturbative Quantization of Gravity

A very successful classical theory of the gravitational field has been established and tested for over a hundred years. Solving Einstein's General Relativity[3] equations,

$$\mathcal{R}_{\mu\nu} - \frac{1}{2}g_{\mu\nu}\mathcal{R} + \Lambda g_{\mu\nu} = 8\pi G_N \mathcal{T}_{\mu\nu} \quad , \tag{2.1}$$

where $\mathcal{R}_{\mu\nu}$ is the Ricci curvature tensor, $\mathcal{R}$ is the Ricci curvature scalar, $g_{\mu\nu}$ is the metric tensor, $\mathcal{T}_{\mu\nu}$ is the energy-momentum tensor, G_N is Newton's constant and Λ is the cosmological constant, has provided us with a good model of classical gravity.

GR predicts numerous exciting gravitational effects[21], from the deflection of light rays to gravitational waves, the Big Bang and black holes. The Big Bang and black hole singularities signal a regime where Einstein's theory loses its validity. It is conjectured that an understanding of quantum gravitational effects at very short length scales might help remove these singularities. However, the scale of such effects dwells below the Planck length scale, a distance scale that is much smaller than the scales of the other fundamental interactions' quantum theories. At modern times, the Planck energy scale,

$$P_E = \sqrt{\frac{\hbar c^5}{G_N}} \approx 10^{19}\, GeV \quad , \tag{2.2}$$

is inaccessible (for instance, the LHC (Large Hadron Collider) runs at a maximal collision energy of around 10^4 GeV[22]).

Furthermore, to start a quantization procedure, the degrees of freedom to be quantized must be identified. In the particular case of the weak gravity limit of Einstein's field equations, in which $g_{\mu\nu}$ is perturbed around a fixed background metric (usually taken to be Minkowski's metric, $\eta_{\mu\nu} = diag(-1, 1, 1, 1)$) with a (weak) fluctuation field $f_{\mu\nu}$,

$$g_{\mu\nu}(x) = \eta_{\mu\nu} + f_{\mu\nu}(x), \quad |f_{\mu\nu}| << 1 \quad . \tag{2.3}$$

the physical degrees of freedom at play in GR can be identified. Plugging this solution into equation (2.1) in the case of a vanishing cosmological constant ($\Lambda = 0$), a wave equation is obtained. Choosing the harmonic gauge condition on the fluctuation field, $f_{\mu\nu}$,

$$\partial^\nu f_{\mu\nu} - \frac{1}{2}\partial_\mu f^\nu_\nu = 0 \quad , \tag{2.4}$$

Einstein's equations become[23]

$$\Box f_{\mu\nu} = -16\pi G_N[\mathcal{T}_{\mu\nu} - \frac{1}{2}\eta_{\mu\nu}\eta^{\mu\nu}\mathcal{T}_{\mu\nu} + \mathcal{O}_{\mu\nu}] \quad , \tag{2.5}$$

where $\Box$ is the D'Alembertian operator associated with $\eta_{\mu\nu}$. $\mathcal{O}_{\mu\nu}$ gathers "higher-than-linear-order" terms in $f_{\mu\nu}$[23]. They can be read as the fact that not only matter, $\mathcal{T}_{\mu\nu}$, is a source of gravity but gravity is a source of itself, as Einstein's equations are non-linear in $f_{\mu\nu}$. In the linearized gravity (or weak $f_{\mu\nu}$ field) and matterless (vanishing $\mathcal{T}_{\mu\nu}$) case, (2.5) turns into a wave equation, whose solutions are plane waves. In the harmonic gauge, the solution[21] to source-free linearized gravity reveals that the physical degrees of freedom of linearized gravity are the polarization states of the wave,

$$f_{\mu\nu}(x) = \begin{pmatrix} 0 & 0 & 0 & 0 \\ 0 & 0 & 0 & 0 \\ 0 & 0 & f_{22} & f_{23} \\ 0 & 0 & f_{23} & -f_{22} \end{pmatrix} e^{iw(x-t)} \quad . \tag{2.6}$$

If the polarization states of a plane wave transform as $\phi \to e^{ih\theta}\phi$ under a θ rotation about the axis of propagation, they have helicity $\pm h$. The polarization states of the gravitational wave transform accordingly with $h = \pm 2$. Although all that has been said is purely classical, in the quantum theory this translates to the quantum of gravitation - *graviton* - being a *spin 2* particle.

Let us now look at the Feynamn integral of the gravitational field,

$$\mathcal{Z} = \int_{\mathcal{G}(\mathcal{M})} \mathcal{D}[g_{\mu\nu}] e^{iS_{EH}[g_{\mu\nu}]} \quad . \tag{2.7}$$

The integration is taken over all distinct geometries, $\mathcal{G}$, of the 4D manifold $\mathcal{M}$. Due to the freedom in the choice of coordinate system, some metrics are equivalent under the action of the group of diffeomorphisms. Metrics equivalent to one another can be put in a set: a class of metrics. Metrics in different classes are physically non-equivalent. Therefore, $\mathcal{D}[g_{\mu\nu}]$ is an explicit reference to the integration measure being taken over the *physical metrics* only, that is, over classes of metrics. $S_{EH}[g_{\mu\nu}]$ is the Einstein-Hilbert action[24],

$$S_{EH} = \frac{1}{16\pi G_N} \int d^4x \sqrt{|g|}(\mathcal{R} - 2\Lambda) \quad , \tag{2.8}$$

which gives rise to Einstein's equations (2.1). Let us consider, for simplicity, pure gravity (no matter fields) and a vanishing cosmological constant. In particular, following the background-field approach[6], where we decompose the metric $g_{\mu\nu}$ into a fixed background field - which we take to be the Minkowski metric, $\eta_{\mu\nu}$ - plus a fluctuation field, $h_{\mu\nu}$,

$$g_{\mu\nu}(x) = \eta_{\mu\nu} + h_{\mu\nu}(x) \quad . \tag{2.9}$$

Redefining the fluctuation field, as follows,

$$h_{\mu\nu} = \sqrt{16\pi G_N}\tilde{h}_{\mu\nu} \quad , \tag{2.10}$$

the theory's coupling constant is $\sim \sqrt{G_N}$. Quadratic terms in the fields are thus independent of the coupling constant. To proceed with a Feynman diagrammatic expansion of the graviton building blocks, the Einstein-Hilbert Lagrangian is expanded in powers of the fluctuation field. It reduces to the Fierz-Pauli Lagrangian[25],

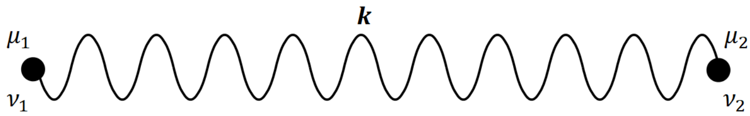

Figure 1: Graviton propagator

$$\mathcal{L}_{FP} = \frac{1}{2}(\partial^\sigma h_{\mu\nu})(\partial_\sigma h^{\mu\nu}) - \frac{1}{2}(\partial_\sigma h^\mu_\mu)(\partial^\sigma h^\nu_\nu) - (\partial^\sigma h^{\mu\nu})(\partial_\mu h_{\mu\nu}) + (\partial_\sigma h^{\sigma\mu})(\partial_\mu h^\nu_\nu) \quad , \tag{2.11}$$

plus higher-order terms in the fluctuation field. The appearance of the Fierz-Pauli Lagrangian as the lowest-order polynomial in the fluctuation field is natural since the field equations of linearized gravity (when $h_{\mu\nu} \to f_{\mu\nu} << 1$) can be obtained from it. Furthermore, it is the only Lagrangian invariant under diffeomorphisms[26], where ξ_μ is a small shift in the coordinate system,

$$\delta f_{\mu\nu} = \partial_\mu \xi_\nu + \partial_\nu \xi_\mu \quad . \tag{2.12}$$

By virtue of appropriate partial integrations, the Fierz-Pauli Lagrangian (2.11) can be cast in the suitable form of a product of fields with an operator insertion, as follows:

$$\mathcal{L}_{FP} \propto h_{\rho\lambda} M^{\rho\lambda\mu\nu} h_{\mu\nu} \quad . \tag{2.13}$$

Similar to QED or QCD, the M matrix is not invertible since it has zero modes. To make it invertible, the harmonic gauge condition, (2.4), may be introduced as a gauge-fixing term[27] and the usual Fadeev-Popov method[28] can be carried out. Having done so[29], the first building block of perturbation theory arises: the *graviton propagator* (figure (1)),

$$\mathcal{D}_{\mu_1\nu_1;\mu_2\nu_2}(k) = \frac{\eta_{\mu_1\mu_2}\eta_{\nu_1\nu_2} + \eta_{\mu_1\nu_2}\eta_{\nu_1\mu_2} - \eta_{\mu_1\nu_1}\eta_{\mu_2\nu_2}}{k^2 - i\epsilon} \quad . \tag{2.14}$$

Albeit technically involved, the higher-order terms in the couplings carry information about the vertices associated with graviton self-interactions, like the three-vertex[7] (figure (2)), represented by the Feynman rule:

$$\mathcal{V}^{\mu_1\nu_1;\mu_2\nu_2;\mu_3\nu_3}(k_1, k_2, k_3) = k_1 k_2 \eta^{\mu_1\nu_1}\eta^{\mu_2\nu_2}\eta^{\mu_3\nu_3} + k_1^{\mu_3} k_2^{\nu_3} \eta^{\mu_1\mu_2}\eta^{\nu_1\nu_2} + (\ldots) \quad , \tag{2.15}$$

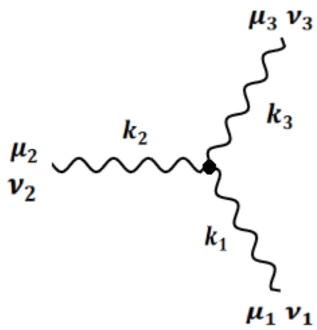

Figure 2: Graviton three-vertex

comprising all the six-index quantities that can be built from the momenta and the Minkowski metric. (Naturally, if a non-flat background is chosen, the expressions are even more complex[30].)

This vertex gives a first taste of the complexity of this type of approach. However, technical complexity is not the only (nor the main) issue. The perturbative path integral approach is not a complete theory of the quantum gravitational field since it is not possible to renormalize the theory within the standard perturbative renormalization procedures of QFT[31]. The divergences in the theory cannot be absorbed in the parameters of the Lagrangian, requiring the addition of counterterms to the Lagrangian at every order of the perturbative expansion. Each counterterm carries a coefficient which is to be fixed experimentally. Hence, at arbitrarily high order, an infinite number of counterterms ought to be fixed in order to renormalize the theory. As such, the theory is deemed incomplete or non-predictive at high energies. (To be precise, the coefficients of the divergent 1-loop order (pure gravity) terms coincidentally cancel out[32]. However, that is not the case at higher loop orders[33][34][35].) This fact could have already been foreseen by looking at the mass dimensions of Newton's constant, $[G_N]$ (and consequently the theory's coupling constant),

$$\sqrt{G_N} \sim \frac{1}{m_{Pl}} \to [G_N] = -2 \quad . \tag{2.16}$$

A momentum cut-off Λ is introduced to allow for finite integrations and then sent to infinity to obtain a UV-complete theory. When computing the amplitude $\mathcal{A}$ - a dimensionless quantity - of a physical process and reading its perturbative expansion in powers of the gravitational coupling constant, one notices that the divergences increase with increasing order of the powers of the coupling constant due to the negative mass dimension of $\sqrt{G_N}$. Schematically, $\mathcal{A}$ depends on powers $(\sqrt{G_N})^a\Lambda^b$ and, in order for such an object to be dimensionless, $b > 0$ to cancel the negative mass dimensions introduced by G_N.

The impossibility to renormalize the theory might, in fact, be rooted in a deeper conceptual problem pertaining the split of the metric field into perturbations around the Minkowski (or any other background) metric.

First, at strong gravitational limits, it might occur that the $h_{\mu\nu}$ field fluctuates in such an unrestricted manner that it alters the metric signature $(-+++)$ of $g_{\mu\nu}$ (which would, for instance, destroy the constraint of $det(g_{\mu\nu}) < 0$). Some alternative decompositions of the metric that restrict the behaviour of the fluctuation field have been studied[36][37] in an attempt to circumvent this problem. Furthermore, the background-field method is an explicitly covariant approach to quantum gravity in the sense that diffeomorphism invariance is preserved for the (fixed) background field. The fluctuation field is considered to exist on the space-time defined by the background metric. However, it is at the core of GR that space-time geometry and the *full* metric field go hand in hand. Space-time is not determined by the background metric alone but by the full metric - which is precisely the unknown variable. Quantum gravity should be defined in a background-independent manner. The BRST symmetry[38] realizes background-independence in QFTs. However, the perturbative non-renormalizability of GR raises some issues[39] regarding the preservation of the symmetry order by order in the perturbative expansion, complicating the use of the metric split as a tool in the quest for a quantum theory of the gravitational field.

In spite of this, perturbative quantum gravity has its use in the setting of an effective field theory[40], valid up to an energy scale beneath that at which it breaks down. Within this framework, some results have been obtained. Quantum corrections to the Newtonian potential have been studied[41] as well as corrections to the Schwarzschild and Kerr metrics[42], and the amplitudes of processes such as the graviton-graviton scattering have been computed[7]. These results can serve as a benchmark to a complete theory of Quantum Gravity.

Some difficulties of the perturbative path integral attempt to quantize gravity have been outlined above. The following subsection is devoted to another classic quantization procedure: the canonical quantization of GR.

2.2 Canonical Quantization of Gravity

A possible approach in the canonical quantization of GR is the casting of the Einstein-Hilbert action, (2.8), into Hamiltonian form. The focus here will be on ADM Gravity[43], a Hamiltonian formulation of GR developed in the 1960's by Richard Arnowitt, Stanley Desner and Charles

Misner. To obtain it from the Einstein-Hilbert action, it is important to recall the definition of the Hamiltonian density, $\mathcal{H}$, as a Legendre transformation of the Lagrangian density, $\mathcal{L}$,

$$\mathcal{H} = \pi \dot{q} - \mathcal{L} \quad , \tag{2.17}$$

where q denotes the chosen canonical variable, π denotes its canonically conjugate momentum and the dot over q denotes the time derivative.

Hence, one must start by defining the appropriate canonical variable. Moreover, a "time" variable must be singled out, with respect to which the evolution of the canonical variable is evaluated. In order to do so, space-time is broken up into space plus time: the Hamiltonian formalism explicitly breaks the space-time covariance of GR.

Let us start with a 4D topological differentiable manifold and a Lorentzian metric, $(\mathcal{M},\, g_{\mu\nu})$. If such a space-time is globally hyperbolic, $\mathcal{M}$ can be foliated, for each "time", into Cauchy hypersurfaces[29], and its topology is given by a direct product of the spatial 3D Cauchy hypersurfaces, Σ_t, and the global "time",

$$\mathcal{M} = \mathbb{R} \times \Sigma_t \quad . \tag{2.18}$$

A time flow vector field, t^μ, can be associated to the global "time" function, t, where μ refers to the 4D space-time indices. Note that this "time" is still not endowed with any physical meaning, as the metric field is still unknown. To understand the meaning of this "time" vector, consider two infinitesimally close hypersurfaces as in figure (3). t^μ is the vector that points along the line identified with ds: it points from the point of coordinates (x^a) in Σ_t to the point of coordinates (x^a) in Σ_{t+dt} (a references spatial indices). Since the two surfaces are, in general, geometrically different from one another, the two (x^a, t) and $(x^a, t+dt)$ do not lie normally above one another. t^μ can be decomposed into a normal and a tangential component, respectively,

$$t^\mu = N n^\mu + N^\mu \quad , \tag{2.19}$$

where n^μ denotes the unit vector normal to Σ_t, pointing from (x^a, t) to a point $(y^a, t+dt)$ normally above it, N^μ is the shift vector, pointing from $(y^a, t + dt)$ to the point $(x^a, t + dt)$, and N is the lapse function, such that $ds = N dt$.

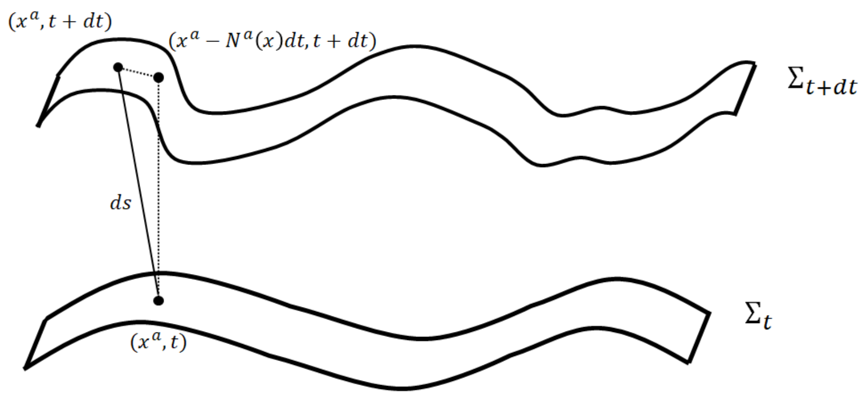

Figure 3: Two infinitesimally close hypersurfaces

A three-dimensional metric is induced on each hypersurface, the spatial components of which,

$$h_{ab} = g_{ab} + n_a n_b \quad , \tag{2.20}$$

constitute the canonical variable in the ADM formalism. g^{ab} can be expressed[44] in terms of the geometrical quantities (h^{ab}, N, N^a) as follows:

$$g^{ab} = h^{ab} - N^{-2}(t^a - N^a)(t^b - N^b) \quad . \tag{2.21}$$

Therefore, the 10 degrees of freedom of the Lorentzian metric, $g_{\mu\nu}$, (a 4×4 symmetric matrix) are now expressed as 6 degrees of freedom from the induced spatial metric, h_{ab}, (a 3×3 symmetric matrix), 1 degree of freedom from the lapse function, N, and 3 degrees of freedom from the shift vector, N^a.

The goal is now to rewrite (2.8), namely the volume element and the Ricci scalar, in terms of these new variables. To that end, it is useful to introduce the concept of extrinsic curvature, given in terms of a Lie derivative[29],

$$K_{\mu\nu} = \frac{1}{2} L_{\mathbf{n}} h_{\mu\nu} \quad , \tag{2.22}$$

where $\mathbf{n}$ is the normal to the surface. This tensor is purely spatial and its spatial components can be written in terms of the new variables[45],

$$K_{ab} = \frac{1}{2N}(\dot{h}_{ab} - D_a N_b - D_b N_a) \tag{2.23}$$

where D_a is the spatial covariant derivative.

The Ricci scalar and the volume element are given, respectively, as follows (see Wald[44] or Kiefer[29] for details),

$$\mathcal{R} = \mathcal{R}^{(3)} + K^2 - K_{ab}K^{ab} - 2\mathcal{R}_{\mu\nu}n^\mu n^\nu = \mathcal{R}^{(3)} - K^2 + K_{ab}K^{ab} \quad , \tag{2.24}$$

$$\sqrt{-g} = N\sqrt{h} \quad , \tag{2.25}$$

where $\mathcal{R}^{(3)}$ is the 3D Ricci scalar and K is the trace of the extrinsic curvature.

With (2.8), (2.24) and (2.25), one obtains the ADM form of the Einstein-Hilbert action[45],

$$S_{EH} = \int \frac{dtd^3x}{16\pi G_N} N\sqrt{h}(\mathcal{R}^{(3)} - 2\Lambda - K^2 + K_{ab}K^{ab}) = \int \frac{dtd^3x}{16\pi G_N} N(\mathcal{G}_{abcd}K^{ab}K^{cd} + \sqrt{h}(\mathcal{R}^{(3)} - 2\Lambda)), \tag{2.26}$$

where the DeWitt super-metric[5] (a "metric" in the space of all metrics) has been introduced,

$$\mathcal{G}_{abcd} = \frac{1}{2\sqrt{h}}(h_{ac}h_{bd} + h_{bc}h_{ad} - h_{ab}h_{cd}) \quad . \tag{2.27}$$

The Lagrangian density does not depend on times derivatives of either N or N^a: they do not play the role of dynamical variables. Their canonically conjugate momenta (generically given by $\pi = \frac{\partial \mathcal{L}}{\partial \dot{q}}$) vanish. On the other hand, the canonical momentum associated to the induced metric, π_{ab}, is non-vanishing, given as follows[45]:

$$\pi_{ab} = \frac{1}{16\pi G_N}\mathcal{G}_{abcd}K^{cd} = \frac{\sqrt{h}}{16\pi G_N}(K_{ab} - Kh_{ab}) \quad . \tag{2.28}$$

In order to apply the Legendre transformation, (2.17), $\dot{h}_{ab}$ must be expressed in terms of the canonical momentum. To that end, one inverts (2.28) in order to express K_{ab} in terms of π_{ab} and plugs it into (2.23). This leads to:

$$\dot{h}_{ab} = \frac{32\pi G_N N}{\sqrt{h}}(\pi_{ab} - \frac{1}{2}\pi_{ab}h^{ab}h_{ab}) + D_a N_b + D_b N_a \quad . \tag{2.29}$$

This is the first set of the Hamiltonian equations of motion, formally given by $\dot{h}_{ab} = \frac{\delta H}{\delta \pi^{ab}}$. The (rather lengthy) expression for the second set of the Hamiltonian equations of motion, $\dot{\pi}_{ab} = -\frac{\delta H}{\delta h^{ab}}$, can be found, for example, in Wald[44].

The Hamiltonian density of GR can now be written,

$$\mathcal{H} = 16\pi G_N N \mathcal{G}_{abcd}\pi^{ab}\pi^{cd} - N\frac{\sqrt{h}(\mathcal{R}^{(3)} - 2\Lambda)}{16\pi G_N} - 2N_b D_a \pi^{ab} \quad , \tag{2.30}$$

and the Einstein-Hilbert action can be rewritten as follows:

$$S_{EH} = \frac{1}{16\pi G_N}\int dt d^3x(\pi^{ab}\dot{h}_{ab} - N\mathcal{H}_\perp - N^a\mathcal{H}_a) \quad . \tag{2.31}$$

As previously pointed out, N and N^a are non-dynamical variables. They are called Lagrange multipliers. From their equations of motion, $\frac{\delta S}{\delta N} = 0$ and $\frac{\delta S}{\delta N^a} = 0 \rightarrow \mathcal{H}_\perp = 0$ and $\mathcal{H}_a = 0$. $\mathcal{H}_\perp$ and $\mathcal{H}_a$ are called constraints. Therefore, this is a constrained Hamiltonian formulation of GR, one in which, aside from the Hamiltonian equations of motion, there are two constraints on the Hamiltonian: the diffeomorphism (or momentum) constraint and the Hamiltonian constraint, respectively,

$$\mathcal{H}_a = -2D_b\pi_a^b = 0 \quad , \tag{2.32}$$

$$\mathcal{H}_\perp = 16\pi G_N \mathcal{G}_{abcd}\pi^{ab}\pi^{cd} - \frac{\sqrt{h}(\mathcal{R}^{(3)} - 2\Lambda)}{16\pi G_N} = 0 \quad . \tag{2.33}$$

In the 1970's, the formulation developed by Hojman *et al.*[46], known as geometrodynamics, shone new light on the meaning of these objects. The approach is based solely on the algebra of surface deformations and, under some general principles, it is shown that (2.32) and (2.33) are the generators of such surface deformations. (A review of the approach can be found in Kiefer[29].)

The constraints restrict the degrees of freedom of the theory. (2.32) and (2.33) sum up to 4 (one scalar and one vectorial) constraints on each point of phase space, $4 \times \infty^{(3)}$. Subtracting that from the $6 \times \infty^{(3)}$ degrees of freedom coming from the pair (h_{ab}, π_{ab}) of canonical variables, one is left with $2 \times \infty^{(3)}$ degrees of freedom, in line with the two polarization states of the gravitational wave of (2.6). The existence of the constraints is an indication that the configuration space is not yet narrowed down to the physical one. The diffeomorphism constraint (2.32) can be eliminated[44] by taking as canonical variable the set of equivalence classes of h_{ab} - the set of all physically non-equivalent metrics (up to diffeomorphisms of Σ_t). This configuration space is known as superspace[47]. However, a configuration space that can eliminate the Hamiltonian constraint (2.33) is not known.

The constraints represent an obstacle to the quantization of ADM Gravity. The problem can be posed as follows. Should the constrained classical theory be quantized and then some quantum mechanical reduction of the degrees of freedom be performed or should the classical degrees of freedom be reduced and then the unconstrained classical theory be quantized? Is there a guarantee of the equivalence of the two *modi operandi*?

In general, the equivalence between the two approaches cannot be guaranteed. In practice, the quantization of the unconstrained classical theory is based on a much more complicated configuration space and is rarely attempted. The quantization of the constrained classical theory can be done through the quantization procedure set up by Paul Dirac[48]. A comprehensive step-by-step discussion of the procedure can be found in Kiefer[29]. For the current purposes the following statement suffices: the classical constraint is promoted to an operator equation that restricts the physical states,

$$\phi_a = 0 \rightarrow \hat{\phi}_a |\psi\rangle = 0 \quad . \tag{2.34}$$

However, there is no general recipe to predict the behaviour of constraints after quantization. Consider, for example, two classical constraints, $\phi_a = 0$ and $\phi_b = 0$, such that they satisfy the usual Poisson brackets, $\{\phi_a, \phi_b\} = f^c_{ab}\phi_c = 0$. The Poisson brackets should then be promoted to $[\hat{\phi}_a, \hat{\phi}_b]|\psi\rangle = 0$. As $f^c_{ab}\phi_c$ is subject to quantization, a factor-ordering problem arises: it could be that $f^c_{ab}\phi_c \rightarrow \hat{f}^c_{ab}\hat{\phi}_c$ but it could also be that the order of the products turns out to be different. Due to $[\hat{\phi}_a, \hat{\phi}_b]|\psi\rangle = 0$, constraints other than the classical ones would then be imposed on (already physical) degrees of freedom. The classical symmetry would be broken at the quantum level and a gauge anomaly would arise. This is why one cannot guarantee the equivalence of the procedures outlined above. Different degrees of freedom of either approach might lead to different quantum constraints and anomalies that are present in one quantization scheme might not be present in the other. Hypothetical experimental evidence of the existence/nonexistence of such anomalies could be of use in this setting.

The simplest quantum promotion of (2.33) is given by promoting $h_{ab} \rightarrow \hat{h}_{ab}$, $\pi_{ab} \rightarrow \hat{\pi}_{ab} = \frac{\delta}{\delta \hat{h}_{ab}}$ (a functional derivative with respect to $\hat{h}_{ab}$) and assuming the operator ordering where all momenta appear to the right of their respective term. The equation is known as the Wheeler-DeWitt equation[5],

$$\hat{\mathcal{H}}_{\perp}|\psi\rangle = (-16\pi G_N \hbar^2 G_{abcd} \frac{\delta^2}{\delta h_{ab} \delta h_{cd}} - \frac{\sqrt{h}}{16\pi G_N}(\mathcal{R}^{(3)} - 2\Lambda))|\psi\rangle = 0 \quad . \tag{2.35}$$

As it stands, there is no general solution to this equation. It has, however, been studied in cosmological models[49][50]. Even before solving the equation, an interesting question is raised by it: the question of the meaning of time. If one is to interpret it as a Schrödinger-like equation, $i\hbar \frac{d}{dt}\psi = \hat{\mathcal{H}}_{\perp}\psi = 0$, then nothing is happening dynamically to the system. The question of the nature of time in QG has been addressed many times, both from a philosophical and a mathematical viewpoint and many great reviews on the subject can be found[51][52][53].

In the 1980's, in an attempt to simplify the equations of motion and constraints of ADM Gravity, Abhay Ashtekar proposed the adoption of a new set of canonical variables[54], inspired by the possibility of writing the metric h_{ab} in terms of a set of orthonormal vectors known as triads, such that $h_{ab} = e_i^a e_i^b$. The new index i, referent to the internal symmetry of the vectors, gives rise to a new gauge (SU(2)) symmetry of the metric. This prompted Lee Smolin and Carlo Rovelli to formulate GR as a gauge theory in 1990[55]. This formulation gave rise to the modern day canonical approach to the quantization of gravity, known as Loop Quantum Gravity. Many exciting predictions are made in this formalism[56][57] and research is highly active.

2.3 Asymptotically Safe Gravity

Having discussed the perturbative and canonical approaches to QG, this subsection discusses another approach, doing so very lightly, as the ideas put forth here will be made more concrete in sections further along the thesis.

The idea of (Gravitational) Asymptotic Safety was introduced by Steven Weinberg[58] in the end of the 1970's. As we have seen in subsection [2.1], the perturbative QFT approach to GR fails at delivering a UV-complete theory. The goal of the Asymptotic Safety scenario is a rather simple one: to make a perturbatively non-renormalizable QFT UV-complete by means of non-perturbative techniques.

Scale symmetry is an important feature of classical field theories as the theory's couplings are constant and thus independent of the energy scale, k. This means that the theory is consistent at all energy scales. However, scale symmetry is broken upon quantization (often due to the measure of the path integral) and, as such, divergences in the theory's couplings, u_α, may appear at high energy scales, where the theory is no longer consistent. The way that couplings vary with the energy scale is portrayed by the couplings' *beta functions*, $\beta(u_\alpha)$. In order for scale symmetry to be recovered at the quantum level, one should then find a set of values for the couplings, $\{u_\alpha,\ \alpha = 1, 2, ...\} = u^*$, known as a *fixed point*, at which $\beta(u_\alpha) = 0$ - that is, the couplings cease to have a scale dependence. If the fixed point has all coordinates, u_α, equal to zero, it is called a Gaussian Fixed Point, and one speaks of Asymptotic Freedom. If the fixed point has some non-vanishing coordinate(s), it is called a Non-Gaussian Fixed Point (NGFP), and one speaks of Asymptotic Safety. The goal of Asymptotically Safe Gravity is thus to define a quantum gravitational theory whose UV limit ($k \to \infty$) is a fixed point, such that at arbitrarily high energy scales the theory is (asymptotically) safe from divergences.

Evidence[18][59][60][61] for the existence of such a fixed point for 4D gravity is not definitive but enough to make a good case for it and to still be pushing active research in the field. However, lower-dimensional versions of GR are generally simpler and easier to explore[9][10]. Therefore, they can be looked at as possible starting points for lower-dimensional models of a quantum theory of the gravitational field.

In this thesis, we will focus specifically on the quantization of $2D$ gravity. We will show that $2D$ Quantum Gravity (2DQG) is equivalent to a matrix formulation - Matrix Models - to which we will apply the necessary procedures in order to evaluate the hypothesis of Asymptotic Safety in such models. The hope is that the results found in a $2D$ setting can serve as a toy model for higher-dimensional settings to be tackled afterwards. The following chapter is thus devoted to the quantization of $2D$ gravity and to presenting the results relevant for the work developed further along the thesis.

3 Two-Dimensional Quantum Gravity

Two-dimensional gravity - with one temporal and one spatial dimension - is a topological field theory, as the $2D$ Einstein-Hilbert action leads to non-dynamical equations for the metric field. It is thus classically trivial. However, in two dimensions, Einstein's field equations are equivalent to Liouville's equation. Liouville's equation can be generalized to be the equation of motion of a $2D$ Conformal Field Theory, appropriately named Liouville Field Theory, which can thus provide a framework for a quantum theory of gravity - Liouville Gravity. The quantum theory turns out to be non-trivial due to the presence of a conformal anomaly. Furthermore, Liouville Gravity is shown to be equivalently described by Matrix Models: different types of matter interactions are described by different types/restrictions to the matrices. This chapter is devoted to presenting these two approaches: Liouville Gravity, Matrix Models and the bridge between them.

3.1 Liouville Gravity

The Einstein-Hilbert action (2.8) in two-dimensions leads to no dynamical field equations for the metric tensor due to the fact that the corresponding Lagrangian, $-\sqrt{|g|}\mathcal{R}$, is a total divergence. Another way of looking at it is that Einstein's tensor identically vanishes in two dimensions,

$$\mathcal{G}_{\mu\nu} = \mathcal{R}_{\mu\nu} - \frac{1}{2} g_{\mu\nu}\mathcal{R} = 0 \quad , \tag{3.1}$$

and, as such, any metric is a solution of the equations of motion.

To obtain the Liouville equation from the Einstein-Hilbert action[11][12] additional fields must be introduced, known as Liouville modes. Liouville Field Theory had long been (classically) established and studied as a $2D$ conformal field theory but its quantization is far from trivial.

Alexander Polyakov's seminal paper[13] of 1981 paved the way for the path integral quantization of Liouville Gravity. In it, inspired by the fact that the amplitudes of free particles are given by the sum of all possible paths in the particle's history, the author outlined a model for summing over all possible surfaces along which free strings (the model's analogue of particles) would move. This is ultimately the problem of QG: the summation over metrics - or surfaces - modulo diffeomorphisms and over topologies, as stated in equation (2.7).

Following Polyakov[13], one can start with the purely bosonic string action, describing the $2D$ worldsheet of a D-dimensional bosonic string,

$$S_M(X,g) = \frac{1}{8\pi}\int d^2\xi\sqrt{g}g_{ab}h_{ij}\partial^a X^i \partial^b X^j \quad , \tag{3.2}$$

where h is the metric of the D-dimensional target manifold, g is the metric field of the worldsheet, Σ, a $2D$ Riemannian genus h surface (where the genus is, intuitively, the number of holes of the surface), and X is the bosonic D-dimensional matter field. $\vec{X}(\xi)$ specifies the embedding of Σ into the D-dimensional space-time. Choosing to work in flat D-dimensional Euclidean space, (3.2) is simplified,

$$S_M(X,g) = \frac{1}{8\pi}\int d^2\xi\sqrt{g}g_{ab}\partial^a X^i \partial^b X^i \quad . \tag{3.3}$$

The a, b indices refer to the $2D$ worldsheet and i refers to the D-dimensional embedding space.

The action is invariant under a conformal/Weyl transformation of the metric,

$$g_{ab} \to g'_{ab} = e^{\sigma} g_{ab} \quad , \tag{3.4}$$

where σ is the Liouville mode. The quantum theory, however, is not invariant under (3.4),

The partition function, where μ_0 is an explicit bare cosmological constant and the configurations related by diffeomorphisms of the 2D surface Σ are divided out, is written as follows,

$$\mathcal{Z} = \int \frac{\mathcal{D}g\mathcal{D}_g X}{vol(diff)} e^{-S_M(X,g)-\frac{\mu_0}{2\pi}\int d^2\xi\sqrt{g}} \quad . \tag{3.5}$$

An anomaly arises due to the integration measures, and conformal invariance is broken upon quantization. While the integration measures are invariant under diffeomorphisms of the surface Σ - hence the division by the volume of the diffeomorphism group - they depend on the metric by their very definition[13][62] in a way that makes them non-invariant under the Weyl rescaling of the metric, (3.4). The integration measures are determined by requiring they respect the following constraints,

$$\int \mathcal{D}_g \delta X e^{-||\delta X||_g^2} = 1 \quad ,$$
$$\int \mathcal{D}_g \delta g e^{-\frac{1}{2}||\delta g||_g^2} = 1 \quad , \tag{3.6}$$

where the norms are defined as follows, δg and δX being metric/matter fluctuations on Σ,

$$||\delta X||_g^2 = \int d^2\xi \sqrt{g} \delta X^i \delta X^i \quad , \tag{3.7}$$

$$||\delta g||_g^2 = \int d^2\xi \sqrt{g} (g_{ac} g_{bd} + 2 g_{ab} g_{cd}) \delta g^{ab} \delta g^{cd} \quad , \tag{3.8}$$

The dependence on the metric in equation (3.7) means the matter field integration measure is not conformally invariant. The anomaly is given by

$$\mathcal{D}_{g'} X = e^{\frac{D}{48\pi} S_L(\sigma)} \mathcal{D}_g X \quad , \tag{3.9}$$

where D is the dimension of the flat space-time in which the $2D$ surface Σ is embedded and $S_L(\sigma)$ is the Liouville action,

$$S_L(\sigma) = \int d^2\xi \sqrt{g} \left(\frac{1}{2} g_{ab} \partial^a \sigma \partial^b \sigma + R\sigma + \mu e^{\sigma} \right) \quad . \tag{3.10}$$

The metric integration measure also carries a conformal anomaly. To integrate over the metric field, one must get rid of the degeneracies and integrate only over the non-equivalent metrics. The space of metrics on a surface Σ modulo diffeomorphisms and Weyl transformations (3.4) is a finite dimensional compact space named moduli space[14], $\mathcal{M}_h$, whose dimensions depend on the genus of the surface. With a representative fiducial metric, $\hat{g}$, for each point τ of the moduli space, the full space of metrics on Σ can be recovered via the action of the diffeomorphism and Weyl groups' generated orbits on the fiducial metric, $\hat{g}$. Hence, the metric can be parameterized by a diffeomorphism f and a Weyl scaling ϕ,

$$f * g = e^{\phi} \hat{g}(\tau) \quad . \tag{3.11}$$

The metric integration is thus split into an integration over the vector fields, v_a, that generate infinitesimal diffeomorphisms, an integration over the Liouville mode, ϕ, and an integration over moduli space. The definition of the partition function (3.5) divides out the diffeomorphisms and one is left with the integration over the Liouville mode and over the moduli space. The Fadeev-Popov method[28] can be used to extract the Jacobian for the change of variables by taking convenient advantage of the complex coordinate language of $2D$ CFT[14] (see appendix [A]). The Jacobian is given by

$$J(\phi, \hat{g}) = \int \mathcal{D}b\mathcal{D}c\mathcal{D}\bar{b}\mathcal{D}\bar{c}\, e^{-\int d^2\xi\sqrt{g}(b\bar{\nabla}c+\bar{b}\nabla\bar{c})} \quad , \tag{3.12}$$

where b ($\bar{b}$) and c ($\bar{c}$) are the ghosts (and anti-ghosts). The anomaly associated to the ghost integration measure (from here on out abbreviated to $\mathcal{D}(bc)$) is finally extracted:

$$\mathcal{D}_{e^\sigma g}(bc) = e^{-\frac{26}{48\pi}S_L(\sigma)}\mathcal{D}_g(bc) \quad . \tag{3.13}$$

This is Polyakov's seminal result[13]: the origin of the critical $D = 26$ dimension in string theory. At this value of D, the conformal invariance of the classical theory is preserved upon quantization and the Weyl transformation, (3.4), is a gauge symmetry of the theory. However, at any other value, the anomaly impedes the division of the integration measure by the volume of Weyl transformations and one has to integrate over the Liouville mode.

The partition function can thus be rewritten,

$$\mathcal{Z} = \int [d\tau]\mathcal{D}_g\phi\mathcal{D}_g(bc)\mathcal{D}_g X\, e^{-S_M(X,g)-S_{gh}(b,c,g)-\frac{\mu_0}{2\pi}\int d^2\xi\sqrt{g}} \quad . \tag{3.14}$$

The main problem from now on is how to deal with the Liouville mode integration measure. As first pointed out by Distler and Kawai[62], having constructed this measure to be explicitly diffeomorphism invariant, the norm is dependent not only on the metric but also on the Liouville mode itself in a non-trivial manner due to the fiducial decomposition, (3.11),

$$||\delta\phi||_g^2 = \int d^2\xi\sqrt{g}(\delta\phi)^2 = \int d^2\xi\sqrt{\hat{g}}e^{\phi}(\delta\phi)^2 \quad . \tag{3.15}$$

If the exponential of the Liouville mode were absent from the expression above, the Liouville mode integration measure would reduce to that of a free field, and everything would be facilitated; that is, if the norm took a form akin to (3.7),

$$||\delta\phi||^2_{\hat{g}} = \int d^2\xi \sqrt{\hat{g}}(\delta\phi)^2 \quad . \tag{3.16}$$

To transform from (3.15) to (3.16), one would have to find the Jacobian of such transformation. In Distler and Kawai's paper[62], the form of the Jacobian was assumed to be that of an exponential of a renormalizable local action, diffeormorphism and conformally invariant, $J(\phi, \hat{g}) = e^{-S(\phi,\hat{g})}$. As pointed out in Ginsparg and Moore[14] and in Nakayama's review[63] of Liouville Field Theory, there have been attempts[64][65] to justify this assumption. Furthermore, canonical formulations of Liouville Gravity also validate this assumption[14]. The action that respects these requirements is a Liouville-like action, akin to (3.10), with arbitrary coefficients attached to each term. The integration measures are now dependent only on the fiducial metric,

$$\mathcal{Z} = \int [d\tau]\mathcal{D}_{\hat{g}}\phi\mathcal{D}_{\hat{g}}(bc)\mathcal{D}_{\hat{g}}(X)e^{-S_M(X,\hat{g})-S_{gh}(b,c,\hat{g})-\int d^2\xi\sqrt{\hat{g}}(\alpha\hat{g}_{ab}\partial^a\phi\partial^b\phi+Q\hat{R}\phi+\mu e^{\gamma\phi})} \quad , \tag{3.17}$$

where μ is a combination of μ_0 and some term μ_1 analog to that of the Liouville action. Hence, μ can be set to zero due to the freedom to adjust the bare cosmological constant μ_0. All that is left is to determine the arbitrary coefficients. To do so, two further aspects are essential. First, the theory ought to be dependent on the metric alone and not on the particular choice of fiducial metric. It should thus be invariant under the following simultaneous transformations,

$$\hat{g}_{ab} \to \hat{g}'_{ab} = e^{\sigma}\hat{g} \;\; || \;\; \phi \to \phi' = \phi - \frac{\sigma}{\gamma} \quad . \tag{3.18}$$

Applying the infinitesimal version of these transformations to (3.17) and upholding the theory's invariance under them, one finds

$$Q = \frac{25 - D}{48\pi} \;\; || \;\; \alpha = \frac{1}{2}Q \quad . \tag{3.19}$$

The Liouville field can be rescaled in order to obtain a standard kinetic term, $\sim \int(\partial\phi)^2$. The definition of Q is altered accordingly:

$$Q = \sqrt{\frac{25 - D}{3}} \quad . \tag{3.20}$$

Second, in order for the theory to be conformally invariant, the total central charge (see appendix [A]) must vanish. Recalling the matter (3.9) and ghost (3.13) anomalies, one can extract the central charge for the Liouville mode,

$$c_{matter} + c_{ghosts} + c_{liouville} = D - 26 + c_{liouville} = 0 \Leftrightarrow c_{liouville} = 1 + 3Q^2 \quad . \tag{3.21}$$

Due to the rescaling of the Liouville mode, the physical and fiducial metric are related via

$$g = e^{\gamma\phi}\hat{g} \quad , \tag{3.22}$$

which means the area of the surface is now given by

$$A = \int d^2\xi \sqrt{\hat{g}} e^{\gamma\phi} \quad . \tag{3.23}$$

Conformal invariance demands that $e^{\gamma\phi}$ behaves as a tensor of conformal weight (see appendix [A]) $(h, \bar{h}) = (1, 1)$[62]. The last coefficient of (3.17) is thus obtained:

$$\gamma_{\pm} = -\frac{1}{\sqrt{12}}(\sqrt{25 - D} \mp \sqrt{1 - D}) \quad . \tag{3.24}$$

As duly noted by Ginsparg and Moore[14], before rescaling the Liouville mode, the Liouville action's effective coupling in (3.17) goes with $\sim \frac{1}{25-D}$. Therefore, the classical limit of the Liouville action is obtained with $D \to -\infty$, which will take the effective coupling to zero. The root that carries this classical behaviour $\gamma \to 0$ is the $+$ root.

Distinct regimes appear depending on the value of the matter central charge. At $D \leq 1$, both γ and Q are real; this is the range in which the cosmological constant is real, and where Liouville Gravity is well defined. At $D = 1$ a phase transition might occur; above this value of the matter central charge, Liouville's model of gravity is incomplete. Particularly at $D = 25$, $Q = 0$ and γ is purely imaginary, which means the reality of the metric is lost. A conjecture can be made:

to account for this, one can perform a Wick rotation on $\phi \to i\phi$, which reverses the sign of the kinetic term, making it as though ϕ is a timelike dimension; in this sense, the noncritical string propagating in a 25-dimensional Euclidean space is analog to the critical string propagating in a 26-dimensional Minkowski space. At $D > 25$, both Q and γ are purely imaginary, and the reversal of the Liouville mode kinetic term sign still occurs. Despite being undisclosed in the Liouville formalism of 2DQG, it is this regime that could model higher-dimensional QG[66].

An important quantity to establish the link between Liouville Gravity, Matrix Models and the FRG is the string susceptibility, Γ_{str}, an exponent that governs the behaviour of the partition function for large areas of the surface. This quantity was first conjectured by Knizhnik, Polyakov, Zamolodchikov[15] for genus zero surfaces, working in the light-cone gauge, and then formally derived by Distler and Kawai[62] and David[67] for arbitrary genus, working in the conformal gauge, (3.11) - the one that's been followed throughout this section. Consider the partition function for the theory for a fixed area A of the Riemannian surface,

$$\mathcal{Z}(A) = \int \mathcal{D}\phi\mathcal{D}\psi e^{-S}\delta\left(A - \int d^2\xi\sqrt{\hat{g}}e^{\gamma\phi}\right) \quad , \tag{3.25}$$

where $\mathcal{D}\psi$ conveniently encompasses the matter, ghost and moduli integration measures. Following Ginsparg and Moore[14], we define the string susceptibility in terms of the Euler characteristic,

$$\chi = 2 - 2h \quad , \tag{3.26}$$

where h is the genus of the surface, as follows:

$$\mathcal{Z}(A) \sim A^{\frac{\chi}{2}(\Gamma_{str}-2)-1} \quad . \tag{3.27}$$

Consider a shift $\phi \to \phi + \frac{\rho}{\gamma}$, where ρ is a constant, similar to the second transformation in (3.18). The Liouville mode integration measure is invariant under such a transformation. The only variation will thus come from the integrand of (3.25), particularly from the Liouville rescaled action,

$$\frac{Q}{8\pi}\int d^2\xi\sqrt{\hat{g}}\hat{R}\phi \to \frac{Q}{8\pi}\left[\int d^2\xi\sqrt{\hat{g}}\hat{R}\phi + \frac{\rho}{\gamma}\int d^2\xi\sqrt{\hat{g}}\hat{R}\right] \quad , \tag{3.28}$$

and from the δ term,

$$\delta\left(\int d^2\xi\sqrt{\hat{g}}e^{\gamma\phi}-A\right)\rightarrow e^{-\rho}\delta\left(\int d^2\xi\sqrt{\hat{g}}e^{\gamma\phi}-e^{-\rho}A\right) \quad . \tag{3.29}$$

Therefore, (3.25) is shifted to the following form:

$$\mathcal{Z}(A)=\int\mathcal{D}\phi\mathcal{D}\psi e^{-S}e^{-\frac{Q}{8\pi}\frac{\rho}{\gamma}\int d^2\xi\sqrt{\hat{g}}\hat{R}}e^{-\rho}\delta\left(\int d^2\xi\sqrt{\hat{g}}e^{\gamma\phi}-e^{-\rho}A\right) \quad . \tag{3.30}$$

Upon identifying the Gauss-Bonnet formula,

$$\int d^2\xi\sqrt{\hat{g}}\hat{R}=4\pi\chi \quad , \tag{3.31}$$

and setting $A=e^{\rho}$[68] on the remaining expression,

$$\mathcal{Z}(A)=e^{-\frac{Q\rho\chi}{2\gamma}-\rho}\mathcal{Z}(e^{-\rho}A) \quad , \tag{3.32}$$

the dependence of the partition function on the area of the surface is found,

$$\mathcal{Z}(A)\sim A^{-\frac{Q\chi}{2\gamma}-1} \quad . \tag{3.33}$$

Finally, equating (3.27) and (3.33), the expression for the string susceptibility for a genus zero surface is retrieved. The generalization for higher genus comes from an extra dependence on the genus in the integrand shift (3.28). The general formula is given as follows[62][67]:

$$\Gamma_{str}=(1-h)\frac{D-25-\sqrt{(25-D)(1-D)}}{12}+2 \quad . \tag{3.34}$$

Due to its dependence on the dimension of the embedding space, or, equivalently, the matter field central charge, the string susceptibility plays a crucial role in determining which Matrix Model describes which type of conformal matter. At the time of the discovery of (3.34), the agreement of the formula with exact results obtained from the Matrix Model[69][70][71][72] point of view helped strengthen the validity of both approaches.

The string susceptibility is the quantity that guides the work developed in this thesis. However, it is not the only quantity that acts as a scaling law. The conformal weight of a field operator is changed after coupling (dressing) to gravity. The relationship between dressed, h, and bare, h_0, conformal weights was first extracted in the light-cone gauge[15] and later in the conformal gauge[62] formulation, through arguments similar to the ones employed in the previous derivation of the string susceptibility. The dressed conformal weight is found to be dependent on the dimension of the embedding space[62],

$$h = \frac{\sqrt{1 - D + 24h_0} - \sqrt{1 - D}}{\sqrt{25 - D} - \sqrt{1 - D}} \quad , \tag{3.35}$$

and, acting as a scaling law, it can also help determine which Matrix Model describes which type of conformal matter. We will, however, not make use of this quantity and thus refer to the original articles[15][62] for a detailed discussion.

Due to the lack of empirical evidence to support the results of quantum gravitational models, it is important that more than one approach achieves the same outcomes. Quantities such as the string susceptibility are crucial in the identification of the connection between Liouville Gravity and Matrix Models - which will be carried out in the following subsection.

3.2 Random Surfaces and Matrix Models

In the previous subsection devoted to Liouville Gravity, the computation of the integral over metrics of two-dimensional surfaces has been studied. In higher dimensions, this integral is even more difficult to evaluate[73]. Therefore, the interest in an equivalence between Liouville Gravity and Matrix Models is two-fold. First, it can ground Liouville Gravity's results in the face of absent empirical data. Second, if there is an equivalence in a $2D$ setting, there is a possibility that such an equivalence holds at higher dimensions. If so, and if a higher-dimensional "Matrix" Model - to be precise, Tensor Model - is easier to solve than its "Liouville counterpart", more results pointing toward a theory of 4DQG might be obtained. A similar situation occurs, for example, with Yang-Mills theories: calculations in the continuum and lattice simulations are different perspectives of the same problem.

Integrating over the metric is, geometrically, integrating over all possible configurations of a given surface. This can be realized by considering a zero dimensional string theory, that is, the propagation of strings in non-existent embedding space, creating a $2D$ pure worldsheet without any additional matter. This random surface can then be divided into a set of polygons, glued together, which will transform the integral over the metric into a discrete sum of the polygonal structures,

$$\int \mathcal{D}g = \lim_{continuum} \sum_{polygons} \quad . \tag{3.36}$$

These polygons can then be related to their dual graphs[74] and, using the equivalence of Statistical and Quantum Mechanics, these graphs can be dealt with like Gaussian integrals. However, in the case of QG, it is not the graphs alone that are of interest. The graphs must be promoted to maps[75][76] - in simple terms, they serve as a generalization of graphs that are aware of the topology of the surface they belong to. These maps can still be dealt with like Gaussian integrals but the integration is now performed over matrices. This is where the idea of Matrix Models stems from.

Consider the following partition function for such a zero dimensional string theory,

$$\mathcal{Z} = \sum_h \int \mathcal{D}g e^{-\beta A + \gamma\chi} \quad , \tag{3.37}$$

where the sum is performed over topologies (represented by a summation over the genus h of the surface), A is the area of the surface and χ is the Euler characteristic previously defined in (3.26) and (3.31). (Note: the coupling constants β and γ are not related to the β and γ quantities used in the previous subsection.) This partition function is reminiscent of the classical Einstein-Hilbert action (2.8).

Consider also a one degree of freedom system with a quartic interaction term,

$$Z = \int \frac{dx}{\sqrt{2\pi}} e^{-\frac{x^2}{2} + \frac{g}{4}x^4} = \sum_n \frac{g^n}{n!} \int \frac{dx}{\sqrt{2\pi}} e^{-\frac{x^2}{2}} \left(\frac{x^4}{4}\right)^n \quad . \tag{3.38}$$

From the equivalence between such quantum formulations and their statistical counterparts[77], (3.38) is known to be equivalent to a partition function that counts the number of graphs of valency 4 (4 lines leaving the vertex) and n vertices, divided out by $\Gamma(\mathcal{G})$, the automorphism of the graph (the number of ways it can be invariantly symmetrized),

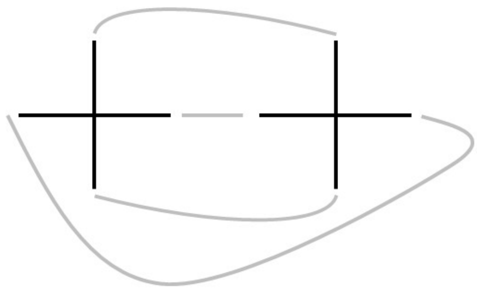

Figure 4: One possible way of connecting two vertices of valency four

$$Z = \sum_{n\, vertices\, graphs\, of\, valency\, 4} g^n \frac{1}{\Gamma(\mathcal{G})} \quad . \tag{3.39}$$

Such an equivalence can be made concrete upon adding a source to the problem:

$$\int \frac{dx}{\sqrt{2\pi}} e^{-\frac{x^2}{2}} x^{2k} = \frac{\partial^{2k}}{\partial J^{2k}} \int \frac{dx}{\sqrt{2\pi}} e^{-\frac{x^2}{2}+Jx}|_{J=0} = \frac{\partial^{2k}}{\partial J^{2k}} e^{\frac{J^2}{2}}|_{J=0} \quad . \tag{3.40}$$

The first derivative on the source pulls out a J outside the exponential, which is why only an even number of derivatives gives terms that don't vanish upon setting $J = 0$. Each pair of vertices is thus linked through lines known as the propagator, such as those seen in figure (4).

This is simply the Feynman diagrammatic approach to QFT[31]. However, such graphs are insufficient when dealing with graphs on a topological surface with arbitrary genus and a generalization to maps must be performed. For example, when choosing a certain polygon to fill out the surface, one readily knows the number of vertices and edges of the map by design; however, although in a genus zero surface the number of faces might be easy to infer, it is generally not trivial to do so in a higher genus setting. This is important in quantities such as the the Euler characteristic, (3.26), which can be related to the vertices, V, the edges E, and the faces, F, of a map,

$$\chi = V + F - E \quad . \tag{3.41}$$

To deal with this problem, graphs such as the one in figure (4) are widened into ribbons by doubling the points where the propagators link to the vertices - figure (5). With this construction, one can calculate the number of faces of a map and, combining (3.26) and (3.41), extract the genus of the map.

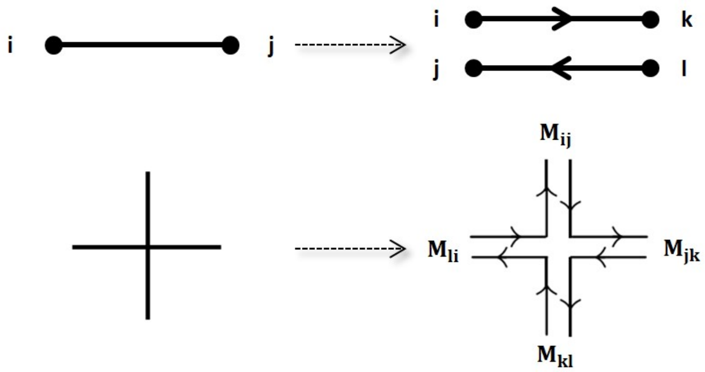

Figure 5: From propagator to ribbon, from graph to map

Figure 6: Face count of two different graphs built from a single valency-four vertex

To obtain the number of faces consider, for example, a single valency-four vertex, and two different ways of connecting it, as in figure (6). Both maps are of a single vertex. Hence, on the expansion of (3.39), both contribute with a power-one g coupling. In order to count the number of faces, one counts the closed loops of the map. Each closed loop (identified in figure (6) with a different colour) is equivalent to saying that one has N ways for the index of that loop to be chosen. Thus, the left-hand map has weight gN^3 and the right-hand map has weight gN^1. Counting the closed loops is essentially counting the number of boundaries of the faces: this is why one can extract the number of faces of each map by looking at the powers of N of each map[78]. To represent the ribbons and the extra index structure, the integration in (3.38) is upgraded from an integration over a scalar to an integration over matrices as follows:

$$Z = \int \mathcal{D}\mathcal{M} e^{-\frac{1}{2}tr(\mathcal{M}^2)+\frac{g}{4}tr(\mathcal{M}^4)} \quad . \tag{3.42}$$

The propagator is upgraded to a 4-tensor,

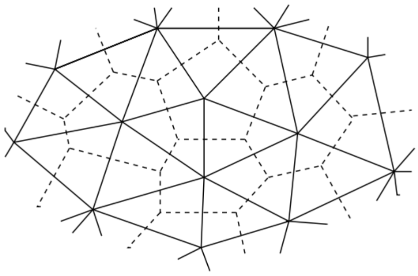

Figure 7: Random triangulation of a surface - figure taken from F. David, *Simplicial quantum gravity and random lattices*

$$\langle \mathcal{M}_{ij}\mathcal{M}_{kl}\rangle = \delta_{ik}\delta_{jl} \quad , \tag{3.43}$$

and Wick's theorem is still valid in extracting the maps created by the interaction term - such as, for example, the one in figure (5):

$$\begin{aligned} \langle tr(\mathcal{M}^4)\rangle &= \langle \mathcal{M}_{ij}\mathcal{M}_{jk}\mathcal{M}_{kl}\mathcal{M}_{li}\rangle \\ &= \langle \mathcal{M}_{ij}\mathcal{M}_{jk}\rangle\langle \mathcal{M}_{kl}\mathcal{M}_{li}\rangle + \langle \mathcal{M}_{ij}\mathcal{M}_{kl}\rangle\langle \mathcal{M}_{jk}\mathcal{M}_{li}\rangle + \langle \mathcal{M}_{ij}\mathcal{M}_{li}\rangle\langle \mathcal{M}_{jk}\mathcal{M}_{kl}\rangle \\ &= 2N^3 + N \quad . \end{aligned} \tag{3.44}$$

Many great and more detailed reviews on the combinatorial and graphical approach to quantum field theories can be found[79][75][76][80]. However, for the purposes of this thesis, these notions suffice.

Having made the transition from graphs to maps, we can now establish the contact between (3.37) and the partition function for a matrix model. To that end, the polygons with which to discretize the surface must be chosen to make a connection with the coupling constants β and γ in (3.37). While some polygons might be practically more suitable to implement, any polygon (or general mixture of polygons) can, in principle, reproduce the continuum result. It is usual to consider random triangulations of the surface, as in figure (7), taken from F. David's review on random surfaces[74]. The dashed lines are the dual complex of the discretized manifold: the dual of a triangle (or another polygon) is a point, the dual of an edge is a line segment and the dual of a vertex is a polygon.

Consider, in particular, the scenario in which all the triangles are equilateral. Then, with six triangles joined by a common vertex, this construction is intrinsically flat, as each angle, α, of each triangle is measured at $\pi/3$. To endow the surface with (Gaussian) curvature one can remove or add a certain number of triangles to the vertex: in the first case, one gains a deficit angle (positive curvature) and, in the second case, one gains an excess angle (negative curvature). The deficit angle is given simply by

$$\delta = 2\pi - \sum_i \alpha_i \quad , \tag{3.45}$$

where the sum is labelled over the triangles i sharing a common vertex v.

With this approach of fixed edge lengths, one sums over the ways of gluing together equilateral triangles with different deficit angles, counting all such configurations. A different approach could be followed. In particular, one where the edge lengths are left as variables and the overall display of the triangles with relation to one another is held fixed; one would thus set a configuration globally and sum over all the ways of creating that particular configuration. The latter is inspired by Regge calculus[81]. A striking difference between the two approaches is that the first one sums over all different manifolds created with fixed triangle edge lengths - that sum is, in general, discrete - while the second one sums over all edge lengths - naturally, a continuous sum. At the classical level, the sum over edge lengths is more suitable. However, at the quantum level, where one wants to sum over different geometries, the sum over configurations with fixed edge lengths is the most sensible[82].

In analogy with (3.42), one can write a matrix model partition function for the specific case of a triangulated surface.

$$Z = \int d\mathcal{M} e^{-\frac{1}{2}tr(\mathcal{M}^2)+\frac{g}{\sqrt{N}}tr(\mathcal{M}^3)} \tag{3.46}$$

Recall, however, that (3.46) generates both connected and disconnected surfaces, of which we want only the connected surfaces to make the identification with (3.37). Therefore, it is the free energy of the matrix model that is equivalent to the 2DQG partition function,

$$\mathcal{Z} = \ln(Z) \quad . \tag{3.47}$$

Following Di Francesco *et al.*[68], one can set the area of each triangle to be unitary. Hence, the area of the surface is given by the number of triangles or, equivalently, the number of vertices

n - the power of the coupling in the expansion of the cubic term of (3.46). Thus, one can make the identification $g = e^{-\beta}$. Furthermore, performing a change of variables $\mathcal{M} \rightarrow \mathcal{M}\sqrt{N}$, the partition function becomes (in its diagrammatic expanded form):

$$e^{\mathcal{Z}} = \sum_n \int d\mathcal{M} e^{-\frac{1}{2}Ntr(\mathcal{M}^2)} \frac{g^n}{n!} N^n (tr(\mathcal{M}^3))^n \quad . \tag{3.48}$$

With this change of variables, the power of N (previously identified as the number of indices, or equivalently the matrix size) associated to any diagram can be extracted. The propagator (edge) is given by the inverse of the quadratic term and, as such, contributes with a power N^{-1}. Due to N^n, each vertex contributes with a power N. And, as discussed after figure (6), each face contributes with a power N. Hence, each diagram carries a factor $N^{V+F-E} = N^{\chi}$. Thus, one can make the identification $N = e^{\gamma}$. At last, the formal identification between the continuum limit of the matrix model and the zero dimensional string partition function that governs 2DQG is made:

$$\mathcal{Z} = \ln \int d\mathcal{M} e^{-\frac{1}{2}Ntr(\mathcal{M}^2)+gNtr(\mathcal{M}^3)} \xrightarrow[limit]{continuum} \sum_h \int \mathcal{D}g e^{-\beta A + \gamma\chi} \quad . \tag{3.49}$$

More information can be extracted about the continuum limit of the matrix model. In the previous paragraphs, it has been established that the coupling g counts the number of vertices, V, and the matrix size N counts the number of faces, F. There is a behaviour of the following type:

$$\ln(Z) \propto g^V N^F \quad . \tag{3.50}$$

The relation between the number of vertices and edges can be defined for a fixed polygon. For example, with triangles, each edge connects two vertices and the vertices are cubic. Therefore, $V = \frac{2E}{3}$ and, from (3.41), $F = \frac{1}{2}V - (2h-2)$. Hence, one can rewrite (3.50) as the product of a term dependent on the vertices and a term dependent on the genus of the surface,

$$\ln(Z) \propto (gN^{\frac{1}{2}})^V \frac{1}{N^{2h-2}} \quad . \tag{3.51}$$

The term independent of the genus is called the 't-Hooft coupling[78], λ. The matrix model partition function (or its associated free energy) can thus be written as a sum over topologies.

For each genus, there is a term, Z_h, that gathers the contributions of all the possible maps of vertices V in surfaces of that genus,

$$Z = \sum_{h=0}^{\infty} \frac{1}{N^{2h-2}} Z_h = \sum_{h=0}^{\infty} \frac{1}{N^{2h-2}} \sum_V \lambda^V \quad . \tag{3.52}$$

Higher genus maps can be read to have a smaller contribution to the partition function. In the limit where $N \to \infty$, only the genus zero, Z_0, contribution survives. Z_0 itself can be expanded in a perturbation series in the coupling g[79], which, for large n, is given as follows,

$$Z_0(g) \sim \sum_n n^{\Gamma_{str}-3} \left(\frac{g}{g_c}\right)^n \sim (g_c - g)^{2-\Gamma_{str}} \quad , \tag{3.53}$$

and the expectation value of the area of the surface can be extracted[68] from this expansion,

$$\langle A \rangle = \langle n \rangle \sim \frac{1}{g - g_c} \quad , \tag{3.54}$$

where g_c is the critical value of the coupling at which (when $g \to g_c$) $n \to \infty$. With an infinite number of triangles/vertices, their individual areas must be sent to zero in order for the area of the (continuum) $2D$ Riemannian surface to remain finite.

The remaining $Z_h(g)$ also diverge at the same critical value of the coupling, g_c. Their large n expansion is given by[68]

$$Z_h(g) \sim \sum_n n^{(\Gamma_{str}-2)\frac{\chi}{2}-1} \left(\frac{g}{g_c}\right)^n \sim (g_c - g)^{\frac{(2-\Gamma_{str})}{2}\chi} \quad , \tag{3.55}$$

which, finally, makes the contact between the Matrix Models' continuum limit and the results for the critical exponents ((3.27), (3.34)) derived for large area partition functions in the Liouville Gravity approach. It is relevant to single out the quantity known as the critical exponent,

$$\theta = \frac{2}{2 - \Gamma_{str}} \quad , \tag{3.56}$$

which appears in the exponent of $1/(g - g_c)$ in (3.55). This will be a reoccurring quantity throughout the remainder of this thesis. In particular, for Euclidean 2DQG, it is found that[68]

$$\Gamma_{str} = -\frac{1}{2} \quad . \tag{3.57}$$

In the previous paragraphs, it has been seen how the $N \to \infty$ limit suppresses higher genus contributions to the partition function of Matrix Models. However, from the right-hand side of (3.55) and the definition of the Euler characteristic, (3.26), one can notice that when $g \to g_c$ contributions from higher genus - and, consequently, smaller χ - will give rise negative powers and, as such, larger contributions to the partition function. Higher genus contributions are suppressed as $N \to \infty$ and, in contrast, are enhanced as $g \to g_c$. This leads to the abandonment of the naive continuum limit of $N \to \infty$ in exchange for the double scaling limit, where $N \to \infty$ and $g \to g_c$ are taken together in a correlated manner, such that

$$N(g - g_c)^{-\theta} = constant \quad , \tag{3.58}$$

in order for the effects of non-spherical topologies to be taken into account[83][84]. This is the limit that is of interest, in general, to the construction of Matrix Models and, in particular, to the results obtained in the work developed in this thesis.

Several methods have been developed in order to solve the Matrix Models. It is not the purpose of this subsection to give a detailed account of the existing approaches (Di Francesco *et al.*[68] provides a good review on the subject). Naturally, the reason for the existence of an array of methods is that there is neither an easy nor a perfect one. The sum over genus (3.52) is problematic in most perturbative methods[85]. Non-perturbative methods exist - and can even obtain precise differential equations[86] - but are practically very difficult to implement. Of course, there is an advantage to the discrete (matrix) approach: even when analytical solutions are impossible or impractical to obtain, computational power can be utilized due to the large body of work on computational Statistical Mechanics - for instance, Monte Carlo methods can be applied to Matrix Models[87].

The work developed in this thesis employs the Functional Renormalization Group as the tool to study Matrix Models. We will attempt to mimic results established analytically - in particular, the critical exponents (3.56) - making use of this formalism. To do so, the Functional Renormalization Group must be introduced. We do so in the next chapter.

4 Functional Renormalization Group

The perturbative renormalizability of a theory is no longer seen as a guarantee of its UV-completion. An illustrative example is that of QED, which is simultaneously a perturbatively renormalizable theory and a UV-incomplete theory, ill-defined at arbitrarily high energies. At the same time, the perturbative non-renormalizability of a theory does not render it useless or wrong. In general, there are two ways of approaching such theories. First, valuable information may be extracted within an Effective Field Theory setting, as pointed out in [2.1]. Second, a picture larger than perturbative renormalizability may be pursued through non-perturbative approaches. The Renormalization Group (RG) approach to QFT provides one such approach. Within it, several frameworks exist. The Functional Renormalization Group (FRG) is one such framework, particularly suited to the study of several concepts previously introduced, such as UV-completion and asymptotic safety. This chapter is devoted to presenting the Functional Renormalization Group. First, the idea and process behind the RG approach to QFT, as well as some of its core concepts, are laid out. Second, the way the FRG (in particular) conveys those very concepts (and how they are of use to our work) is studied in detail.

4.1 Quantum Field Theory *à la* Wilson

In subsection (2.1), GR was treated in the setting of perturbative QFT. In that setting, divergences appear at every order of the perturbative expansion, making it necessary to introduce a set of renormalized quantities to take care of them. The divergences are, in a sense, covered by the relation between the bare and renormalized couplings. The relation is determined experimentally by matching computations in the QFT - performed at some energy scale, Λ - with experimental data. Having determined the relation, the QFT can make predictions for further experiments at energy scales below Λ. The process is then repeated for higher and higher Λ in order to access higher energy physics.

A different view of QFT, however, was proposed early on[88]. In it, the evolution of the renormalization of the bare coupling constant could be evaluated with respect to the energy scale, Λ, as the solution of a differential equation. The idea was made possible due to the introduction of ideas from Statistical Mechanics to QFT.

In the 1980's, Kenneth Wilson[17] noted that the divergences were of physical nature. The renormalized couplings have contributions from not only a single energy scale but from a range of momenta up to Λ or, conversely, a range of distances from a short distance cut-off, $a(=1/\Lambda)$, to a large macroscopic correlation length, ξ. If the short-distance cut-off is read as a lattice spacing, the connection to Statistical Mechanics arises and taking $\Lambda \to \infty$ is equivalent to taking the continuum limit, $a \to 0$, of a discretized theory, defining it at progressively smaller UV scales. Wilson then realized that for the continuum limit to exist in a QFT, the field theory must be tuned to a specific (critical) value of its couplings at which the macroscopic length, ξ, diverges, such that $\xi >> a$. Finding the regime in which ξ is divergent is, however, precisely the problem of finding a continuous phase transition in Statistical Mechanics. This viewpoint is the so called Renormalization Group approach to QFT.

This is, naturally, the idea from Statistical Mechanics that long-distance physics should not be sensitive to short-distance fluctuations. A procedure must be implemented to sum over the short distance degrees of freedom, averaging them out into a renormalized theory for the long distance degrees of freedom. The FRG is one such procedure. Before studying it, it is worth briefly mentioning Kadanoff's[89][16] block-spin transformations as they provide an intuitive picture of the idea of RG transformations in general.

4.1.1 Block-Spin Transformations

Consider the simple Ising model, defined on a square lattice with lattice spacing a; on each site, an Ising spin, s, pointing up or down (± 1) exists. The partition function is given by the sum over all possible configurations of the Ising spins, $\{s\}$,

$$Z = \sum_{\{s\}} e^{-S(s)/T} \quad , \tag{4.1}$$

where S is the action, given by the interaction of nearest neighbour spins, and T is the temperature. Now, consider a new lattice in which the lattice spacing is doubled to $2a$, as the following image indicates.

The shaded area is a cell. For each cell, $\mathcal{C}$, an effective degree of freedom is defined[77],

$$s' = \frac{\sum_{i\in\mathcal{C}} s(i)}{||\sum_{i\in\mathcal{C}} s(i)||} \quad , \tag{4.2}$$

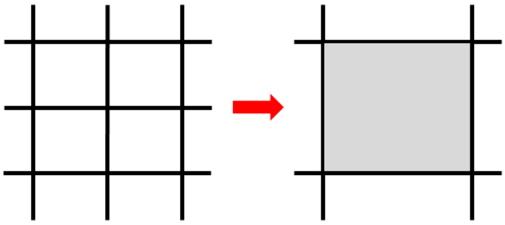

Figure 8: Coarse-graining procedure

where the sum is performed over the lattice sites of the cell $\mathcal{C}$. The number of degrees of freedom on the new lattice is half the original one. The next step is to define a block-spin transformation, $B[s', s]$, demanding that $\sum_{s'} B[s', s] = 1$[77], such that the partition function (4.1) can be rewritten as follows:

$$Z = \sum_{\{s\}} e^{-S(s)/T} = \sum_{\{s'\}} \sum_{\{s\}} B[s', s] e^{-S(s)/T} \quad . \tag{4.3}$$

The procedure gives rise to a block-spin effective action,

$$e^{-S_{eff}(s')} = \sum_{\{s\}} B[s', s] e^{-S(s)/T} \quad . \tag{4.4}$$

The new *coarse-grained* system's partition function is defined with respect to this action. The procedure is repeated until the quantities measured by the block-spin effective action stabilize. Then, the point is reached in which the effects of short (UV) distance fluctuations are so diluted that they have no impact on the long distance physics. (Naturally, since $B[s', s]$ is a technical choice, stability with respect to the block-spin transformation must also be taken into account.)

4.1.2 Beta Functions and Fixed Points 1.0

Now consider a general theory. Assume that it can be defined in terms of a set of local operators, $\mathcal{O}_\alpha$,

$$S(s) = \sum_{\alpha} u_\alpha \mathcal{O}_\alpha(s) \quad , \tag{4.5}$$

where u_α are the coupling constants. The set must be complete - that is, it is the set of all possible local operators generated under the action of the RG transformation. If it is complete, then the coarse-grained system is defined by the same set of operators,

$$S_{eff}(s') = \sum_\alpha \bar{u}_\alpha \mathcal{O}_\alpha(s') \quad , \tag{4.6}$$

where $\bar{u}_\alpha$ are the renormalized coupling constants. Having performed the coarse-graining, the couplings acquire a non-trivial scale dependence. The beta function is defined as the measurement of the rate of change of the bare couplings with respect to the change in scale,

$$\beta \equiv \frac{\bar{u}_\alpha - u_\alpha}{\ln(r)} \quad , r = \frac{a'}{a} \quad , \tag{4.7}$$

where a' is the lattice spacing after coarse-graining. Let the relationship between the bare and the renormalized coupling be given by a homogeneous scale transformation, as follows[77],

$$\bar{u}_\alpha = r^{\gamma_\alpha} u_\alpha \quad , \tag{4.8}$$

(Remember that there is freedom in the choice of block transformation, (4.3); therefore, it can be generally chosen such that (4.8) is respected.)

The Wilsonian viewpoint on the large energy limit of QFT is the identification of the limit in which the coarse-grained macroscopic length diverges, that is, $r \to \infty$. In that limit, operators can be categorized in terms of their γ_α exponent by reading (4.8). When $r \to \infty$, operators with $\gamma_\alpha < 0$ have vanishing contribution to the theory - they are appropriately named *irrelevant* operators. Operators with $\gamma_\alpha > 0$ and $\gamma_\alpha = 0$, on the other hand, contribute to the theory and are named *relevant* and *marginal* operators, respectively. Wilson[17] proposed the existence of theories that are invariant under the RG transformations. Therefore, a general renormalized theory has the form of a *fixed point* action, S^*, plus a set of relevant (and marginal) operators:

$$S = S^* + \sum_\alpha u_\alpha \int d^D x \, \mathcal{O}_\alpha(s(x)) \quad . \tag{4.9}$$

A theory defined on a fixed point retains (quantum) scale symmetry. As such, it does not depend on the UV cut-off a (or Λ) and each fixed point defines a renormalizable QFT. Before going deeper into how to reach a fixed point with RG transformations, let us introduce a specific RG transformation: the Functional Renormalization Group.

4.2 Functional Renormalization Group

We have now understood the principles of the Wilsonian RG approach to QFT. The partition function of a field theory,

$$Z = e^{-\Gamma[\phi]} = \int \mathcal{D}\phi \, e^{-S[\phi]} \quad , \tag{4.10}$$

(where $S[\phi]$ is the bare action and $\Gamma[\phi]$ is the renormalized (effective) action) is evaluated at different values of the UV cut-off, Λ, varying it as exemplified in the block-spin coarse-graining procedure, [4.1.1]. When the lattice spacing is doubled, the UV cut-off is halved, and a new action - the Wilsonian Effective Action - arises as the result of the integration over the momentum shell $[\Lambda', \Lambda]$. Performing this procedure repeatedly, the space of all possible actions - *theory space* - is covered by the RG flow.

The FRG has an additional characteristic. Instead of a variable UV cut-off parameter, Λ, an additional IR cut-off parameter, k, is introduced. The functional integral (4.10) is thus performed in the range $k < p < \Lambda$, instead of integrating over all field modes below Λ. The functional defined with this "double cut-off" is the scale-dependent *Effective Average Action* (EAA), Γ_k. In the limit $k \to \Lambda$, the EAA recovers the bare action, $\Gamma_k \to S$; in the limit, $k \to 0$, the EAA recovers the renormalized action, $\Gamma_k \to \Gamma$. This formulation is particularly advantageous as the EAA's dependence on k can be cast in the form of an exact RG flow - the *Wetterich equation*[19]. Therefore, the functional integration over momentum shells is replaced by a functional differential equation governing the change in the action with the variation of the cut-off.

We will now analyze the Effective Average Action and its underlying Wetterich equation in detail, following closely Codello[90], Reuter and Saueressig[61] and Berges, Tetradis and Wetterich[91].

4.2.1 Effective Average Action

Following Codello[90], consider the case of a single scalar field, ϕ on a manifold $\mathcal{M}$ with Riemannian metric $g_{\mu\nu}$ and a gauge connection A_μ - considered fixed external fields. The generating functional of correlation functions is defined by adding the usual auxiliary currents, J, to the partition function (4.10) as follows:

$$Z = \int \mathcal{D}_g\phi \, e^{\left(-S[\phi,A,g]+\int d^dx \, \sqrt{g}J\cdot\phi\right)} \quad . \tag{4.11}$$

Z generates connected and non-connected correlation functions. It is the free energy,

$$W = \ln(Z) \quad , \tag{4.12}$$

that generates only connected correlation functions. They are given by taking functional derivatives of W and setting the source, J, to zero:

$$\langle\phi(x_1)\,...\,\phi(x_n)\rangle_C = \frac{\delta}{\delta J(x_1)}\,...\,\frac{\delta}{\delta J(x_n)}W[J]\bigg|_{J=0} \quad . \tag{4.13}$$

The simplest of the correlation functions is the vacuum expectation value of the ϕ in the presence of the source, J, φ_J, given as follows:

$$\frac{\delta W(J)}{\delta J(x)} = \langle\phi(x)\rangle_J = \varphi_J(x) \quad . \tag{4.14}$$

The effective action, $\Gamma[\varphi]$, is a functional of φ_J, defined by obtaining $J_\varphi(\equiv J(\varphi))$ from (4.14) and taking a Legendre transformation of W, as follows:

$$\Gamma[\varphi] = \int d^dx \, \sqrt{g}J_\varphi\cdot\varphi - W[J_\varphi] \quad . \tag{4.15}$$

(It is straightforward to see that the effective action generates the current associated with the vacuum expectation value of the field, $\frac{\delta\Gamma[\varphi]}{\delta\varphi(x)} = J_\varphi(x)$.)

In order to make the generalization from the effective action to a scale-dependent effective action, an IR regulator (or cut-off) mass-like term, ΔS_k,

$$\Delta S_k[\phi,A,g] = \frac{1}{2}\int d^dx \, \sqrt{g}\,\phi R_k\phi \quad , \tag{4.16}$$

is added to the bare action, where R_k is an operator whose role is the suppression of field modes below the cut-off scale, k. The modes above the cut-off scale are integrated without suppression. In spite of freedom in the choice of R_k, its limiting behaviours are set[61],

$$\begin{aligned} \lim_{k\to 0} R_k(p^2) = 0 \quad , \\ \lim_{k\to\infty} R_k(p^2) = k^2 \quad . \end{aligned} \tag{4.17}$$

Then, (4.11) is generalized to a scale-dependent generating functional,

$$Z_k = \int \mathcal{D}_g\phi \, e^{\left(-S[\phi,A,g]-\Delta S_k[\phi,A,g]+\int d^dx\,\sqrt{g}J\cdot\phi\right)} \quad , \tag{4.18}$$

and the scale-dependent generating functional of connected correlation functions is given - in line with (4.12) - by the free energy of Z_k,

$$W_k = \ln(Z_k) \quad . \tag{4.19}$$

The *Effective Average Action* is the scale-dependent generalization of the effective action, obtained through the modified Legendre transform as follows,

$$\Gamma_k[\varphi, A, g] = \int d^dx\,\sqrt{g}J_\varphi\cdot\varphi - W_k[J_\varphi, A, g] - \Delta S_k[\varphi, A, g] \quad , \tag{4.20}$$

where J_φ is now obtained, in line with (4.14), from $\frac{\delta W_k}{\delta J} = \varphi_J$.

It is possible to cast the EAA in the form of an integro-differential equation, akin to (4.10). To do so, one can invert (4.19), $Z_k = e^{W_k}$, and isolate W_k in (4.20), plugging it in (4.18), which leads to (omission of the external fields is understood)

$$e^{-\Gamma_k[\varphi]} = \int \mathcal{D}_g\phi \, e^{-S[\phi]} e^{-\Delta S_k[\phi]+\Delta S_k[\varphi]} e^{\int d^dx\,\sqrt{g}J_\varphi\cdot(\phi-\varphi)} \quad . \tag{4.21}$$

Moreover, (4.20) can be differentiated with respect to the vacuum expectation value of the field, as follows:

$$\frac{\delta\Gamma_k}{\delta\varphi(x)}+\frac{\delta\Delta S_k}{\delta\varphi(x)}=\int d^dy\,\sqrt{g}\left(\frac{\delta J_\varphi}{\delta\varphi(x)}\varphi+J_\varphi\frac{\delta\varphi(y)}{\delta\varphi(x)}\right)-\frac{\delta W_k}{\delta\varphi(x)}\quad . \tag{4.22}$$

$\frac{\delta\varphi(y)}{\delta\varphi(x)}=\delta_{xy}$ is readily identified - δ_{xy} stands for the Kronecker delta. Furthermore, expanding $\frac{\delta W_k}{\delta\varphi(x)}=\int d^dy\,\sqrt{g}\frac{\delta W_k}{\delta J_\varphi}\frac{\delta J_\varphi}{\delta\varphi}$ and identifying $\frac{\delta W_k}{\delta J}=\varphi_J$, the first and third terms of (4.22) are seen to cancel out and one finds that (4.22) reduces to

$$\frac{\delta\Gamma_k}{\delta\varphi(x)}+\frac{\delta\Delta S_k}{\delta\varphi(x)}=\int d^dy\,\sqrt{g}J_\varphi(y)\delta_{xy}=J_\varphi(x)\quad . \tag{4.23}$$

Plugging (4.23) into (4.21) and introducing the fluctuation field, $\chi=\phi-\varphi$, the integro-differential equation for the EAA is expressed as follows:

$$e^{-\Gamma_k[\varphi]}=\int\mathcal{D}_g\chi\,e^{-S[\varphi+\chi]}e^{-\Delta S_k[\varphi+\chi]+\Delta S_k[\varphi]}e^{\int d^dx\,\sqrt{g}\left(\frac{\delta\Gamma_k[\varphi]}{\delta\varphi}+\frac{\delta\Delta S_k[\varphi]}{\delta\varphi}\right)\chi}\quad . \tag{4.24}$$

The IR regulator terms can be further rewritten by taking the following functional derivative into account,

$$\frac{\delta}{\delta\varphi}\int d^dx\,\sqrt{g}\chi\frac{\delta\Delta S_k}{\delta\varphi}\chi=\int d^dx\,\sqrt{g}\left(\frac{\delta\chi}{\delta\varphi}\frac{\delta\Delta S_k}{\delta\varphi}\chi+\chi\frac{\delta\Delta S_k}{\delta\varphi}\frac{\delta\chi}{\delta\varphi}+\chi\frac{\delta^2\Delta S_k}{\delta\varphi^2}\chi\right)\quad . \tag{4.25}$$

Notice that, by definition of the fluctuation field, $\frac{\delta\chi}{\delta\varphi}=-1$. Furthermore, in the small fluctuation limit, one can approximate derivatives with differences,

$$\frac{\Delta S_k[\varphi+\chi]-\Delta S_k[\varphi]}{\chi}=\frac{\delta\Delta S_k[\varphi]}{\delta\chi}=\frac{\delta\Delta S_k[\varphi]}{\delta\varphi}\frac{\delta\varphi}{\delta\chi}\to-\Delta S_k[\varphi+\chi]+\Delta S_k[\varphi]=\chi\frac{\delta\Delta S_k[\varphi]}{\delta\varphi}\,. \tag{4.26}$$

With these two ingredients, the IR regulator terms in (4.24) are rewritten as follows:

$$-\Delta S_k[\varphi+\chi]+\Delta S_k[\varphi]+\int d^dx\,\sqrt{g}\frac{\delta\Delta S_k[\varphi]}{\delta\varphi}\chi=-\frac{1}{2}\int d^dx\,\sqrt{g}\chi\frac{\delta^2\Delta S_k[\varphi]}{\delta\varphi^2}\chi\quad . \tag{4.27}$$

By definition, (4.16) is quadratic in the field, ϕ, and, as such, it is also quadratic in φ. Therefore, differentiating twice with respect to φ will eliminate the field dependence and leave only the R_k operator, that is, $-\frac{1}{2}\int d^dx\,\sqrt{g}\chi\frac{\delta^2\Delta S_k[\varphi]}{\delta\varphi^2}\chi = -\frac{1}{2}\int d^dx\,\sqrt{g}\chi R_k\chi = -\Delta S_k[\chi]$. The final form of the integro-differential equation satisfied by the EAA is achieved,

$$e^{-\Gamma_k[\varphi]} = \int \mathcal{D}_g\chi\, e^{-S[\varphi+\chi]-\Delta S_k[\chi]+\int d^dx\,\sqrt{g}\frac{\delta\Gamma_k[\varphi]}{\delta\varphi}\chi} \quad . \tag{4.28}$$

As previously stated, the IR regulator term suppresses modes below the cut-off scale, $p^2 < k^2$, and leaves modes above the cut-off scale, $p^2 > k^2$, unaffected. Let us analyze the two limiting cases, (4.17), $k \to \infty$ ($p^2 << k^2$) and $k \to 0$ ($p^2 >> k^2$). $R_k \to 0$ when $p^2 >> k^2$; therefore, $\Delta S_k[\chi]$ vanishes from (4.28) and the integro-differential equation satisfied by the EAA, (4.28), reduces to the one satisfied by the effective action in the IR limit,

$$\lim_{k\to 0}\Gamma_k[\varphi, A, g] = \Gamma[\varphi, A, g] \quad . \tag{4.29}$$

Low momentum modes are suppressed by the IR regulator. (Notice that, due to the negative sign accompanying ΔS_k in (4.28), $\Delta S_k > 0$.) The simplest cut-off operator would be $R_k = k^2$ for $p^2 << k^2$. In general, the IR regulator behaves as[61] $Ck^2\int d^dx\,\sqrt{g}\chi^2$ in the $k \to \infty$ limit, where C is a constant dependent on the cut-off operator chosen. Using a redefinition of the fluctuation field, $\chi \to \chi/\sqrt{C}k$, and noticing, from (4.16), that $\Delta S_k[\chi/\sqrt{C}k] = \Delta S_k[\chi]/Ck^2$, (4.28) can be rewritten as follows:

$$e^{-\Gamma_K[\varphi]} = \int \mathcal{D}_g\chi\, e^{-S[\varphi+\chi/\sqrt{C}k]}e^{-\Delta S_k[\chi]/Ck^2}e^{\frac{1}{\sqrt{C}k}\int d^dx\,\sqrt{g}\frac{\delta\Gamma_k}{\delta\varphi}\chi} \quad . \tag{4.30}$$

When $k \to \infty$, the third exponential vanishes (assuming the current stays finite). Moreover, $\chi/\sqrt{C}k \to 0$, leading (4.30) to

$$e^{-\Gamma_k[\varphi]} \xrightarrow[k\to\infty]{} e^{-S[\varphi]}\int \mathcal{D}_g\chi\, e^{-\Delta S_k[\chi]/Ck^2} = e^{-S[\varphi]}\int \mathcal{D}_g\chi\, e^{-\int d^dx\,\sqrt{g}\chi^2} \quad . \tag{4.31}$$

The remaining functional integral is Gaussian and is thus equal to a constant. The integro-differential equation satisfied by the EAA, (4.28), reduces to the bare action in the UV limit,

$$\lim_{k\to\infty}\Gamma_k[\varphi, A, g] = S[\varphi, A, g] \quad . \tag{4.32}$$

We have thus demonstrated, as previously stated, that the EAA interpolates between the effective (renormalized) action in the IR limit and the bare action in the UV limit.

4.2.2 Wetterich Equation

Following Codello[90], consider φ to be a multiplet of fields, whose components are labeled by $(i, j, ...)$. To obtain the differential equation governing the scale dependence of the EAA, consider the differentiation of (4.24) with respect to the RG "time" parameter,

$$t = \ln k/k_0 \quad , \tag{4.33}$$

where k_0 is an arbitrary scale:

$$e^{-\Gamma_k}\partial_t\Gamma_k = \int \mathcal{D}_g\chi \left[-\partial_t\Delta S_k + \int d^dx\,\sqrt{g}\left(\partial_t\frac{\delta\Gamma_k}{\delta\varphi_i}\right)\chi_i\right] e^{-S-\Delta S_k+\int d^dx\,\sqrt{g}\frac{\delta\Gamma_k}{\delta\varphi}\chi} \quad . \tag{4.34}$$

By definition, the expectation value of an operator O is given as follows:

$$\langle O[\phi]\rangle = \frac{1}{Z}\int \mathcal{D}_g\chi\; O[\chi]e^{-S[\varphi+\chi]-\Delta S_k[\chi]+\int d^dx\,\sqrt{g}\frac{\delta\Gamma_k[\varphi]}{\delta\varphi_i}\chi_i} \quad . \tag{4.35}$$

Therefore, (4.34) can be rewritten as

$$\partial_t\Gamma_k[\varphi] = -\langle\partial_t\Delta S_k[\chi]\rangle + \int d^dx\,\sqrt{g}\partial_t\frac{\delta\Gamma_k[\varphi]}{\delta\varphi_i}\langle\chi_i\rangle \quad . \tag{4.36}$$

By construction, $\langle\chi_i\rangle = 0$, since it is a quantum fluctuation. Then,

$$\partial_t\Gamma_k[\varphi] = \frac{1}{2}\int d^dx\,\sqrt{g}\langle\chi_i\chi_j\rangle\partial_t R_{k_{ij}} \quad , \tag{4.37}$$

where the symmetry of the cut-off operator in the indices i and j was used[90]. The relationship between the non-connected and connected two-point correlation functions is given generically by $\langle\phi_i\phi_j\rangle = \langle\phi_i\phi_j\rangle_C + \langle\phi_i\rangle\langle\phi_j\rangle$. Given the vanishing vacuum expectation value of the fluctuation field, $\langle\chi_i\rangle = 0$, $\langle\chi_i\chi_j\rangle$ in (4.37) can be taken to be the connected one. Furthermore, from (4.13),

$\langle \chi_i \chi_j \rangle = \frac{\delta^2 W_k[J]}{\delta J(x_i) \delta J(x_j)}$. Moreover, there is a general inverse proportionality relation between the Hessian of the connected piece generating functional and the Hessian of the effective action:

$$\begin{aligned} \frac{\delta W[J]}{\delta J(x_i)} &= \varphi(x_i) \to \frac{\delta^2 W[J]}{\delta J(x_i) \delta J(x_j)} = \frac{\delta \varphi(x_i)}{\delta J(x_j)} \quad , \\ \frac{\delta \Gamma[\varphi]}{\delta \varphi(x_j)} &= J(x_j) \to \frac{\delta^2 \Gamma[\varphi]}{\delta \varphi(x_i) \delta \varphi(x_j)} = \frac{\delta J(x_j)}{\delta \varphi(x_i)} \quad . \end{aligned} \tag{4.38}$$

Therefore, from the definition of the Legendre transformation of the EAA, (4.20),

$$\langle \chi_i \chi_j \rangle = \frac{\delta^2 W_k[J]}{\delta J(x_i) \delta J(x_j)} = \left(\frac{\delta^2 \left(\Gamma_k[\varphi] + \Delta S_k[\varphi] \right)}{\delta \varphi_i \delta \varphi_j} \right)^{-1} = \left(\frac{\delta^2 \Gamma_k[\varphi]}{\delta \varphi_i \delta \varphi_j} + R_{k_{ij}} \right)^{-1} \quad . \tag{4.39}$$

Plugging (4.39) into (4.37), the *Wetterich equation* is obtained,

$$\partial_t \Gamma_k[\varphi] = \frac{1}{2} \mathrm{Tr} \left[\left(\frac{\delta^2 \Gamma_k[\varphi]}{\delta \varphi^2} + R_k \right)^{-1} \partial_t R_k \right] \quad , \tag{4.40}$$

where Tr is a functional trace, condensing the integration over space-time, $\int d^d x \sqrt{g}$, the trace over the space-time indices and the trace over the internal symmetry indices.

4.2.3 Beta Functions and Fixed Points 2.0

As done in (4.5) and (4.6), $\Gamma_k[\varphi]$ may be expanded in a basis of functionals, $\{\mathcal{O}_\alpha\}$, as follows[92]:

$$\Gamma_k[\varphi] = \sum_{\alpha=1}^{\infty} \bar{u}_\alpha \mathcal{O}_\alpha[\varphi] \quad . \tag{4.41}$$

Inserting (4.41) into (4.40), the scale dependence of the dimensionful (renormalized) couplings, $\partial_t \bar{u}_\alpha$, can be extracted. From the right-hand side of (4.40), it is readily identified that each $\partial_t \bar{u}_\alpha$ depends, in general, on all $\{\bar{u}_\alpha, \alpha = 1, 2, ...\}$. As such, a system of infinitely many coupled differential equation for the dimensionful couplings arises. Therefore, in practice, truncations to (4.41) must be applied in order for results to be extracted.

However, we are interested in finding fixed points. It is the dimensionless (bare) couplings, u_α, that tend to a constant, u^*_α, at a fixed point[93]. Indeed, from the relationship between dimensionful and dimensionless couplings,

$$\bar{u}_\alpha = k^{d_\alpha} u_\alpha \quad , \tag{4.42}$$

where d_α is the canonical mass dimension of $\bar{u}_\alpha$, one can read that the dimensionful couplings keep running with k, $\bar{u}_\alpha = u^*_\alpha k^{d_\alpha}$, at a fixed point. We are thus interested, in particular, in the dimensionless couplings. (In a standard QFT, couplings can be related to physically measurable quantities, such as cross sections, and it is the dimensionless ratio of couplings that must remain finite in such scattering processes[93][94].) Therefore, the beta functions are defined by the dimensionless scale derivatives (it can be read as a "continuous framework upgrade" of (4.7)):

$$\partial_t u_\alpha = \beta_\alpha(u_1, u_2, ...) \quad . \tag{4.43}$$

From the very definition of the beta function, a fixed point is obtained simply by finding the values of the (dimensionless) couplings at which all beta functions vanish,

$$\beta_\alpha|_{\vec{u}=\vec{u}^*} = 0, \quad \forall \alpha \quad . \tag{4.44}$$

Let us now finish the discussion we halted in [4.1.2]. As stated in [2.3], the fixed point of the Asymptotic Safety Scenario is a Non-Gaussian Fixed Point (NGFP), one in which there is at least one non-vanishing coordinate, u^*_α. Knowing the coordinates of the NGFP and the scale evolution of the couplings, an RG flow that emanates from the (UV) fixed point towards the IR is defined. That flow defines an asymptotically safe theory, that is, a renormalizable QFT. The set of points in theory space that are pulled into the NGFP by the inverse RG flow is the critical hypersurface[92], $\mathcal{S}_{UV}$. Around the fixed point, the beta functions can be linearized, resulting in a linear differential equation for each coupling,

$$\beta_\alpha = \beta_\alpha|_{\vec{u}=\vec{u}^*} + \sum_\sigma \left.\frac{\partial \beta_\alpha}{\partial u_\sigma}\right|_{\vec{u}=\vec{u}^*} (u_\sigma - u^*_\sigma) = \sum_\sigma \left.\frac{\partial \beta_\alpha}{\partial u_\sigma}\right|_{\vec{u}=\vec{u}^*} (u_\sigma - u^*_\sigma) \quad , \tag{4.45}$$

and the solution to (4.45) is given as follows,

$$u_\alpha(k) = u_\alpha^* + \sum_I C^I V_\alpha^I \left(\frac{k}{k_0}\right)^{-\theta_I} \quad , \tag{4.46}$$

where k_0 is the scale at which the generic trajectory enters the linearized regime, C^I are the constants of integration, V_α^I are the eigenvectors of the stability matrix, $\frac{\partial \beta_\alpha}{\partial u_\sigma}\Big|_{\vec{u}=\vec{u}^*}$, and $-\theta_I$ are the eigenvalues of the stability matrix.

In principle, infinitely many C_I must be known in order for a generic trajectory to be determined. However, some conditions arise from the existence of a UV fixed point[95]. As the RG flow is taken to the IR - $k/k_0 \to 0$ - eigenvectors with $\theta_I < 0$ have vanishing contribution to the values of the couplings. The directions defined by these eigenvectors are the *irrelevant* directions we mentioned previously in [4.1.2]. As $k \to \infty$ and $\mathcal{S}_{UV}$ is approached, the parameters C^I corresponding to irrelevant directions - $\theta_I < 0$ - are accordingly set to zero, ensuring that u_α tends to a constant. Conversely, eigenvectors with $\theta_I > 0$ lend a growing contribution to the values of the couplings as the flow is taken to the IR. The associated C^I are thus called *relevant*. RG flows on $\mathcal{S}_{UV}$ are determined solely by the relevant directions, reducing the number of free parameters, C^I, from an infinite (non-predictive) to a finite (predictive) one.

Lastly, let us mention that the critical exponents, θ_I, are universal quantities, as they characterize the universality class a system belongs to when certain parameters are tuned to their critical values. This means they are independent of FRG artifacts, such as the choice of regulator. Naturally, since truncations must be applied to theory space in order for calculations to be carried out, the stability of the critical exponent with respect to the regulator is a good indicator of the results' quality. On the other hand, the coordinates of the fixed points are not universal. Therefore, our focus is the calculation of the critical exponents when applying the procedure generically discussed in the last few pages to Matrix Models.

5 FRG and Matrix Models

Having introduced the FRG formalism for the evaluation of the RG flows of a QFT, this chapter is devoted to the implementation of the FRG to Matrix Models. As discussed previously, Matrix Models reproduce Liouville Gravity. In applying the FRG to Matrix Models, we attempt to mimic the results for the critical exponents known from exact calculations. To do so, this chapter begins by outlining the differences between the FRG in a standard QFT setting and the FRG in the framework of a Matrix Model. After doing so, we proceed with the calculations. The work developed in this thesis and, in particular, in this chapter, is directly influenced by the article by Eichhorn and Koslowski from 2013[20] which, inspired by previous works[96][97] dedicated to the RG analysis of Matrix Models, builds the tools necessary to an FRG analysis of Matrix Models.

5.1 The Absence of a Standard Scale

A kinetic operator is an essential part in the Lagrangian of a standard QFT. A Matrix Model, such as (3.42) or (3.46), is substantially different from a standard QFT in that regard: it has no kinetic operator (or it can be said to be trivial). As such, it has no fundamental notion of momentum (or energy) scale and therefore of RG flow. Without it, there is no standard canonical mass dimension to govern the change in the couplings under scale transformations, (4.42), and the Wetterich equation, (4.40), cannot be evaluated as formulated in [4.2.2].

In essence, there is no fundamental identification of IR and UV. The identification can, however, be implemented by hand, utilizing the indices of the $N \times N$ matrices as a scale. The simplest way to do so is to define the upper-left corner of the matrices, with indices below a cut-off scale, as IR and, conversely, the lower-right corner of the matrices as UV. Therefore, the matrix size works as the scale, expressed in the RG "time" parameter, (4.33), now written as $t = \ln N$. The cut-off is introduced via an IR regulator identical to the one introduced in (4.16),

$$\Delta S_N[\phi] = \frac{1}{2}\phi_{ab} R_N^{abcd}(a,b)\phi_{cd} \quad , \tag{5.1}$$

where the latin indices refer to the matrix entries. Similarly to (4.28), matrix entries in the "IR" block, $a, b < N$, are suppressed whereas entries in "UV" block, $a, b > N$, are integrated out unaffectedly. The arguments follow in line with those presented in [4.2.2] and the Wetterich equation, (4.40), is formally the same,

$$\partial_t \Gamma_N = \frac{1}{2} Tr \left[\left(\Gamma_N^{(2)} + R_N \right)^{-1} \partial_t R_N \right] \quad , \tag{5.2}$$

with $k \to N$ and the trace now only over the matrix entries. $\delta^2 \Gamma_N / \delta \phi^2$ was abbreviated to $\Gamma_N^{(2)}$.

Despite the absence of a fundamental energy scale with respect to which the scaling of couplings can be evaluated, the couplings do have an inherent dimensionality that determines their scaling with N. In the continuum space-time limit, $N \to \infty$, this inherent N-dimensionality can be said to give rise to the standard canonical mass dimension. Consider an effective average action comprised of single-trace terms,

$$\Gamma_N = \frac{Z_N}{2} Tr\left(\phi^2\right) + \sum_i \bar{g}_i Tr\left(\phi^i\right) \quad , \tag{5.3}$$

where Z_N is a renormalization factor. To extract the N-dimensionality of the couplings, the argument used in [3.2] (around (3.48)) in order to connect the matrix model, (3.46), with 2DQG, (3.37), is utilized. The fields are rescaled, $\phi \to \sqrt{N}\phi$, and the $MM \equiv 2DQG$ connection is made. Furthermore, performing a second rescaling, $\phi \to \phi/\sqrt{Z_N}$, in order to set the kinetic term to its canonical coefficient, 1/2, (5.3) is rewritten as follows,

$$\Gamma_N = N \left(\frac{1}{2} Tr\left(\phi^2\right) + \sum_i \bar{g}_i N^{\frac{i-2}{2}} Z_N^{-i/2} Tr\left(\phi^i\right) \right) \quad , \tag{5.4}$$

and the N-dimensionality of the couplings is expressed in the relationship between their dimensionless and dimensionful counterparts:

$$g_i = \bar{g}_i \frac{N^{\frac{i-2}{2}}}{Z_N^{i/2}} \quad . \tag{5.5}$$

Accordingly, the beta functions have two terms next to the quantum fluctuations are taken into account: the canonical term and the anomalous term (due to the running of the renormalization factor),

$$\beta_{g_i} = \frac{i-2}{2} g_i + \frac{i}{2}\eta g_i + (...) \quad , \tag{5.6}$$

where (...) refers to quantum fluctuation terms and η is known as the anomalous dimension,

$$\eta = -\partial_t \ln Z_N \quad . \tag{5.7}$$

Let us make two more comments on the N-dimensionality of the couplings. The aim is to find NGFPs of the FRG flows with the matrix size, N, that correspond to the double scaling limit, (3.58), where $N \to \infty$ and one (and only one) coupling is tuned to its critical value, $g \to g_c$. The first condition is another way of fixing the couplings' N-dimensionality, since it requires that the N-dimensionality is such that all beta functions are $1/N$-expandable (in order for the limit $N \to \infty$ to be taken). The second condition means that only NGFPs with one (and only one) relevant critical exponent are of interest in this case. Quantum fluctuations work as a push toward/away from relevance. From (5.5), one can read that the most relevant coupling for a single-trace action, g_4, is irrelevant before quantum fluctuations are taken into account, since it has negative N-dimensionality, -1. Hence, quantum fluctuations must shift this coupling (and only this one) into relevance. Let us now see how to obtain the quantum fluctuations by solving the Wetterich equation, (5.2), for the case of a Euclidean (single-)matrix model.

5.2 Hermitian Matrix Model

The starting point for the work to be developed from now on is the single-trace action, (5.3), where we additionally restrict the analysis to even powers of the matrix, ϕ,

$$\Gamma_N = \frac{Z_N}{2} Tr\left(\phi^2\right) + \sum_i \bar{g}_{2i} Tr\left(\phi^{2i}\right) \quad . \tag{5.8}$$

Therefore, aside from the $U(N)$ symmetry of the model, there is an additional Z_2 symmetry, as it is invariant under $\phi \to -\phi$. The Wetterich flow generates infinitely many operators compatible with the model's symmetries. Naturally, it also generates operators beyond the original theory space since the presence of the IR regulator breaks the $U(N)$ symmetry due to the introduction of a mass-like term to the functional generator below N. We will only consider single-trace operators allowed by the original symmetry, as indicated by the second term on the right-hand side of (5.8).

5.2.1 Flow Setup

The setup considered here is the one put forth in Eichhorn and Koslowski's work[20]. The matrix, ϕ, is considered to be Hermitian (which corresponds to the case of orientable Feynman diagrams, [3.2]). Therefore, one can take advantage of its decomposition into a real symmetric matrix, A - $A_{ab} = A_{ba}$ - and a real anti-symmetric matrix, B - $B_{ab} = -B_{ba}$:

$$\phi_{ab} = A_{ab} + iB_{ab} \quad . \tag{5.9}$$

Another appropriate decomposition is employed. In order to evaluate the Wetterich equation, (5.2), the $\mathcal{P}^{-1}\mathcal{F}$ expansion is used, in which the inverse regularized propagator is split as follows,

$$\Gamma_N^{(2)} + R_N = \mathcal{P}_N + \mathcal{F}_N \quad , \tag{5.10}$$

where $\mathcal{P}_N$ is the (field-independent) inverse propagator and $\mathcal{F}_N$ is the fluctuation matrix, gathering all field-dependent contributions. Plugging it into (5.2), the $\mathcal{P}^{-1}\mathcal{F}$ expansion is readily obtained by expanding the geometric series, as follows:

$$\begin{aligned} \partial_t \Gamma_N &= \frac{1}{2}\mathrm{Tr}\left[(\Gamma_N^{(2)} + R_N)^{-1}\partial_t R_N\right] \\ &= \frac{1}{2}\mathrm{Tr}\left[\left(\mathbf{1} - \left(-\mathcal{P}_N^{-1}\mathcal{F}_N\right)\right)^{-1}\left(\partial_t R_N\right)\mathcal{P}_N^{-1}\right] \\ &= \frac{1}{2}\mathrm{Tr}\left[\left(\partial_t R_N\right)\mathcal{P}_N^{-1} + \sum_{n=1}^{\infty}(-1)^n\left(\partial_t R_N\right)\mathcal{P}_N^{-1}\left(\mathcal{F}_N\mathcal{P}_N^{-1}\right)^n\right] \end{aligned} \quad . \tag{5.11}$$

Let us take a more detailed look at the derivation of (5.11), explicitly taking into account the Hermitian decomposition, (5.9). According to it, $\Gamma_N^{(2)}$ takes the form of a matrix of matrices:

$$\Gamma_N^{(2)} = \begin{pmatrix} \Gamma_{(AA)}^{(2)} & \Gamma_{(AB)}^{(2)} \\ \Gamma_{(BA)}^{(2)} & \Gamma_{(BB)}^{(2)} \end{pmatrix} \quad . \tag{5.12}$$

Since $\Gamma_{(AB)}^{(2)}$ and $\Gamma_{(BA)}^{(2)}$ contain only terms with odd powers of B, they vanish due to the anti-symmetry of B[20] (see [B] for an illustrative example). This diagonal structure facilitates calculations.

The components of the propagator for the matrix modes can be obtained considering the quadratic term of (5.8), $\Gamma_N^{quad} = \frac{Z_N}{2}\mathrm{Tr}(\phi^2)$. Upon plugging the Hermitian decomposition, (5.9), into it, $\Gamma_N^{quad} = \frac{Z_N}{2}\left(\mathrm{Tr}(A^2) - \mathrm{Tr}(B^2)\right)$. Given the derivatives,

$$\begin{aligned} \frac{\delta}{\delta A_{ab}} A_{cd} &= \frac{1}{2}\left(\delta_{ad}\delta_{bc} + \delta_{ac}\delta_{bd}\right) \quad , \\ \frac{\delta}{\delta B_{ab}} B_{cd} &= -\frac{1}{2}\left(\delta_{ad}\delta_{bc} - \delta_{ac}\delta_{bd}\right) \quad , \end{aligned} \tag{5.13}$$

it follows directly that:

$$\begin{aligned} \frac{\delta^2 \Gamma_N^{quad}}{\delta A_{ab}\delta A_{cd}} &= \frac{Z_N}{2}\left(\delta_{ad}\delta_{bc} + \delta_{ac}\delta_{bd}\right) \quad \equiv Z_N \mathbf{1}^{sym}_{abcd}, \\ \frac{\delta^2 \Gamma_N^{quad}}{\delta B_{ab}\delta B_{cd}} &= -\frac{Z_N}{2}\left(\delta_{ad}\delta_{bc} - \delta_{ac}\delta_{bd}\right) \quad \equiv Z_N \mathbf{1}^{asym}_{abcd}, \\ \frac{\delta^2 \Gamma_N^{quad}}{\delta A_{ab}\delta B_{cd}} &= \frac{\delta^2 \Gamma_N^{quad}}{\delta B_{ab}\delta A_{cd}} = 0 \quad . \end{aligned} \tag{5.14}$$

The regulator components are chosen as follows,

$$\begin{aligned} R^{(A)}_{N_{abcd}} &= Z_N \mathbf{1}^{sym}_{abcd}\mathcal{R}_N(a,b,c,d) \quad , \\ R^{(B)}_{N_{abcd}} &= Z_N \mathbf{1}^{asym}_{abcd}\mathcal{R}_N(a,b,c,d) \quad , \end{aligned} \tag{5.15}$$

where $\mathcal{R}_N(a,b,c,d)$ is the cut-off function. (The terminology of (5.12) has been (and will, from now on, be) abbreviated from (AA) and (BB) to (A) and (B), respectively, since there is no ambiguity with the mixed matrix modes, (AB) or (BA) - as they vanish.) Therefore, from (5.10), $\mathcal{P}_{\mathcal{N}} = \frac{\delta^2\Gamma_N^{quad}}{\delta\phi^2} + R_N$, and the form of the propagators for the two matrix modes comes readily as follows:

$$\begin{aligned} \mathcal{P}^{-1}_{(A)_{abcd}} &= \frac{1}{Z_N(1+\mathcal{R}_N(a,b,c,d))}\mathbf{1}^{sym}_{abcd} \quad , \\ \mathcal{P}^{-1}_{(B)_{abcd}} &= \frac{1}{Z_N(1+\mathcal{R}_N(a,b,c,d))}\mathbf{1}^{asym}_{abcd} \quad . \end{aligned} \tag{5.16}$$

Having defined these structures, the right-hand side of (5.2) can be expanded. Firstly,

$$\Gamma_N^{(2)} + R_N = \begin{pmatrix} \Gamma^{(2)}_{(AA)} & 0 \\ 0 & \Gamma^{(2)}_{(BB)} \end{pmatrix} + \begin{pmatrix} R_N^{(A)} & 0 \\ 0 & R_N^{(B)} \end{pmatrix} = \begin{pmatrix} \mathcal{P}_{(A)} & 0 \\ 0 & \mathcal{P}_{(B)} \end{pmatrix} + \begin{pmatrix} \mathcal{F}_{(A)} & 0 \\ 0 & \mathcal{F}_{(B)} \end{pmatrix} \quad , \tag{5.17}$$

and, consequently,

$$\left(\Gamma_N^{(2)} + R_N\right)^{-1} = \left(\begin{pmatrix} \mathcal{P}_{(A)} & 0 \\ 0 & \mathcal{P}_{(B)} \end{pmatrix} \left[\mathbf{1} + \begin{pmatrix} \mathcal{P}^{-1}_{(A)} & 0 \\ 0 & \mathcal{P}^{-1}_{(B)} \end{pmatrix} \begin{pmatrix} \mathcal{F}_{(A)} & 0 \\ 0 & \mathcal{F}_{(B)} \end{pmatrix} \right] \right)^{-1} \quad . \tag{5.18}$$

Therefore,

$$\partial_t \Gamma_N = \frac{1}{2} \mathrm{Tr} \left\{ \left[\mathbf{1} - (-1) \begin{pmatrix} \mathcal{P}^{-1}_{(A)} \mathcal{F}_{(A)} & 0 \\ 0 & \mathcal{P}^{-1}_{(B)} \mathcal{F}_{(B)} \end{pmatrix} \right]^{-1} \begin{pmatrix} \mathcal{P}^{-1}_{(A)} & 0 \\ 0 & \mathcal{P}^{-1}_{(B)} \end{pmatrix} \begin{pmatrix} \partial_t R_N^{(A)} & 0 \\ 0 & \partial_t R_N^{(B)} \end{pmatrix} \right\} , \tag{5.19}$$

which, upon identifying the geometric series, becomes

$$\begin{aligned} \partial_t \Gamma_N &= \frac{1}{2} \mathrm{Tr} \left\{ \sum_n (-1)^n \begin{pmatrix} \mathcal{P}^{-1}_{(A)} \mathcal{F}_{(A)} & 0 \\ 0 & \mathcal{P}^{-1}_{(B)} \mathcal{F}_{(B)} \end{pmatrix}^n \begin{pmatrix} \mathcal{P}^{-1}_{(A)} & 0 \\ 0 & \mathcal{P}^{-1}_{(B)} \end{pmatrix} \begin{pmatrix} \partial_t R_N^{(A)} & 0 \\ 0 & \partial_t R_N^{(B)} \end{pmatrix} \right\} \\ &= \frac{1}{2} \left\{ \mathrm{tr} \left(\mathcal{P}^{-1}_{(A/B)} \partial_t R_N^{(A/B)} \right) - \mathrm{tr} \left(\mathcal{P}^{-1}_{(A/B)} \mathcal{F}_{(A/B)} \mathcal{P}^{-1}_{(A/B)} \partial_t R_N^{(A/B)} \right) + (...) \right\} \quad , \end{aligned} \tag{5.20}$$

where $\left(\mathcal{P}^{-1}_{(A/B)} \partial_t R_N^{(A/B)}\right)$ abbreviates $\left(\mathcal{P}^{-1}_{(A)} \partial_t R_N^{(A)}\right) + \left(\mathcal{P}^{-1}_{(B)} \partial_t R_N^{(B)}\right)$ - and equivalently for the remaining terms of the expansion.

It is now clearer how to proceed with the evaluation of the flow equation. $\mathcal{F}_{(A)}$ and $\mathcal{F}_{(B)}$ are, schematically, of the form $\sum_i \bar{g}_{2i} \mathcal{F}^{(2i)}_{(A)/(B)}$. For example, upon derivation, ϕ^4 terms feedback into the running of ϕ^2 terms at order $n = 1$ - that is, the beta function of Z_N depends on g_4; at order $n = 2$, they contribute to the running of $(\phi^2)^2 = \phi^4$ - that is, the beta function of g_4 depends on g_4^2; and so on.

Naturally, it is impossible to obtain results for the complete infinite-dimensional theory space. In practice, the action must be truncated. Once a truncation of Γ_N is chosen, it is possible to know the highest order of n of interest for the beta functions. Stability of the results with respect to the truncation is one of the key ingredients in evaluating the quality of the results. We call these ingredients spurious in the sense that they are mathematical artifacts upon which the results for the critical exponents should depend as lightly as possible. Two others of such ingredients exist. One is the subspace on which the matrices are projected (after the derivations). In the present thesis, we begin by employing the same projection scheme of the original article[20], in which we project onto a subspace of purely symmetric diagonal matrices,

$$\begin{aligned} A_{ab} &= a\delta_{ab} \quad , \\ B_{ab} &= 0 \quad , \end{aligned} \tag{5.21}$$

where δ_{ab} is the Kronecker delta. The other is the cut-off function, $\mathcal{R}_N$, introduced above, (5.15). We choose it to be slightly different from the one used in the original article[20],

$$\mathcal{R}_N(a,b,c,d) = \left(\frac{(2N)^r}{a^r+b^r} - 1\right)\Theta\left(1 - \frac{a^r+b^r}{(2N)^r}\right) \quad , \tag{5.22}$$

where r is a real parameter and Θ is the Heaviside step function,

$$\Theta(x) = \begin{cases} 1, & x > 0 \\ 0, & x < 0 \end{cases} \quad . \tag{5.23}$$

The exact critical exponent for Euclidean 2DQG is known[68]; from (3.56) and (3.57),

$$\theta_{MM} = \frac{4}{5} \quad . \tag{5.24}$$

In the work[20] that inspires this thesis, despite good accuracy of the critical exponent for very simple truncations, it was reported that there existed a barrier, $\theta = 1$, below which it was impossible to break for the chosen regulator/projection scheme, regardless of the truncation size. We attempt to optimize this result. We do so by allowing the r parameter in the cut-off function, (5.22), to vary as a real number, and see whether the barrier can be broken.

The procedure is, in essence, a simple one, despite possibly lengthy mathematics in performing the flow equation derivatives. The quantum fluctuation terms are obtained and added to the theory's beta functions, (5.6); then, a set of fixed points, (4.44) is derived, from which the one(s) corresponding to the double scaling limit, (3.58), are chosen; then, the linearized regime of the beta functions, (4.45), around the fixed point is studied, and the stability matrix is diagonalized in order to extract its eigenvalues, (4.46), from which the critical exponents, (3.56), are readily obtained.

Presenting the full derivation of all the terms in all the beta functions would originate many and long pages. We refrain from doing so and point to appendix [B] where the extraction of a few terms is exemplified - the process is similar for all of them. All terms in the beta functions can be generically written as follows,

$$\partial_t g_{2i} \propto \left[(-1)^n \frac{1}{2} \times (2i) \times c \times \zeta(p,r)\right] (g_{2j}...g_{2l}) \quad , \tag{5.25}$$

where $(-1)^n \frac{1}{2}$ comes from the Wetterich equation itself, (5.20), $2i$ comes from the left-hand side of the Wetterich equation, $\partial_t (g_{2i}/2i)$, c is a numerical coefficient coming from the $\mathcal{F}_N$ derivatives and $\zeta(r)$ is the contribution from the trace,

$$\frac{1}{Z_N^{p-1}} \zeta(p,r) = \sum_{a,b} (\mathcal{P}_N^{-1})^p (\partial_t R_N) \quad , \tag{5.26}$$

where $p = n+1$. Notice that, due to the projection scheme, (5.21), $\mathcal{F}_N$ does not contribute to the summation.

In practice, as in the original work[20], we approximate the sum by an integral - which is valid to leading order in $1/N$ - whose limits are set by the Heaviside function of the cut-off function. Notice that

$$\partial_t = \frac{\partial}{\partial \ln N} = \frac{\partial N}{\partial \ln N} \frac{\partial}{\partial N} = \left(\frac{1}{N}\right)^{-1} \frac{\partial}{\partial N} \quad , \tag{5.27}$$

and, consequently,

$$\begin{aligned} \partial_t \left[\frac{(2N)^r}{a^r + b^r}\right] &= r \frac{(2N)^r}{a^r + b^r} \quad , \\ \partial_t \left[\Theta\left(1 - \frac{a^r + b^r}{(2N)^r}\right)\right] &= p \frac{a^r + b^r}{(2N)^r} \delta\left(1 - \frac{a^r + b^r}{(2N)^r}\right) \quad . \end{aligned} \tag{5.28}$$

Therefore, one can write down the derivative,

$$
\partial_t \left(Z_N \mathcal{R}_N(a,b,c,d)\right) = \left[(\partial_t Z_N)\left(\frac{(2N)^r}{a^r+b^r}-1\right) + Z_N r \frac{(2N)^r}{a^r+b^r}\right] \Theta\left(1-\frac{a^r+b^r}{(2N)^r}\right) + Z_N \left(\frac{(2N)^r}{a^r+b^r}-1\right)\delta\left(1-\frac{a^r+b^r}{(2N)^r}\right) \quad , \tag{5.29}
$$

and, consequently, the integral $\zeta(r)$ is defined (notice that the δ term in (5.29) vanishes upon integration):

$$
\begin{aligned}
\zeta(p,r,\eta) &= \frac{1}{Z_N}\int_0^{2N} db \int_0^{((2N)^r-b^r)^{\frac{1}{r}}} da \left\{ \frac{1}{\left(\frac{(2N)^r}{a^r+b^r}\right)^p} \left[\partial_t Z_N \left(\frac{2N}{a+b}-1\right) + Z_N \frac{2N}{a+b}\right\}\right] \\
&= \frac{1}{N^2}\int_0^{2N} db \int_0^{((2N)^r-b^r)^{\frac{1}{r}}} da \left\{ \left[\frac{a^r+b^r}{(2N)^r}\right]^{p-1} (-\eta + r) + \eta \left[\frac{a^r+b^r}{(2N)^r}\right]^p \right\} \quad .
\end{aligned} \tag{5.30}
$$

The integrals can be solved numerically for each p. For all p, they return a conditional expression for $r > 0$.

5.2.2 Flow Analysis: r-dependence

The smallest truncation,

$$
\Gamma_N = \frac{Z_N}{2}\mathrm{Tr}(\phi^2) + \frac{\bar{g}_4}{4}\mathrm{Tr}(\phi^4) \quad , \tag{5.31}
$$

is simple enough that analytical expressions for the critical exponents can be found for a generic r, which give a good preview of their r-dependence for larger truncations. The beta functions are given as follows:

$$
\eta = 2 g_4 \zeta(2,r,\eta) \quad , \tag{5.32}
$$

$$
\beta_{g_4} = (1+2\eta) g_4 + 4 g_4^2 \zeta(3,r,\eta) \quad . \tag{5.33}
$$

Aside from the trivial Gaussian fixed point ($g_4^* = 0$), there are two NGFPs,

$$g_4^* = \frac{-10u - 8v - 8ur - 12vr \pm \sqrt{-32uvr + (10u + 8v + 8ur + 12vr)^2}}{16uvr} \quad , \tag{5.34}$$

where u and v are given by the following expressions,

$$\begin{aligned} u &= \frac{2^{1-\frac{2}{r}}\sqrt{\pi}\Gamma[\frac{1}{r}]}{r(1+r)\Gamma_f[\frac{3}{2}+\frac{1}{r}]} \quad , \\ v &= \frac{2^{1-\frac{2}{r}}\sqrt{\pi}r\Gamma_f[1+\frac{1}{r}]}{(2+3r)(1+r)\Gamma_f[\frac{1}{2}+\frac{1}{r}]} \quad , \end{aligned} \tag{5.35}$$

where $\Gamma_f[x]$ is the gamma function.

The critical exponents are obtained via (4.46). Their limiting behaviours are clearly distinct. Let θ_{NGFP1} be the critical exponent related to the $-\surd$ solution of (5.34) and θ_{NGFP2} be the one related to the $+\surd$ solution of (5.34). Then,

$$\begin{aligned} \lim_{r\to+\infty} \theta_{NGFP1} &= +\infty \quad , \\ \lim_{r\to+\infty} \theta_{NGFP2} &= 1 \quad , \end{aligned} \tag{5.36}$$

and, at $r = 1$,

$$\begin{aligned} \theta_{NGFP1}(r=1) &= 16.137 \quad , \\ \theta_{NGFP2}(r=1) &= 1.066 \quad . \end{aligned} \tag{5.37}$$

At $r < 1$, θ_{NGFP2} grows away from its value at $r = 1$. On the other hand, θ_{NGFP1} tends to a smaller value than the one it holds at $r = 1$. However, it does not do so fast enough and it does not get sufficiently close to (5.24) before numerical issues arise from the proximity of $r = 0$. Hence, it is θ_{NGFP2} that is closer to matching (5.24). Its value at $r = 1$ is, indeed, the one reported in the original article[20]. However, the problem stands with regards to the $\theta = 1$ barrier.

We proceed by enlarging the truncation up to $\bar{g}_{12}$, to determine whether a combination of high r parameter and larger truncations can break the barrier. The beta functions are given as follows (the anomalous dimension, (5.32), stands unaltered):

$$\beta_{g_4} = (1+2\eta)g_4 + 4\left(-g_6\zeta(2,r,\eta) + g_4^2\zeta(3,r,\eta)\right) \quad , \tag{5.38}$$

$$\beta_{g_6} = (2+3\eta)g_6 + 6\left(-g_8\zeta(2,r,\eta) + 2g_4g_6\zeta(3,r,\eta) - g_4^3\zeta(4,r,\eta)\right) \quad , \tag{5.39}$$

$$\beta_{g_8} = (3+4\eta)+8\left(-g_{10}\zeta(2,r,\eta) + \left(g_6^2 + 2g_8g_4\right)\zeta(3,r,\eta) - 3g_4^2g_6\zeta(4,r,\eta) + g_4^4\zeta(5,r,\eta)\right) \quad , \tag{5.40}$$

$$\begin{aligned}\beta_{g_{10}} = (4+5\eta) + 10\Big(&- g_{12}\zeta(2,r,\eta) + \left(2g_4g_{10} + 2g_6g_8\right)\zeta(3,r,\eta) \\ &- \left(3g_4^2g_8 + 3g_4g_6^2\right)\zeta(4,r,\eta) + 4g_4^3g_6\zeta(5,r,\eta) - g_4^5\zeta(6,r,\eta)\Big) \quad ,\end{aligned} \tag{5.41}$$

$$\begin{aligned}\beta_{g12} = (5+6\eta) + 12\Big(&\left(2g_4g_{12} + 2g_6g_{10} + g_8^2\right)\zeta(3,r,\eta) - \left(g_6^3 + 3g_4^2g_{10} + 6g_4g_6g_8\right)\zeta(4,r,\eta) \\ &+ (6g_4^2g_6^2 + 4g_4^3g_8)\zeta(5,r,\eta) - 5g_4^4g_6\zeta(6,r,\eta) + g_4^6\zeta(7,r,\eta)\Big) \; .\end{aligned} \tag{5.42}$$

In the following plots, we report the evolution of the critical exponent's relevant direction, θ, with growing r, in the range $r \in [1, 10]$ for four growing truncations: $\{\phi^2, \phi^4, \phi^6\}$ ($n = 3$), $\{\phi^2, \phi^4, \phi^6, \phi^8\}$ ($n = 4$), $\{\phi^2, \phi^4, \phi^6, \phi^8, \phi^{10}\}$ ($n = 5$) and $\{\phi^2, \phi^4, \phi^6, \phi^8, \phi^{10}, \phi^{12}\}$ ($n = 6$), respectively. In the table that follows the graphs, we report, in particular, on the value for $r = 1000$.

As noted in the original article[20], the difference in the critical exponent's relevant direction between subsequent truncation orders, n, becomes smaller in every step. Therefore, an extrapolation of $n \to \infty$ yields $\theta \to 1$. We observe that the same happens between subsequent values of the r parameter - this is quite clear in figures (9), (10), (11) and (12). Combined with the analytical functions of r obtained for the $\{\phi^2, \phi^4\}$ truncation, this constitutes evidence that an extrapolation of $r \to \infty$ also yields $\theta \to 1$. The $\theta = 1$ barrier cannot be resolved by the new cut-off function, (5.22), for positive r. Despite that, the new regulator shows itself useful. Notice, for example, that, with $r = 10$, the smallest truncation's critical exponent's relevant direction is already closer to the exact value, (5.24), than the critical exponent reported in the original article for the truncation up to ϕ^{14} - $\theta = 1.022$. Calculations for $\{\phi^2, \phi^4\}$ with $r = 10$ are much simpler than the ones necessary for larger truncations, even at $r = 1$. This points to a practical advantage of (5.22) over its "predecessor"[20].

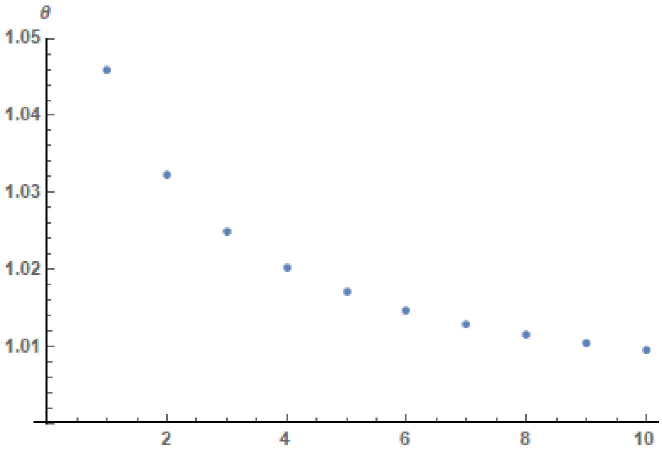

Figure 9: $\theta(r)$ in the $n = 3$ truncation

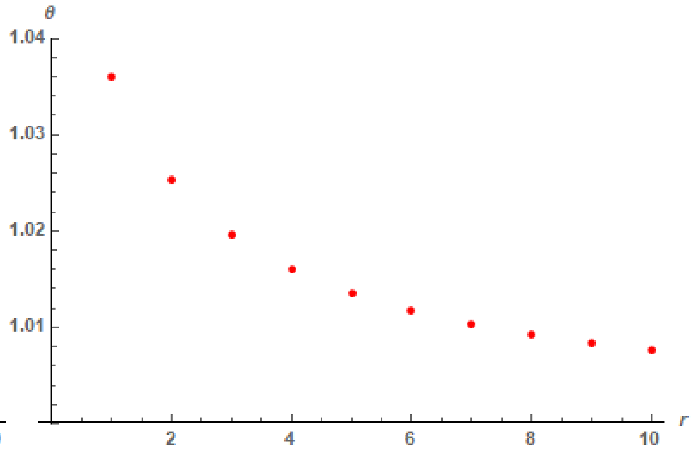

Figure 10: $\theta(r)$ in the $n = 4$ truncation

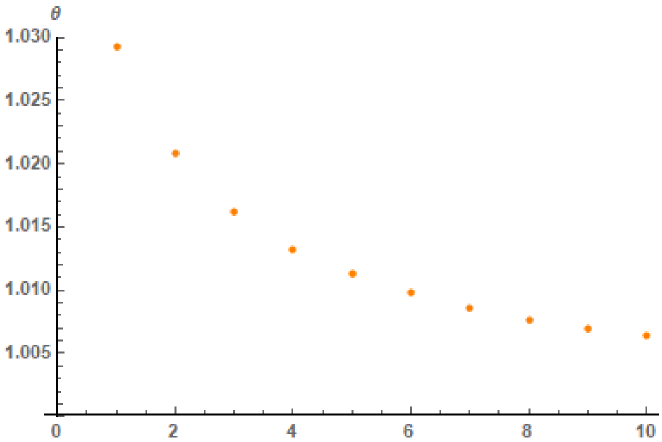

Figure 11: $\theta(r)$ in the $n = 5$ truncation

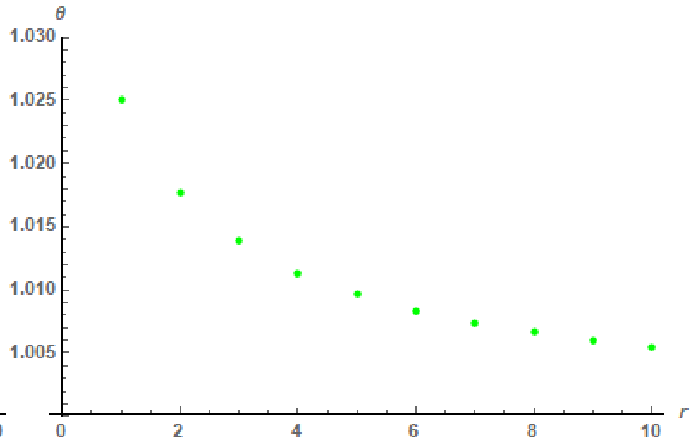

Figure 12: $\theta(r)$ in the $n = 6$ truncation

Truncation	r=1	r=10	r=1000
$\{\phi^2, \phi^4\}$	1.066	1.0131	1.00015
$\{\phi^2, \phi^4, \phi^6\}$	1.046	1.0096	1.00011
$\{\phi^2, \phi^4, \phi^6, \phi^8\}$	1.036	1.0076	1.00009
$\{\phi^2, \phi^4, \phi^6, \phi^8, \phi^{10}\}$	1.029	1.0064	1.00007
$\{\phi^2, \phi^4, \phi^6, \phi^8, \phi^{10}, \phi^{12}\}$	1.025	1.0060	1.00005

Table 1: Critical exponent: evolution with growing r and truncation

5.2.3 Flow Analysis: Negative r

The integrals, (5.30), return conditional expressions for $r > 0$. In the previous analysis we have restricted to this regime. However, within it, it is not possible to resolve the $\theta = 1$ barrier problem. Therefore, we decide to perform an "analytic continuation" of the integrals to negative r values.

To do so, it is important to note that the first integral, $\int da$, returns a conditional expression for $r > -1/p$ (which was irrelevant in the previous subsection since $r > 0$). Moreover, the integrals up to $p = 7$ (equivalently, ϕ^{10}) return an expression $\sim \frac{1}{1+r}$. For $p = 2$, there is also an $r = 0$ pole. We should thus be careful with the singularities and ill-behaved points in the range $r \in [-1, 0]$ as they can spoil the results.

We start, once again, by analyzing the smallest truncation, (5.31), with its two NGFPs, (5.34). Because we have an analytical expression for r, we can set their respective critical exponents to 0.8 and see which value of r respects the equality. The following r values are found,

$$\begin{aligned} \theta_{NGFP1} &= 0.8 \rightarrow r \approx -1.063 \quad , \\ \theta_{NGFP2} &= 0.8 \rightarrow r \approx -2.133 \quad , \end{aligned} \tag{5.43}$$

which do occur outside the $[-1, 0]$ regime. However, it is noted that slightly below $r = -1$, the r-dependence is quite unstable and the values - and even the nature - of the critical exponents change rapidly. For instance, while at $r \approx -1.063$, θ_{NGFP1} describes the double scaling limit accurately and is equal to (5.24), at $r \approx -1.08$, θ_{NGFP1} is not even a real quantity. The proximity to the $r = -1$ singularity might still have an unwanted effect on the critical exponents, such that we disregard this value of r.

The limiting behaviours of both critical exponents are, once again, quite distinct. At $r \approx -1.7$, θ_{NGFP1} becomes real but negative. From then on, it grows in magnitude and thus never goes back to a positive regime. θ_{NGFP2} grows toward an asymptotic behaviour, similar to that of its positive r evolution:

$$\begin{aligned} \lim_{r \to -\infty} \theta_{NGFP1} &= -\infty \quad , \\ \lim_{r \to -\infty} \theta_{NGFP2} &= 1 \quad , \end{aligned} \tag{5.44}$$

The points made in the previous paragraphs bring our focus to the $r^* \approx -2.133$ value of the r parameter, in which we have successfully broken the $\theta = 1$ barrier and obtained a single NGFP suitable for the double scaling limit that matches the exact critical exponent, (5.24), for the simplest truncation, (5.31). We now expand the truncation order step by step in order to evaluate the stability of the results.

For the $\{\phi^2, \phi^4, \phi^6\}$ truncation, the $r \in (-2, -1]$ range is notable for the absence of NGFPs between $r \approx -1.17$ and $r \approx -1.93$. From $r \approx -1.93$ down, they do exist and their qualitative structure is stable. Specifically, we find a set of two NGFPs, one with two relevant directions, $\vec{\theta}_{NGFP1}$, and one with a single relevant direction, $\vec{\theta}_{NGFP2}$. At $r = -2.133$, we find them to be given as follows:

$$\begin{aligned} \vec{\theta}_{NGFP1} &= (1.093,\ 0.686) \quad , \\ \vec{\theta}_{NGFP2} &= (0.818,\ -0.681) \quad . \end{aligned} \tag{5.45}$$

Their limiting behaviours are distinct: $\vec{\theta}_{NGFP1}$ grows up to an asymptotic value with increasing r and is thus never a suitable double scaling limit candidate for negative r; $\vec{\theta}_{NGFP2}$ reaches the $\theta = 1$ barrier from below once again for $r \to -\infty$:

$$\begin{aligned} \lim_{r \to -\infty} \vec{\theta}_{NGFP1} &= (2,\ 1) \quad , \\ \lim_{r \to -\infty} \vec{\theta}_{NGFP2} &= (1,\ -1) \quad . \end{aligned} \tag{5.46}$$

We should note that the limiting behaviours of (5.46) - and of subsequent truncation orders - are not computed analytically but rather inferred by taking very large values of r, as large as 10000000, perhaps one or two orders of magnitude below (depending on whether numerical accuracy can be obtained for such a high r value).

Therefore, as for the smallest truncation, we find only one critical exponent, $\vec{\theta}_{NGFP2}$, suitable to describe the double scaling limit. Moreover, remarkable numerical proximity to (5.24) is found. Naturally, it does not precisely equal 0.8 since $r \approx -2.133$ was specifically fine-tuned for $\{\phi^2, \phi^4\}$. We can do the same fine-tuning for $\{\phi^2, \phi^4, \phi^6\}$ and find that $\theta = 0.8$ at $r^* \approx -2.087$. The proximity to $r^* \approx -2.133$ inspires us to keep expanding the truncation.

For the $\{\phi^2, \phi^4, \phi^6, \phi^8\}$ truncation, NGFPs are once again absent between $r \approx -1.29$ and $r \approx -1.82$. At $r = -2.133$, we find the following set of fixed points,

$$
\begin{aligned}
\vec{\theta}_{NGFP1} &= (0.481 - 8.516i,\ 0.481 + 8.516i,\ -2.387) \quad , \\
\vec{\theta}_{NGFP2} &= (1.597,\ 0.764,\ 0.523) \quad , \\
\vec{\theta}_{NGFP3} &= (1.255,\ 0.713,\ -0.437) \quad , \\
\vec{\theta}_{NGFP4} &= (-1.344,\ 0.833,\ -0.770) \quad ,
\end{aligned}
\tag{5.47}
$$

where $\vec{\theta}_{NGFP4}$ is identified as the one and only suitable candidate for the double scaling limit. Like in the smaller truncation orders, the qualitative behaviour of the NGFPs is stable for $r < -2$. $\vec{\theta}_{NGFP1}$, in its generic form $(a - bi, a + bi, -c)$, stable throughout $r < -2$, appears to have a, b and c grow unrestrictedly as $r \to -\infty$. The real critical exponents exhibit the following asymptotic behaviours,

$$
\begin{aligned}
\lim_{r\to-\infty} \vec{\theta}_{NGFP2} &= (3,\ 2,\ 1) \quad , \\
\lim_{r\to-\infty} \vec{\theta}_{NGFP3} &= (2,\ 1,\ -1) \quad , \\
\lim_{r\to-\infty} \vec{\theta}_{NGFP4} &= (-2,\ 1,\ -1) \quad ,
\end{aligned}
\tag{5.48}
$$

in line with the two smaller truncation orders. The fine-tuned value of r for $\{\phi^2, \phi^4, \phi^6, \phi^8\}$ occurs at $r^* \approx -2.062$.

For the $\{\phi^2, \phi^4, \phi^6, \phi^8, \phi^{10}\}$ truncation, NGFPs are absent between $r \approx -1.39$ and $r \approx -1.99$. At $r = 2.133$, the set of fixed points is given as follows,

$$
\begin{aligned}
\vec{\theta}_{NGFP1} &= (1.371,\ -0.917,\ 0.737,\ -0.579) \quad , \\
\vec{\theta}_{NGFP2} &= (-2.113,\ -1.374,\ -0.858,\ 0.845) \quad ,
\end{aligned}
\tag{5.49}
$$

where only two NGFPs appear. The number of NGFPs varies within (roughly) $r \approx -2$ and $r \approx -4$ between two and four NGFPs. However, as r grows in magnitude, it stabilizes at four NGFPs. Their limiting behaviours are in line with the smaller truncation orders' results:

$$
\begin{aligned}
\lim_{r\to-\infty} \vec{\theta}_{NGFP1} &= (4,\ 3,\ 2,\ 1) \quad , \\
\lim_{r\to-\infty} \vec{\theta}_{NGFP1} &= (3,\ 2,\ 1,\ -1) \quad , \\
\lim_{r\to-\infty} \vec{\theta}_{NGFP3} &= (2,\ -2,\ 1,\ -1) \quad , \\
\lim_{r\to-\infty} \vec{\theta}_{NGFP4} &= (-3,\ -2,\ -1,\ 1) \quad .
\end{aligned} \tag{5.50}
$$

The fine-tuned value of r continues to exhibit good stability: $\theta = 0.8$ occurs for $r^* \approx -2.048$.

For the $\{\phi^2, \phi^4, \phi^6, \phi^8, \phi^{10}, \phi^{12}\}$ truncation, NGFPs are absent between $r \approx -1.47$ and $r \approx -1.87$. The number of NGFPs once again fluctuates until it stabilizes for slightly larger magnitudes of r - roughly between $r \approx -3$ and $r \approx -10$ - at six NGFPs. At $r = -2.133$,

$$
\begin{aligned}
\vec{\theta}_{NGFP1} &= (3.460 - 11.652i,\ 3.459 + 11.652i,\ -0.634 - 7.045i,\ -0.634 + 7.045i,\ -1.967) \quad , \\
\vec{\theta}_{NGFP2} &= (2.274,\ 1.206,\ 0.648,\ -0.343,\ -0.201) \quad , \\
\vec{\theta}_{NGFP3} &= (-1.479,\ 1.459,\ -1.165,\ 0.727,\ -0.612) \quad , \\
\vec{\theta}_{NGFP4} &= (-2.912,\ -2.024,\ -1.647,\ 0.849,\ -0.818) \quad .
\end{aligned} \tag{5.51}
$$

The stability of the single critical exponent suitable for the double scaling limit remains noteworthy. The fine-tuned value of r at which $\theta = 0.8$ occurs for $r^* \approx -2.042$.

It is difficult to infer the limiting behaviour of the critical exponents as numerical accuracy issues arise at relatively low values of r. For example, at $r = 100$, the number of NGFPs drops to three and, at $r = 1000$, it is already reduced to two.

The stability of the r value that leads to the exact double scaling limit with growing truncation order is quite relevant. We can, however, identify a pattern: as the truncation order grows, the r^* value that corresponds to $\theta = 0.8$ grows (slightly) toward zero. Furthermore, the difference between values of r^* of subsequent truncation orders becomes smaller in every step, as can be seen in (13).

This points to the existence of an asymptotic behaviour or r^* at arbitrarily high truncation order, n. We conjecture that this asymptotic behaviour occurs at a value of r^* before it reaches -2. Indeed, for all the truncation orders presented above, we have noticed that, for $r = -2$, there is always a single critical exponent suitable for the double scaling limit whose relevant direction

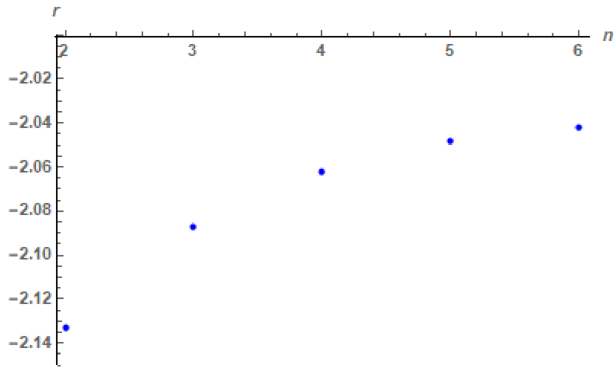

Figure 13: Evolution of the fine-tuned r parameter, r^*, with respect to the truncation order, n

remains the same from $\{\phi^2, \phi^4\}$ to $\{\phi^2, \phi^4, \phi^6, \phi^8, \phi^{10}, \phi^{12}\}$: $\theta(r=-2) = \frac{3}{4}$. There is no indication that this behaviour should change at higher truncation orders. Therefore, we conjecture that, for arbitrarily high truncation order, one can always find a parameter $r^* \in (-2.133, -2)$ that leads to $\theta = 0.8$. This points to a remarkable stability of r^*. Furthermore, it points to the fact that r^* is always above the undesired range of singularities and ill-behaved r points mentioned previously.

5.2.4 Flow Analysis: Multi-Trace Terms

As made explicit in appendices [B] and [C], the theory space is not just composed of single-trace terms. For instance, (B.8) and (B.9) show that g_4 contributes to the running coupling associated to $\mathrm{Tr}^2(\phi)$. Multi-trace terms of the form $\mathrm{Tr}(\phi^i)...\mathrm{Tr}(\phi^l)$, with i and l even powers, are allowed by the original symmetry of the model. Therefore, they must be considered alongside single-trace terms in the process of filling out the theory space.

Herein, we consider only double-trace terms, $\mathrm{Tr}(\phi^i)\mathrm{Tr}(\phi^j)$. With the addition of one trace, the N-dependence of the beta functions is altered. In accordance, the canonical N-dimensionality, (5.5), assigned to such terms must be altered in order to respect the $1/N$-expandability of the beta functions. A simple possibility is the assignment of an additional $1/N$ factor for each additional trace[20], immediately cancelling the N factor introduced by the additional trace,

$$g_{i,j} = \bar{g}_{i,j} \frac{N^{\frac{i+j}{2}}}{Z_N^{\frac{i+j}{2}}} \quad . \tag{5.52}$$

altering (5.6) accordingly. As pointed out by Eichhorn and Koslowski[20], terms with $n-1$ traces are generated from terms with n traces of the form $\mathrm{Tr}(\phi^2)\mathrm{Tr}(\phi^i)...\mathrm{Tr}(\phi^j)$. Therefore, $\mathrm{Tr}(\phi^2)\mathrm{Tr}(\phi^i)$

terms couple directly to β_{g_i}. We thus consider a truncation - $\{\phi^2, \phi^4, \phi^6, \phi^2\phi^2, \phi^2\phi^4\}$ - including the terms that couple directly up to g_4: the two double-trace terms that couple directly to η and β_{g_4}, $g_{2,2}$ and $g_{2,4}$, respectively, and g_6,

$$\Gamma_N = \frac{Z_N}{2}\mathrm{Tr}(\phi^2) + \frac{\bar{g}_4}{4}\mathrm{Tr}(\phi^4) + \frac{\bar{g}_6}{6}\mathrm{Tr}(\phi^6) + \frac{\bar{g}_{2,2}}{4}\mathrm{Tr}(\phi^2)\mathrm{Tr}(\phi^2) + \frac{\bar{g}_{2,4}}{2}\mathrm{Tr}(\phi^2)\mathrm{Tr}(\phi^4) \quad . \tag{5.53}$$

The beta functions read

$$\eta = (2g_4 + g_{2,2})\zeta(2, r, \eta) \quad , \tag{5.54}$$

$$\beta_{g_4} = (1 + 2\eta)g_4 - (4g_6 + 2g_{2,4})\,\zeta(2, r, \eta) + 4g_4^2\zeta(3, r, \eta) \quad , \tag{5.55}$$

$$\beta_{g_6} = (2 + 3\eta)g_6 + 6\left(2g_4g_6\zeta(3, r, \eta) - g_4^3\zeta(4, r, \eta)\right) \quad , \tag{5.56}$$

$$\beta_{g_{2,2}} = (2 + 2\eta)g_{2,2} - (8g_{2,4} + 2g_6)\zeta(2, r, \eta) + (6g_4^2 + 2g_{2,2}^2 + 8g_4g_{2,2})\zeta(3, r, \eta) \quad , \tag{5.57}$$

$$\begin{aligned}\beta_{g_{2,4}} = (3 + 3\eta)g_{2,4} + (12g_4g_6 + 4g_{2,2}g_6 + 12g_4g_{2,4} + 2g_{2,2}g_{2,4})\zeta(3, r, \eta)& \\ - (12g_4^3 - 6g_4^2g_{2,2})\zeta(4, r, \eta).&\end{aligned} \tag{5.58}$$

For $r = 1$, three NGFPs that can describe the double scaling limit are found:

$$\begin{aligned}\vec{\theta}_{NGFP1} &= (77.268,\ -49.896,\ -30.604,\ -2.250) \quad , \\ \vec{\theta}_{NGFP2} &= (16.983,\ -14.983,\ -9.655,\ -5.328) \quad , \\ \vec{\theta}_{NGFP3} &= (1.219,\ -1.883,\ -1.008,\ -0.685) \quad .\end{aligned} \tag{5.59}$$

$\vec{\theta}_{NGFP3}$ is the critical exponent indicated by Eichhorn and Koslowski[20]. Indeed, if we let r vary as a positive number, the relevant directions of $\vec{\theta}_{NGFP1}$ and $\vec{\theta}_{NGFP2}$ are found to increase. Therefore, for all $r > 0$, there are three NGFPs with (only) one relevant direction but only one of them is sufficiently close to (5.24).

This truncation behaves qualitatively similar to the single-trace truncations with respect to the positive r evolution, as shown in figure (14). However, the value of θ is higher, for $r = 1$, than that of any one of the single-trace truncations evaluated previously. Therefore, a much larger

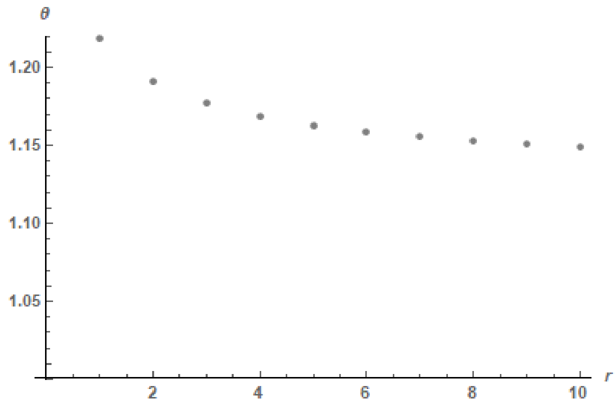

Figure 14: r-dependence of θ in the $\{\phi^2, \phi^4, \phi^6, \phi^2\phi^2, \phi^2\phi^4\}$ truncation

value of r is needed for $\theta \to 1$. In fact, it takes such a large value of r that numerical accuracy issues arise before that limit can be realized. For example, at $r = 20000$, the critical exponent is still relatively high, $\theta = 1.13$, when compared to the results of the single-trace truncations.

We can perform an analysis similar to that of [5.2.3]. For our reference r value, $r = -2.133$, there are two NGFPs suitable to describe the double scaling limit,

$$\begin{aligned} \vec{\theta}_{NGFP1} &= (319.594,\ -269192.008,\ -19035.228,\ -10.609) \quad , \\ \vec{\theta}_{NGFP2} &= (0.863,\ -1.668,\ -1.002,\ -0.679) \quad . \end{aligned} \tag{5.60}$$

Remarkably, $\vec{\theta}_{NGFP2}$ sits very close to the exact value, (5.24). At $r = -2$ we find the following results,

$$\begin{aligned} \vec{\theta}_{NGFP1} &= \left(1,\ -\frac{3}{2},\ -1,\ -\frac{1}{2}\right) \quad , \\ \vec{\theta}_{NGFP2} &= \left(\frac{3}{4},\ -\frac{3}{2},\ -1,\ -\frac{1}{2}\right) \quad , \end{aligned} \tag{5.61}$$

where we recognize $\theta(r = -2) = \frac{3}{4}$, the value found for all the single-trace truncations examined in [5.2.3]. Moreover, it is found that the relevant direction of $\vec{\theta}_{NGFP1}$ grows extremely fast with growing r magnitude (notice, for example, the change from $r = -2$ to $r = -2.133$, (5.61) $\to$ (5.60)). Therefore, it is $\vec{\theta}_{NGFP2}$ that is closer to (5.24) for $r < -2$. The fine-tuned value, r^*, at which the relevant direction of $\vec{\theta}_{NGFP2}$ matches (5.24) is found at $r^* \approx -2.042$, once again pointing to a good stability of r^*. If truncations with more multi-trace terms are found to have an r^* in the vicinity, $r^* \in (-2.133, -2)$, and the $\theta(r = -2)$ behaviour is replicated, then it would be safe to say that the form of the cut-off function, (5.22), with $r = r^*$, is not accidental.

5.2.5 Flow Analysis: Anti-Symmetric Projection

In order to evaluate the stability of the results with respect to the projection scheme, we adopt a projection scheme opposite to (5.21) in which we project onto a subspace of purely anti-symmetric matrices:

$$\begin{aligned} A_{ab} &= 0 \quad , \\ B_{ab} &= a\varepsilon_{N_{ab}} \quad , \end{aligned} \tag{5.62}$$

where $\boldsymbol{\varepsilon_N}$ is a block-diagonal matrix, built from the $2D$ Levi-Civita symbol, $\boldsymbol{\varepsilon}$,

$$\boldsymbol{\varepsilon_N} = \begin{pmatrix} \varepsilon & 0 & \cdots \\ 0 & \varepsilon & \cdots \\ \vdots & \vdots & \ddots \end{pmatrix} , \quad \boldsymbol{\varepsilon} = \begin{pmatrix} 0 & 1 \\ -1 & 0 \end{pmatrix} \quad . \tag{5.63}$$

The relationship between the Levi-Civita symbol and the Kronecker delta,

$$\varepsilon_{ij}\varepsilon_{kl} = \begin{vmatrix} \delta_{ik} & \delta_{il} \\ \delta_{jk} & \delta_{jl} \end{vmatrix} = \delta_{ik}\delta_{jl} - \delta_{il}\delta_{jk} \quad , \tag{5.64}$$

is useful in the derivation of the beta functions. Notice, from the Wetterich equation, (5.20), that the change of projection only affects the $\mathcal{F}_N$ functional derivatives. Therefore, it only changes the c coefficient in the generic form of the beta functions, (5.25). In appendix [C], we zoom in on the terms derived in appendix [B] under the new projection scheme as an example of the changes that come about in the derivation of the beta functions.

We have concluded that the beta functions remain unaltered with respect to their form, (5.32) and (5.38)-(5.42), in the symmetric projection, (5.21). The main point is that the c coefficient in (5.25) remains the same whether a symmetric, (5.21) or an anti-symmetric, (5.62), projection is employed. While this statement was verified only up to g_{12} order in the single-trace truncation, the consistent behaviour of the $1/N$ expansion - as exemplified in the two terms derived in appendix [C] - serves as an indication that the equivalence between symmetric and anti-symmetric projection should hold at higher - presumably arbitrary - order.

6 Conclusion and Outlook

The goal of this thesis was the optimization of the procedure[20] of the application of the FRG formalism to Matrix Models describing $2D$ Euclidean (pure) Gravity. In the original article[20], interesting numerical accuracy was found with small truncations. However, a barrier was found for the value of the relevant critical exponent, $\theta = 1$, below which it was not possible to break, regardless of the effective action's truncation size. It was important to resolve this issue, since the exact value of θ lies below 1, specifically at $4/5$. Furthermore, only one matrix projection scheme was tested. It was also important to test the effect of a different projection scheme on the results.

We have been able to go beyond the $\theta = 1$ barrier by introducing a new cut-off function, inspired by the one utilized in the original article, with an additional variable r parameter. For positive r, both the single-trace [5.2.2] and the multi-trace [5.2.4] truncations were unable to break the $\theta = 1$ barrier. The behaviour of the critical exponents with growing r was found to be qualitatively identical to their behaviour with growing truncation order, n. However, relatively small values of r are able to optimize the critical exponent to a degree that relatively large truncation orders are unable to. The computational cost of integration with variable r is much smaller compared to the computational cost of extending the truncation, making (5.22) interesting in a practical sense. The true virtue of the new cut-off function is, however, found after performing an analytical continuation of r to negative values. There, the $\theta = 1$ barrier is finally crossed. The value of r at which the critical exponent for the smallest effective average action truncation order matched its exact value was found at $r \approx -2.133$, serving as a guide for the expansion in higher truncation orders. Remarkable stability of r was found with increasing single-trace truncation order, with $r \approx -2.133$ matching $\theta = 4/5$ for the smallest truncation order ($n = 2$) and $r \approx -2.042$ matching $\theta = 4/5$ for the highest truncation order studied ($n = 6$). Furthermore, we conjectured that r should, in principle, tend asymptotically to $r = -2$ as $n \to \infty$. The evaluation of the simple multi-trace truncation in [5.2.4] strengthened this conjecture, as we found the critical exponent's relevant direction's behaviour with r to be similar to that of the single-trace truncations. More multi-trace operators ought to be included in the effective average action in order for a more definitive conclusion to be made. These results' relevance is two-fold. First, the fact that $r \to -2$ (from below) as $n \to \infty$ places r away from the undesired range of $r \in [-1, 0]$, where several singularities occur. Second, the $\theta = 1$ barrier was successfully crossed, showing that the barrier was merely technical in nature, rather than rooted in some undisclosed fundamental theorem.

In the original article, stability of the procedure with respect to the matrix projection scheme was not tested. In this thesis, aside from a purely symmetric projection, we have considered a purely anti-symmetric projection. In the literature, projections are frequently purely symmetric since they are very easily implemented in calculations. We found the beta functions to remain unchanged with the anti-symmetric projection scheme (up to $n = 6$). This paves the way for future work that can use more general projections mixing the symmetric and anti-symmetric sides of the Hermitian matrices, rather than restricting to either one, broadening the projection subspace.

As future work regarding the Matrix Model studied in this thesis, the inclusion of terms that explicitly break the model's symmetry is yet to be understood. Traces with odd powers of the fields are generated by the flow of the couplings (for example, the flow of g_8 generates terms $\sim \mathrm{Tr}(\phi^3)\mathrm{Tr}(\phi^3)$). It would be useful to understand how to treat these quantum fluctuation terms.

It would also be interesting to see the new cut-off function's behaviour in other Matrix Models. The Benedetti-Henson (BH) Matrix Model[98] is a particularly simple model, which reproduces Causal Dynamical Triangulations[99] (CDT) in $2D$, thus introducing a notion of causality, necessary in the transition from a Euclidean to a Lorentzian setting. In the original application of the FRG to the (BH) Matrix Model[100], results were rather inconclusive. An optimization procedure similar to the one applied in this thesis can help retrieve a critical exponent closer to the exact one known for CDT[101].

Appendices

A Conformal Field Theory

This appendix aims to provide a brief presentation of the concepts of scale(/Weyl/trace) anomalies, central charges, conformal weights and scaling dimensions, found across [3.1].

Conformal Field Theories are QFTs (as they carry the Poincaré symmetry) with an additional ingredient: conformal symmetry. Scale symmetry is a part of conformal symmetry. A Poincaré transformation is a symmetry of flat space-time, leaving its metric invariant,

$$\eta_{\mu\nu}dx^\mu dx^\nu = \eta_{\rho\sigma}d\tilde{x}^\rho d\tilde{x}^\sigma \to \eta_{\mu\nu} = \eta_{\rho\sigma}\frac{\partial\tilde{x}^\rho}{\partial x^\mu}\frac{\partial\tilde{x}^\sigma}{\partial x^\nu} \quad , \tag{A.1}$$

and the general linear transformation that solves it is given as follows[102],

$$\tilde{x}^\mu = a^\mu + \Lambda^\mu_\nu x^\nu \quad . \tag{A.2}$$

To generalize the Poincaré to the conformal algebra, a local rescaling of the line element is introduced, such that the Poincaré isometry equation, (A.1), is upgraded to one that leaves the metric conserved up to a local rescaling[102],

$$\Omega^2(x)\eta_{\mu\nu} = \eta_{\rho\sigma}\frac{\partial\tilde{x}^\rho}{\partial x^\mu}\frac{\partial\tilde{x}^\sigma}{\partial x^\nu} \quad . \tag{A.3}$$

Considering infinitesimal transformations,

$$\begin{aligned} x^\mu \to \tilde{x}^\mu = x^\mu + \xi^\mu(x) \quad , \\ \Omega(x) = 1 + w(x) \quad , \end{aligned} \tag{A.4}$$

and plugging them into the conformal isometry equation, (A.3), the Killing equations for the vector field that generates the conformal transformations are found[103] (to first order in ξ),

$$\partial_\mu\xi_\nu + \partial_\nu\xi_\mu = f(x)\eta_{\mu\nu} = \frac{2}{D}(\partial_\rho\xi^\rho)\eta_{\mu\nu} \to \partial_\mu\partial_\nu\partial_\lambda\xi_\rho = 0 \quad , \tag{A.5}$$

whose general solution is given as follows[103]:

$$\xi^\mu = a^\mu + \Lambda^\mu_\nu x^\nu + \lambda x^\mu + b^\mu x^2 - 2x^\mu b \cdot x \quad . \tag{A.6}$$

The first two terms are identified as the Poincaré transformation (translation and rigid rotation). The third term pertains to the scale transformation (dilation) and the last two terms pertain to the special conformal transformation (SCT). The conformal generators can be extracted from this[103] and, by taking the commutators, the conformal algebra is generated.

In particular, the dilation generator is given as follows[103],

$$D = ix^\mu \partial_\mu \quad . \tag{A.7}$$

The Noether theorem[104] states that for every continuous symmetry there is an associated conserved current. The dilation current, $D^\mu = T^{\mu\nu} x_\nu$, where $T_{\mu\nu} = \frac{2}{\sqrt{g}} \frac{\delta S}{\delta g^{\mu\nu}}$, reveals a feature of scale invariance: the vanishing trace of the stress-energy tensor[105],

$$\partial_\mu D^\mu = T^\mu_\mu = 0 \quad . \tag{A.8}$$

(Note that $T^\mu_\mu = 0$ does not imply conformal symmetry but every CFT has $T^\mu_\mu = 0$.)

Quantum mechanically, however, the right-hand side of (A.8) gains a non-trivial anomalous term. The theory's coupling constants, u, acquire a non-trivial dependence on the energy scale, k, and lose the invariance under a scale transformation,

$$u \to u + \beta(u), \quad \beta = \frac{du}{dk} \quad , \tag{A.9}$$

leading to a *scale*(/Weyl/trace) *anomaly* in the Noether conservation law[106],

$$\langle \partial_\mu D^\mu \rangle = \beta(u) \frac{\partial \mathcal{L}}{\partial u} \quad , \tag{A.10}$$

where $\mathcal{L}$ is the Lagrangian density.

The remaining concepts we wish to point out can be better understood in $2D$. The (otherwise finite) conformal algebra has an infinite number of generators at D=2[103]. This can be shown by setting $\mu = \nu = 1$ and $\mu = \nu = 2$ in the conformal Killing equation (A.5), where one obtains

$$\partial_1 \xi_1 = \partial_2 \xi_2 \quad , \tag{A.11}$$

and, setting $\mu = 1, \nu = 2$, where one obtains

$$\partial_1 \xi_2 = -\partial_2 \xi_1 \quad , \tag{A.12}$$

which are the so-called Cauchy-Riemann equations[107]. In $2D$, one can harness the power of complex coordinates,

$$\begin{aligned} z &= x_1 + i x_2 \quad , \\ \xi &= \xi_1 + i \xi_2 \quad , \\ \partial_z &= \frac{1}{2}(\partial_1 - i \partial_2) \quad , \end{aligned} \tag{A.13}$$

and rewrite the Cauchy-Riemann equations as follows:

$$\partial_{\bar{z}} \xi(z, \bar{z}) = 0 \quad . \tag{A.14}$$

This equation states that a $2D$ conformal transformation is generated by a purely holomorphic map, satisfying $z \to f(z)$. There is an infinite number of such mappings in $2D$: ξ is an arbitrary holomorphic function and the number of conformal generators in $2D$ is infinite. The $2D$ conformal algebra is the DeWitt algebra[103], with the following generators,

$$\begin{aligned} l_n &= -z^{n+1} \partial_z \quad , \\ \bar{l}_n &= -\bar{z}^{n+1} \partial_{\bar{z}} \quad , \end{aligned} \tag{A.15}$$

where $n \in (-\infty, +\infty)$ and, in particular, l_{-1}, l_0 and l_1 (and their anti-holomorphic counterparts) generate the finite subalgebra of global conformal transformations: l_{-1} generates translations on the complex plane, l_0 generates scale transformations and rotations and l_1 generates special conformal transformations[103]. For $n \neq -1, 0, 1$, one speaks of local conformal transformations.

In CFT, operators can be split into two types[108]: primary operators, Φ_A that transform as tensors under conformal transformations, and descendants, which can be obtained from primaries by taking derivatives of them, $\partial_\mu \dots \partial_\nu \Phi_A$. The energy-momentum tensor, particularly important in CFT, is an example of a quasi-primary operator: it transforms as a tensor but only for global conformal transformations. Under a (D-dimensional) conformal mapping, (A.3), a quasi-primary transforms as follows[103],

$$\Phi(x) \to \tilde{\Phi}(\tilde{x}) = \mathbb{J}^{-\frac{\Delta}{D}} \Phi(x) \quad , \tag{A.16}$$

where $\mathbb{J}$ is the Jacobian of the coordinate transformation. Δ is known as the *scaling dimension*: it governs the way an operator behaves under a scale transformation, (if $\tilde{x} = \lambda x$, $\tilde{\Phi}(\tilde{x}) = \lambda^{-\Delta}\Phi(x)$, since $\mathbb{J} = \lambda^D$). In $2D$, with the suitable complex coordinates, $z \to w(z)$, the condition (A.16) is generalized to[103]

$$\Phi(z, \bar{z}) \to \tilde{\Phi}(w, \bar{w}) = \left(\frac{dw}{dz}\right)^{-h} \left(\frac{d\bar{w}}{d\bar{z}}\right)^{-\bar{h}} \Phi(z, \bar{z}) \quad , \tag{A.17}$$

where h and $\bar{h}$ are, respectively, the eigenvalues of l_0 and $\bar{l}_0$, the (holomorphic and anti-holomorphic) *conformal weights*. Since $(l_0 + \bar{l}_0)$ generates dilations and $i(l_0 - \bar{l}_0)$ generates rotations[103], the scaling dimension is given by $\Delta = h + \bar{h}$ and the spin is given by $s = h - \bar{h}$.

Lastly, let us show how to extract the central charge and its interpretation. To do so, let us look at the energy-momentum tensor and its correlation function with itself. To that end, $T_{\mu\nu}$ must first be rewritten in complex coordinates, (A.13). The metric tensor is given as follows[109],

$$g^{\mu\nu} = \begin{pmatrix} g_{zz} & g_{z\bar{z}} \\ g_{z\bar{z}} & g_{\bar{z}\bar{z}} \end{pmatrix} = \begin{pmatrix} 0 & 2 \\ 2 & 0 \end{pmatrix} \quad . \tag{A.18}$$

The energy-momentum tensor is also a symmetric tensor. Therefore, in $2D$, it has 3 independent quantities: T_{zz}, $T_{z\bar{z}}$ and $T_{\bar{z}\bar{z}}$. Its tracelessness, (A.8), implies[109] $T^\mu_\mu = T_{\mu\nu}g^{\mu\nu} = 0 \to T_{z\bar{z}} = 0$. Furthermore, by its conservation law, $\partial_\mu T^{\mu\nu} = 0$, one readily finds[109] $\partial_{\bar{z}} T_{zz} = 0$ and $\partial_z T_{\bar{z}\bar{z}} = 0$, which implies T_{zz} is purely holomorphic, $T_{zz} = T_{zz}(z)(= T(z))$ and $T_{\bar{z}\bar{z}}$ is purely anti-holomorphic, $T_{\bar{z}\bar{z}} = T_{\bar{z}\bar{z}}(\bar{z})(= \bar{T}(\bar{z}))$. One can thus look at the holomorphic part only in what follows.

Consider a coordinate transformation generated by the energy-momentum tensor. Its associated (holomorphic) current is given by the holomorphic part of $T_{\mu\nu}$ and the infinitesimal transformation parameter, $j(z) = T(z)\xi(z)$. The associated charge, $Q_\xi = \oint dz T(z)\xi(z)$, generates the symmetry transformation on an operator Φ defined on a point w of the complex plane[77],

$$\begin{aligned} \delta_\xi \Phi(w) = [Q_\xi, \Phi(w)] &= \lim_{\delta\to 0}\left[\oint_{|z|=|w|+\delta} dz T(z)\xi(z)\Phi(w) - \oint_{|z|=|w|-\delta} dz T(z)\xi(z)\Phi(w)\right] \\ &= \oint_{\mathcal{C}_w} dz \xi(z) T(z)\Phi(w) \quad , \end{aligned} \tag{A.19}$$

where, in the second line, we used the idea from complex analysis that the coincident parts of both paths cancel out and one can perform solely the contour around w, $\mathcal{C}_w$. Furthermore, if $\Phi(w)$ is a primary, the (holomorphic) infinitesimal form of (A.17) is given as follows[77],

$$\delta_\xi \Phi(w) = \xi(w)\partial\Phi(w) + h\partial\xi(w)\Phi(w) \quad . \tag{A.20}$$

If (A.19) is non-vanishing, w must be a pole. Recalling Cauchy's formula for the contour integral around a pole z_0,

$$\oint_{\mathcal{C}_{z_0}} dz \frac{f(z)}{(z-z_0)^{(n+1)}} = \frac{1}{n!} f^{(n)}(z_0) \quad , \tag{A.21}$$

and equating (A.19) and (A.20) with (A.21) in mind, one can readily read that, due to the derivative $\partial\xi$ on the right-hand side of (A.20), $T(z)\Phi(w)$ ought to have a double pole; due to the linear ξ term, there ought to exist a single pole as well. Thus, it is of the following form,

$$T(z)\Phi(w) = \frac{h}{(z-w)^2}\Phi(w) + \frac{\partial\Phi(w)}{(z-w)} \quad , \tag{A.22}$$

plus non-singular terms. This procedure is known as the operator product expansion (OPE) procedure. It allows for the determination of the short-distance singular behaviour of a product of operators, turning it into a sum of local operators. If the procedure is followed similarly when $\Phi(w)$ is $T(w)$ itself, the following OPE (modulo non-singular terms) is obtained[77],

$$T(z)T(w) = \frac{c}{2}\frac{1}{(z-w)^4} + \frac{h}{(z-w)^2}T(w) + \frac{\partial T(w)}{z-w} \quad . \tag{A.23}$$

c is the *central charge*. It depends on the model under study and it is determined by the short-distance behaviour of the model. Modulo the central charge term, (A.23) is equal to the OPE of a primary, (A.22). The central charge functions as an anomalous term in the transformation law of $T(z)$ (the holomorphic part of (A.17)), acting as a measure of the conformal symmetry breaking introduced in an otherwise conformal theory. One very illustrative result of the nature of c is given by defining a CFT on a curved $2D$ manifold: scale invariance is broken by the curvature, R, and the tracelessness (A.8) of $T_{\mu\nu}$ no longer holds, with the scale anomaly being written in terms of the central charge[103], $\langle T^{\mu}_{\mu} \rangle = \frac{c}{24\pi} R$.

For a deeper study of CFT, we refer to Di Francesco, Mathieu and Senechal[103], Polchinski[109] and Fradkin[77].

B Derivation of Beta Functions

We explicitly derive the anomalous dimension flow equation, (5.32), and the g_4 beta function, (5.38), for the single-trace truncation, (5.8), (at least) up to $\bar{g}_6$ in the symmetric projection, (5.21).

First, it is straightforward to notice that $\sim g_4^1$ is the only term of the Wetterich equation expansion, (5.20), that flows into the running of Z_N since, after taking the functional derivatives, it is the only term in which a $\sim \phi^2$ term survives. The first step is thus the Hermitian decomposition, (5.9), of $\frac{\bar{g}_4}{4}\mathrm{Tr}(\phi^4)$:

$$\begin{aligned}\mathrm{Tr}(\phi^4) &= \phi_{am}\phi_{mn}\phi_{nl}\phi_{la} = (A_{am} + iB_{am})(A_{mn} + iB_{mn})(A_{nl} + iB_{nl})(A_{la} + iB_{la}) \\ &= \mathrm{Tr}(A^4) + 4i\mathrm{Tr}(A^3B) - 4i\mathrm{Tr}(AB^3) - 4\mathrm{Tr}(A^2B^2) - 2\mathrm{Tr}(ABAB) + \mathrm{Tr}(B^4)\end{aligned} \tag{B.1}$$

As mentioned previously, the (AB) and (BA) modes of (5.12) vanish due to the anti-symmetry of B. Let us see that explicitly for $4i\mathrm{Tr}(AB^3)$. Making use of the derivatives defined in (5.13),

$$\begin{aligned}\frac{\delta^2}{\delta A_{ab}\delta B_{cd}}\mathrm{Tr}(AB^3) = \frac{\delta^2}{\delta B_{ab}\delta A_{cd}}\mathrm{Tr}(AB^3) = -\frac{1}{4}\{&B_{al}B_{ld}\delta_{bc} - B_{dn}B_{na}\delta_{bc} - B_{bl}B_{ld}\delta_{ac} + B_{dn}B_{nb}\delta_{ac} \\ &- B_{bl}B_{lc}\delta_{ad} + B_{cn}B_{nb}\delta_{ad} + B_{al}B_{lc}\delta_{bd} - B_{cn}B_{na}\delta_{bd} + B_{cb}B_{ad} - B_{ca}B_{bd} + B_{db}B_{ac} - B_{da}B_{bc}\},\end{aligned} \tag{B.2}$$

and the terms can be rearranged due to $B_{ij} = -B_{ji}$, leading to:

$$\frac{\delta^2}{\delta A_{ab}\delta B_{cd}}\mathrm{Tr}(AB^3) = \frac{\delta^2}{\delta B_{ab}\delta A_{cd}}\mathrm{Tr}(AB^3) = -\frac{1}{4}\{B_{al}B_{ld}\delta_{bc} - B_{nd}B_{an}\delta_{bc} - B_{bl}B_{ld}\delta_{ac} + B_{nd}B_{bn}\delta_{ac} - B_{bl}B_{lc}\delta_{ad} + B_{nc}B_{bn}\delta_{ad} + B_{al}B_{lc}\delta_{bd} - B_{nc}B_{an}\delta_{bd} + B_{cb}B_{ad} - B_{ca}B_{bd} + B_{bd}B_{ca} - B_{ad}B_{cb}\} = 0, \tag{B.3}$$

The remaining terms - $4i\mathrm{Tr}(A^3B)$, $4\mathrm{Tr}(A^2B^2)$ and $\mathrm{Tr}(ABAB)$ - follow similarly. Naturally, $\mathrm{Tr}(A^4)$ and $\mathrm{Tr}(B^4)$ vanish instantly upon application of a mixed derivative.

For the (AA) and (BB) modes of (5.12), it is straightforward to see that, due to the choice of a purely symmetrical projection, (5.21), terms in (B.1) with an odd number of B matrices vanish. For the (AA) derivative, $4i\mathrm{Tr}(A^3B) \to \sim AB$ and, upon projecting $B \to 0$, it vanishes. The same reasoning is true for the (BB) derivative of $4i\mathrm{Tr}(AB^3)$. Naturally, the (BB) derivative of $4i\mathrm{Tr}(A^3B)$ and the (AA) derivative of $4i\mathrm{Tr}(AB^3)$ vanish. $\mathrm{Tr}(B^4)$ also vanishes both after the (AA) derivative - self-evidently - and after the (BB) derivative, due to the projection scheme. Therefore, only three relevant terms remain,

$$\frac{\bar{g}_4}{4}\mathrm{Tr}(\phi^4) \to \frac{\bar{g}_4}{4}\mathrm{Tr}(A^4) - \bar{g}_4\mathrm{Tr}(A^2B^2) - \frac{\bar{g}_4}{2}\mathrm{Tr}(ABAB) \quad , \tag{B.4}$$

of which the first term is only non-vanishing for the (AA) mode and, due to the symmetric projection scheme, the second and third terms are only non-vanishing for the (BB) mode. With (5.13) in mind, it is straightforward to obtain the relevant derivatives,

$$\frac{\delta^2}{\delta A_{ab}\delta A_{cd}}\left(\frac{\bar{g}_4}{4}\mathrm{Tr}(A^4)\right) = \frac{\bar{g}_4}{2}\{A_{an}A_{nc}\delta_{bd} + A_{bn}A_{nc}\delta_{ad} + A_{an}A_{nd}\delta_{bc} + A_{bn}A_{nd}\delta_{ac} + A_{bd}A_{ac} + A_{ad}A_{bc}\}, \tag{B.5}$$

$$\frac{\delta^2}{\delta B_{ab}\delta B_{cd}}\left(-\bar{g}_4\mathrm{Tr}(A^2B^2)\right) = \frac{\bar{g}_4}{2}\{A_{bn}A_{nd}\delta_{ac} - A_{bn}A_{nc}\delta_{ad} + A_{an}A_{nc}\delta_{bd} - A_{an}A_{nd}\delta_{bc}\}, \tag{B.6}$$

$$\frac{\delta^2}{\delta B_{ab}\delta B_{cd}}\left(-\frac{\bar{g}_4}{2}\mathrm{Tr}(ABAB)\right) = -\frac{\bar{g}_4}{2}\{A_{ad}A_{bc} - A_{ac}A_{bd}\} \quad , \tag{B.7}$$

which, according to (5.20) and the definition of the propagator, (5.16), are now contracted with $\mathbf{1}^{sym}_{abcd}$ - in the case of (B.5) - and with $\mathbf{1}^{asym}_{abcd}$ - in the case of (B.6) and (B.7) - leading to, respectively:

$$\mathbf{1}^{sym}_{abcd}\frac{\delta^2}{\delta A_{ab}\delta A_{cd}}\left(\frac{\bar{g}_4}{4}\mathrm{Tr}(A^4)\right) = \frac{\bar{g}_4}{2}\{A_{an}A_{na}\delta_{bb} + A_{bn}A_{na}\delta_{ab} + A_{an}A_{nb}\delta_{ab} + A_{bn}A_{nb}\delta_{aa} + A_{bb}A_{aa} + A_{ab}A_{ba}\}, \quad \text{(B.8)}$$

$$\mathbf{1}^{asym}_{abcd}\frac{\delta^2}{\delta B_{ab}\delta B_{cd}}\left(-\bar{g}_4\mathrm{Tr}(A^2B^2)\right) = \frac{\bar{g}_4}{2}\left\{A_{bn}A_{nb}\delta_{aa} - A_{bn}A_{na}\delta_{ab} + A_{an}A_{na}\delta_{bb} - A_{an}A_{nb}\delta_{ba}\right\}, \quad \text{(B.9)}$$

$$\mathbf{1}^{asym}_{abcd}\frac{\delta^2}{\delta B_{ab}\delta B_{cd}}\left(-\frac{\bar{g}_4}{2}\mathrm{Tr}(ABAB)\right) = -\frac{\bar{g}_4}{2}\left\{A_{ab}A_{ba} - A_{aa}A_{bb}\right\} \quad , \quad \text{(B.10)}$$

Notice the terms $\sim A_{aa}A_{bb}$ in (B.8) and (B.10). They exhibit that g_4 also feeds back into the running of a $\sim \mathrm{Tr}(\phi)\mathrm{Tr}(\phi)$ term. Such a term does not exist in a single-trace truncation and we discard those contributions. Applying the projection scheme, (5.21), we get the following:

$$\mathrm{Proj}\left[\mathbf{1}^{sym}_{abcd}\frac{\delta^2}{\delta A_{ab}\delta A_{cd}}\left(\frac{\bar{g}_4}{4}\mathrm{Tr}(A^4)\right)\right] = a^2\frac{\bar{g}_4}{2}\left\{2\delta_{aa}\delta_{bb} + 3\delta_{aa}\right\} = a^2\frac{\bar{g}_4}{2}N^2\left\{2 + 3\frac{1}{N}\right\}, \quad \text{(B.11)}$$

$$\mathrm{Proj}\left[\mathbf{1}^{asym}_{abcd}\frac{\delta^2}{\delta B_{ab}\delta B_{cd}}\left(-\bar{g}_4\mathrm{Tr}(A^2B^2)\right)\right] = a^2\bar{g}_4\left\{\delta_{aa}\delta_{bb} - \delta_{aa}\right\} = a^2\bar{g}_4N^2\left\{1 - \frac{1}{N}\right\}, \quad \text{(B.12)}$$

$$\mathrm{Proj}\left[\mathbf{1}^{asym}_{abcd}\frac{\delta^2}{\delta B_{ab}\delta B_{cd}}\left(-\frac{\bar{g}_4}{2}\mathrm{Tr}(ABAB)\right)\right] = -a^2\frac{\bar{g}_4}{2}\delta_{aa} = -a^2\frac{\bar{g}_4}{2}N \quad . \quad \text{(B.13)}$$

The first term from (B.11) and the first term from (B.12) contribute to leading order in $1/N$. The remaining terms are all sub-leading order when $N \to \infty$ and, therefore, vanish. We have thus found c in (5.25) to be equal to $(1 + 1)$. Ultimately, the flow equation for $\frac{Z_N}{2}\mathrm{Tr}(\phi^2)$ comes as follows,

$$
\begin{aligned}
\partial_t \frac{Z_N}{2}\mathrm{Tr}(\phi^2) &= (-1)^1 \frac{1}{2} a^2 \bar{g}_4 (1+1) \frac{N^2}{Z_N} \zeta(2,r,\eta) \Leftrightarrow \\
\partial_t \frac{Z_N}{2}\mathrm{Tr}(A^2) &= -\frac{1}{2} a^2 g_4 \frac{Z_N^2}{N} (1+1) \frac{N^2}{Z_N} \zeta(2,r,\eta) \Leftrightarrow \\
\partial_t Z_N a^2 N &= -2a^2 g_4 Z_N N \zeta(2,r,\eta) \Leftrightarrow \\
\eta &= 2g_4 \zeta(2,r,\eta)
\end{aligned} \tag{B.14}
$$

where (5.5) and (5.7) were used, as well as $\mathrm{Tr}(\phi^2) \to \mathrm{Tr}(A^2)$ since $\mathrm{Tr}(\phi^2) = \mathrm{Tr}(A^2) - \mathrm{Tr}(B^2)$.

The g_4 beta function is obtained in all too similar fashion. It depends on $\sim g_6$ and $\sim g_4^2$. We can build on the previous results and extract the $\sim g_4^2$ portion readily:

$$
\begin{aligned}
\partial_t \frac{\bar{g}_4}{4}\mathrm{Tr}(\phi^4) &\propto (-1)^2 \frac{1}{2} (a^2)^2 \bar{g}_4^2 (1+1) \frac{N^2}{Z_N^2} \zeta(3,r,\eta) \Leftrightarrow \\
\partial_t \frac{g_4}{4}\mathrm{Tr}(A^4) &\propto \frac{1}{2} a^4 g_4^2 \left(\frac{Z_N^2}{N}\right)^2 (1+1) \frac{N^2}{Z_N^2} \zeta(3,r,\eta) \Leftrightarrow \\
\partial_t g_4 \frac{Z_N^2}{N} a^4 N &\propto 4a^4 g_4^2 Z_N^2 \zeta(3,r,\eta) \Leftrightarrow \\
\beta_{g_4} &\propto 4g_4^2 \zeta(3,r,\eta)
\end{aligned} \tag{B.15}
$$

To derive the $\sim g_6$ term, $\frac{\bar{g}_6}{6}\mathrm{Tr}(\phi^6)$ is decomposed with (5.9):

$$
\begin{aligned}
\mathrm{Tr}(\phi^6) = \mathrm{Tr}(A^6) &+ 6i\mathrm{Tr}(A^5 B) - 6\mathrm{Tr}(A^4 B^2) - 6\mathrm{Tr}(A^3 BAB) - 6i\mathrm{Tr}(A^3 B^3) \\
&- 3\mathrm{Tr}(A^2 BA^2 B) - 6i\mathrm{Tr}(B^2 A^2 BA) - 6i\mathrm{Tr}(A^2 B^2 AB) + 6\mathrm{Tr}(A^2 B^4) \\
&- 2i\mathrm{Tr}(ABABAB) + 6\mathrm{Tr}(ABAB^3) + 3\mathrm{Tr}(AB^2 AB^2) + 6i\mathrm{Tr}(AB^5) - \mathrm{Tr}(B^6)
\end{aligned} \tag{B.16}
$$

Using the same arguments previously laid out, the relevant terms are solely the following,

$$
\frac{\bar{g}_6}{6}\mathrm{Tr}(\phi^6) \to \frac{\bar{g}_6}{6}\mathrm{Tr}(A^6) - \bar{g}_6 \mathrm{Tr}(A^4 B^2) - \bar{g}_6 \mathrm{Tr}(A^3 BAB) - \frac{\bar{g}_6}{2}\mathrm{Tr}(A^2 BA^2 B) \quad , \tag{B.17}
$$

and application of the derivatives yields

$$\frac{\delta^2}{\delta A_{ab}\delta A_{cd}}\left(\frac{\bar{g}_6}{6}\mathrm{Tr}(A^6)\right)=\frac{\bar{g}_6}{2}\{A_{bm}A_{mn}A_{np}A_{pc}\delta_{ad}+A_{am}A_{mn}A_{np}A_{pc}\delta_{bd}+A_{bm}A_{mn}A_{np}A_{pd}\delta_{ac}$$
$$+A_{am}A_{mn}A_{np}A_{pd}\delta_{bc}+A_{bm}A_{mn}A_{nc}A_{ad}+A_{am}A_{mn}A_{nc}A_{bd}+A_{am}A_{mn}A_{nd}A_{bc}$$
$$+A_{bm}A_{mn}A_{nd}A_{ac}+A_{am}A_{md}A_{bn}A_{nc}+A_{am}A_{mc}A_{bn}A_{nd}\},\quad\text{(B.18)}$$

$$\frac{\delta^2}{\delta B_{ab}\delta B_{cd}}\left(-\bar{g}_6\mathrm{Tr}(A^4B^2)\right)=\frac{\bar{g}_6}{2}\{A_{bm}A_{mn}A_{nl}A_{ld}\delta_{ac}-A_{am}A_{mn}A_{nl}A_{ld}\delta_{bc}$$
$$+A_{am}A_{mn}A_{nl}A_{lc}\delta_{bd}-A_{bm}A_{mn}A_{nl}A_{lc}\delta_{ad}\},\quad\text{(B.19)}$$

$$\frac{\delta^2}{\delta B_{ab}\delta B_{cd}}\left(-\bar{g}_6\mathrm{Tr}(A^3BAB)\right)=-\frac{\bar{g}_6}{2}\{A_{am}A_{mn}A_{nd}A_{cb}-A_{bm}A_{mn}A_{nd}A_{ca}$$
$$-A_{am}A_{mn}A_{nc}A_{db}+A_{bm}A_{mn}A_{nc}A_{da}\},\quad\text{(B.20)}$$

$$\frac{\delta^2}{\delta B_{ab}\delta B_{cd}}\left(-\frac{\bar{g}_6}{2}\mathrm{Tr}(A^2BA^2B)\right)=-\frac{\bar{g}_6}{4}\{A_{am}A_{md}A_{cp}A_{pb}-A_{bm}A_{md}A_{cp}A_{pa}$$
$$-A_{am}A_{mc}A_{dp}A_{pb}-A_{bm}A_{mc}A_{dp}A_{pa}\},\quad\text{(B.21)}$$

after which contraction with $\mathbf{1}^{sym}_{abcd}$ - in the case of (B.18) - or $\mathbf{1}^{asym}_{abcd}$ - in the case of (B.19), (B.20) and (B.21) - and projection onto the symmetric subspace, (5.21), lead to the following results,

$$\mathrm{Proj}\left[\mathbf{1}^{sym}_{abcd}\frac{\delta^2}{\delta A_{ab}\delta A_{cd}}\left(\frac{\bar{g}_6}{6}\mathrm{Tr}(A^6)\right)\right]=a^4\frac{\bar{g}_6}{2}\{2\delta_{aa}\delta_{bb}+5\delta_{aa}\}=a^4\frac{\bar{g}_6}{2}N^2\left\{2+5\frac{1}{N}\right\},\quad\text{(B.22)}$$

$$\mathrm{Proj}\left[\mathbf{1}^{asym}_{abcd}\frac{\delta^2}{\delta B_{ab}\delta B_{cd}}\left(-\bar{g}_6\mathrm{Tr}(A^4B^2)\right)\right]=a^4\bar{g}_6\{\delta_{aa}\delta_{bb}-\delta_{aa}\}=a^4\bar{g}_6N^2\left\{1-\frac{1}{N}\right\},\quad\text{(B.23)}$$

$$\mathrm{Proj}\left[\mathbf{1}^{asym}_{abcd}\frac{\delta^2}{\delta B_{ab}\delta B_{cd}}\left(-\bar{g}_6\mathrm{Tr}(A^3BAB)\right)\right]=a^4\bar{g}_6\delta_{aa}=a^4\bar{g}_6N,\quad\text{(B.24)}$$

$$\mathrm{Proj}\left[\mathbf{1}^{asym}_{abcd}\frac{\delta^2}{\delta B_{ab}\delta B_{cd}}\left(-\frac{\bar{g}_6}{2}\mathrm{Tr}(A^2BA^2B)\right)\right]=a^4\frac{\bar{g}_6}{2}\delta_{aa}=a^4\frac{\bar{g}_6}{2}N,\quad\text{(B.25)}$$

where terms that couple onto the running of $\mathrm{Tr}^3(A)\mathrm{Tr}(A)$ and $\mathrm{Tr}(A^2)\mathrm{Tr}(A^2)$ were omitted from (B.22), (B.24) and (B.25). The $\sim g_6$ term in the g_4 beta function comes as follows,

$$
\begin{aligned}
\partial_t \frac{\bar{g}_4}{4}\mathrm{Tr}(\phi^4) &\propto (-1)^1 \frac{1}{2} a^4 \bar{g}_6 (1+1) \frac{N^2}{Z_N} \zeta(2,r,\eta) \Leftrightarrow \\
\partial_t \frac{\bar{g}_4}{4}\mathrm{Tr}(A^4) &\propto -\frac{1}{2} a^4 g_6 \frac{Z_N^3}{N^2} (1+1) \frac{N^2}{Z_N} \zeta(2,r,\eta) \Leftrightarrow \\
\partial_t g_4 \frac{Z_N^2}{N} a^4 N &\propto -4a^4 g_6 Z_N^2 \zeta(2,r,\eta) \Leftrightarrow \\
\beta_{g_4} &\propto -4 g_6 \zeta(2,r,\eta) \quad ,
\end{aligned}
\tag{B.26}
$$

thus concluding the derivation of (5.38). The remaining beta functions, (5.39)-(5.42), are obtained in the same manner. A final word on them. The multiplicative factor in each term can be understood simply in a combinatorial way. For example, in (5.41): the $\sim g_4 g_{10}$ and $\sim g_6 g_8$ have a 2 factor from the fact that we can write their products in two different ways, $g_4 g_{10}$ or $g_{10} g_4$ and $g_6 g_8$ or $g_8 g_6$; the 3 factor in $\sim g_4^2 g_8$ comes from the possibility of writing $g_4^2 g_8$, $g_4 g_8 g_4$ or $g_8 g_4^2$, and the same reasoning goes for $\sim g_4 g_6^2$; $g_4^4 g_6$ can be written as $g_4^4 g_6$, $g_4^3 g_6 g_4$, $g_4^2 g_6 g_4^2$, $g_4 g_6 g_4^3$ and $g_6 g_4^4$, hence the 5 factor; self-evidently, g_{12} can only be written in one way, and the same is true for g_4^5, meaning they simply have a 1 factor attached to them.

C Anti-Symmetric Projection

We explicitly derive the anomalous dimension flow equation and the g_6 contribution to the g_4 beta function, as in the previous appendix, but for the anti-symmetric projection scheme, (5.62). With regards to the fact that the (AB) and (BA) modes of (5.12) vanish, nothing changes since that does not depend on the projection scheme.

However, the relevant terms of (B.1) do change from (B.4). Now the situation reverses: only terms with two A matrices will survive the anti-symmetric projection after the (AA) derivative and only terms without A matrices will survive the anti-symmetric projection after the (BB) derivative. Therefore, the relevant terms are the following,

$$
\frac{\bar{g}_4}{4}\mathrm{Tr}(\phi^4) \to \frac{\bar{g}_4}{4}\mathrm{Tr}(B^4) - \bar{g}_4 \mathrm{Tr}(A^2B^2) - \frac{\bar{g}_4}{2}\mathrm{Tr}(ABAB) \quad , \tag{C.1}
$$

and the respective contracted derivatives come as follows,

$$\mathbf{1}^{asym}_{abcd}\frac{\delta^2}{\delta B_{ab}\delta B_{cd}}\left(\frac{\bar{g}_4}{4}\mathrm{Tr}(B^4)\right) = \frac{\bar{g}_4}{2}\left\{2B_{an}B_{na} - 2B_{an}B_{na}\delta_{bb} + B_{ab}B_{ba} - B_{aa}B_{bb}\right\}, \tag{C.2}$$

$$\mathbf{1}^{sym}_{abcd}\frac{\delta^2}{\delta A_{ab}\delta A_{cd}}\left(-\bar{g}_4\mathrm{Tr}(A^2B^2)\right) = -\bar{g}_4\left\{B_{an}B_{na} + B_{bn}B_{nb}\delta_{aa}\right\}, \tag{C.3}$$

$$\mathbf{1}^{sym}_{abcd}\frac{\delta^2}{\delta A_{ab}\delta A_{cd}}\left(-\frac{\bar{g}_4}{2}\mathrm{Tr}(ABAB)\right) = \frac{\bar{g}_4}{2}\left\{B_{ab}B_{ba} + B_{aa}B_{bb}\right\}, \tag{C.4}$$

which, after applying the anti-symmetric projection scheme, (5.62), realizing that $\mathrm{Tr}(\boldsymbol{\varepsilon}^k_{\boldsymbol{N}}) = \frac{N}{2}\mathrm{Tr}(\boldsymbol{\varepsilon}^k)$ and taking (5.64) into account, becomes - omitting $\sim \mathrm{Tr}^2(B)$ terms:

$$\begin{aligned}\mathrm{Proj}\left[\mathbf{1}^{asym}_{abcd}\frac{\delta^2}{\delta B_{ab}\delta B_{cd}}\left(\frac{\bar{g}_4}{4}\mathrm{Tr}(B^4)\right)\right] &= a^2\frac{\bar{g}_4}{2}\left\{2\varepsilon_{N_{an}}\varepsilon_{N_{na}} - 2\varepsilon_{N_{an}}\varepsilon_{N_{na}}\delta_{bb} + \varepsilon_{N_{ab}}\varepsilon_{N_{ba}}\right\}\\ &= a^2\frac{\bar{g}_4}{2}\frac{N}{2}\left\{3\varepsilon_{ij}\varepsilon_{ji} - 2\varepsilon_{ij}\varepsilon_{ji}\delta_{bb}\right\}\\ &= a^2\bar{g}_4N^2\left\{-3\frac{1}{N} + 1\right\},\end{aligned} \tag{C.5}$$

$$\begin{aligned}\mathrm{Proj}\left[\mathbf{1}^{sym}_{abcd}\frac{\delta^2}{\delta A_{ab}\delta A_{cd}}\left(-\bar{g}_4\mathrm{Tr}(A^2B^2)\right)\right] &= -a^2\bar{g}_4\left\{\varepsilon_{N_{an}}\varepsilon_{N_{na}} + \varepsilon_{N_{bn}}\varepsilon_{N_{nb}}\delta_{aa}\right\}\\ &= -a^2\bar{g}_4\frac{N}{2}\left\{\varepsilon_{ij}\varepsilon_{ji} + \varepsilon_{ij}\varepsilon_{ji}\delta_{aa}\right\}\\ &= a^2\bar{g}_4N^2\left\{\frac{1}{N} + 1\right\},\end{aligned} \tag{C.6}$$

$$\begin{aligned}\mathrm{Proj}\left[\mathbf{1}^{sym}_{abcd}\frac{\delta^2}{\delta A_{ab}\delta A_{cd}}\left(-\frac{\bar{g}_4}{2}\mathrm{Tr}(ABAB)\right)\right] &= a^2\frac{\bar{g}_4}{2}\varepsilon_{N_{ab}}\varepsilon_{N_{ba}} = a^2\frac{\bar{g}_4}{2}\frac{N}{2}\varepsilon_{ij}\varepsilon_{ji}\\ &= -a^2\frac{\bar{g}_4}{2}N^2\left\{\frac{1}{N}\right\}.\end{aligned} \tag{C.7}$$

Maintaining the leading terms in $1/N$, we obtain the anomalous dimension flow equation,

$$
\begin{aligned}
\partial_t \frac{Z_N}{2}\mathrm{Tr}(\phi^2) &= (-1)^1 \frac{1}{2} a^2 \bar{g}_4 (1+1) \frac{N^2}{Z_N}\zeta(2,r,\eta) \Leftrightarrow \\
-\partial_t \frac{Z_N}{2}\mathrm{Tr}(B^2) &= -\frac{1}{2} a^2 g_4 \frac{Z_N^2}{N}(1+1)\frac{N^2}{Z_N}\zeta(2,r,\eta) \Leftrightarrow \\
\partial_t Z_N a^2 N &= -2a^2 g_4 Z_N N \zeta(2,r,\eta) \Leftrightarrow \\
\eta &= 2g_4\zeta(2,r,\eta) \quad ,
\end{aligned} \tag{C.8}
$$

where we used that $-\mathrm{Tr}(B^2) \to -\mathrm{Tr}(\varepsilon_N^2) \to a^2 N$, when $N \to \infty$.

The same procedure is applied to the contribution of g_6^1 to the g_4 beta function. First,

$$
\frac{\bar{g}_6}{6}\mathrm{Tr}(\phi^6) \to -\frac{\bar{g}_6}{6}\mathrm{Tr}(B^6) + \bar{g}_6\mathrm{Tr}(A^2B^4) + \bar{g}_6\mathrm{Tr}(ABAB^3) + \frac{\bar{g}_6}{2}\mathrm{Tr}(AB^2AB^2) \quad , \tag{C.9}
$$

and, to abbreviate the content, (it follows just as the previous derivations) the contracted and projected derivatives come as follows,

$$
\mathrm{Proj}\left[\mathbf{1}^{asym}_{abcd}\frac{\delta^2}{\delta B_{ab}\delta B_{cd}}\left(-\frac{\bar{g}_6}{6}\mathrm{Tr}(B^6)\right)\right] \xrightarrow[N\to\infty]{} a^4\bar{g}_6 N^2, \tag{C.10}
$$

$$
\mathrm{Proj}\left[\mathbf{1}^{sym}_{abcd}\frac{\delta^2}{\delta A_{ab}\delta A_{cd}}\left(\bar{g}_6\mathrm{Tr}(A^2B^4)\right)\right] \xrightarrow[N\to\infty]{} a^4\bar{g}_6 N^2, \tag{C.11}
$$

$$
\mathrm{Proj}\left[\mathbf{1}^{sym}_{abcd}\frac{\delta^2}{\delta A_{ab}\delta A_{cd}}\left(\bar{g}_6\mathrm{Tr}(ABAB^3)\right)\right] \xrightarrow[N\to\infty]{} a^4\bar{g}_6 N^2\left\{\frac{1}{N}\right\}, \tag{C.12}
$$

$$
\mathrm{Proj}\left[\mathbf{1}^{sym}_{abcd}\frac{\delta^2}{\delta A_{ab}\delta A_{cd}}\left(-\frac{\bar{g}_6}{2}\mathrm{Tr}(AB^2AB^2)\right)\right] \xrightarrow[N\to\infty]{} \frac{1}{2}a^4\bar{g}_6 N^2\left\{\frac{1}{N}\right\}, \tag{C.13}
$$

leading to:

$$
\begin{aligned}
\partial_t \frac{\bar{g}_4}{4}\mathrm{Tr}(\phi^4) &\propto (-1)^1\frac{1}{2}a^4\bar{g}_6(1+1)\frac{N^2}{Z_N}\zeta(2,r,\eta) \Leftrightarrow \\
\partial_t \frac{\bar{g}_4}{4}\mathrm{Tr}(B^4) &\propto -\frac{1}{2}a^4 g_6\frac{Z_N^3}{N^2}(1+1)\frac{N^2}{Z_N}\zeta(2,r,\eta) \Leftrightarrow \\
\partial_t g_4 \frac{Z_N^2}{N}a^4 N &\propto -4a^4 g_6 Z_N^2\zeta(2,r,\eta) \Leftrightarrow \\
\beta_{g_4} &\propto -4g_6\zeta(2,r,\eta) \quad .
\end{aligned} \tag{C.14}
$$

The remaining terms follow in similar fashion.

7 References

[1] Paul Adrien Maurice Dirac. *The Principles of Quantum Mechanics*. Clarendon Press, 1930.

[2] Max Abraham. Zur elektrodynamik bewegter körper. *Annalen der Physik*, 332:891–921, 1904.

[3] Albert Einstein. Zur allgemeinen Relativitätstheorie. (German) [Toward a General Theory of Relativity]. *j-S-B-PREUSS-AKAD-WISS-2*, pages 778–786, 799–801, 1915.

[4] Mary K. Gaillard, Paul D. Grannis, and Frank J. Sciulli. The standard model of particle physics. *Reviews of Modern Physics*, 71(2):S96–S111, mar 1999.

[5] Bryce S. DeWitt. Quantum Theory of Gravity. I. The Canonical Theory. *Phys. Rev.*, 160:1113–1148, Aug 1967.

[6] Bryce S. DeWitt. Quantum Theory of Gravity. II. The Manifestly Covariant Theory. *Phys. Rev.*, 162:1195–1239, Oct 1967.

[7] Bryce S. DeWitt. Quantum Theory of Gravity. III. Applications of the Covariant Theory. *Phys. Rev.*, 162:1239–1256, Oct 1967.

[8] Stephen Boughn and Tony Rothman. Aspects of graviton detection: graviton emission and absorption by atomic hydrogen. *Classical and Quantum Gravity*, 23(20):5839–5852, Sep 2006.

[9] Stanley Deser, R. Jackiw, and Gerard 't Hooft. Three-Dimensional Einstein Gravity: Dynamics of Flat Space. *Annals Phys.*, 152:220, 1984.

[10] Steven Giddings, James Abbott, and Karel Kuchar. Einstein's theory in a three-dimensional space-time. *Gen. Rel. Grav.*, 16:751–775, 1984.

[11] Thomas Strobl. Gravity in two spacetime dimensions. *arXiv: High Energy Physics - Theory*, 2000.

[12] Daniel Grumiller and Roman Jackiw. Liouville gravity from einstein gravity. *arXiv: General Relativity and Quantum Cosmology*, 2007.

[13] A.M. Polyakov. Quantum geometry of bosonic strings. *Physics Letters B*, 103(3):207–210, 1981.

[14] Paul H. Ginsparg and Gregory W. Moore. Lectures on 2-D gravity and 2-D string theory. In *Theoretical Advanced Study Institute (TASI 92): From Black Holes and Strings to Particles*, pages 277–469, 10 1993.

[15] V. G. Knizhnik, Alexander M. Polyakov, and A. B. Zamolodchikov. Fractal Structure of 2D Quantum Gravity. *Mod. Phys. Lett. A*, 3:819, 1988.

[16] Kenneth G. Wilson. Renormalization group and critical phenomena. i. renormalization group and the kadanoff scaling picture. *Phys. Rev. B*, 4:3174–3183, Nov 1971.

[17] Kenneth G. Wilson. The renormalization group and critical phenomena. *Rev. Mod. Phys.*, 55:583–600, Jul 1983.

[18] M. Reuter. Nonperturbative evolution equation for quantum gravity. *Physical Review D*, 57(2):971–985, jan 1998.

[19] Christof Wetterich. Exact evolution equation for the effective potential. *Physics Letters B*, 301(1):90–94, feb 1993.

[20] Astrid Eichhorn and Tim Koslowski. Continuum limit in matrix models for quantum gravity from the functional renormalization group. *Physical Review D*, 88(8), oct 2013.

[21] Lewis Ryder. *Introduction to General Relativity*. Cambridge University Press, 2009.

[22] Restarting the LHC: Why 13 TeV? https://home.cern/science/engineering/restarting-lhc-why-13-tev.

[23] Renate Loll. Quantum gravity (review) - lecture 2, jan 2012. PIRSA:12010058 in https://pirsa.org.

[24] David Hilbert. Die grundlagen der physik (german) [foundations of physics]. *Nachrichten von der Gesellschaft der Wissenschaften zu Göttingen – Mathematisch-Physikalische Klasse*, pages 395–407, 1915.

[25] Markus Fierz and Wolfgang E. Pauli. On relativistic wave equations for particles of arbitrary spin in an electromagnetic field. *Proc. Roy. Soc. Lond. A*, 173:211–232, 1939.

[26] E. Álvarez, D. Blas, J. Garriga, and E. Verdaguer. Transverse fierz–pauli symmetry. *Nuclear Physics B*, 756(3):148–170, nov 2006.

[27] Renate Loll. Quantum gravity (review) - lecture 5, jan 2012. PIRSA:12010061 in https://pirsa.org.

[28] L. D. Faddeev and V. N. Popov. Feynman Diagrams for the Yang-Mills Field. *Phys. Lett. B*, 25:29–30, 1967.

[29] Claus Kiefer. *Quantum Gravity*. Oxford University Press UK, 2004.

[30] John F. Donoghue. General relativity as an effective field theory: The leading quantum corrections. *Phys. Rev. D*, 50:3874–3888, Sep 1994.

[31] Michael Edward Peskin and Daniel V. Schroeder. *An Introduction to Quantum Field Theory*. Westview Press, 1995. Reading, USA: Addison-Wesley (1995).

[32] Gerard 't Hooft and M. J. G. Veltman. One loop divergencies in the theory of gravitation. *Ann. Inst. H. Poincare Phys. Theor. A*, 20:69–94, 1974.

[33] Marc H. Goroff and Augusto Sagnotti. Quantum gravity at two loops. *Physics Letters B*, 160(1):81–86, 1985.

[34] Marc H. Goroff and Augusto Sagnotti. The Ultraviolet Behavior of Einstein Gravity. *Nucl. Phys. B*, 266:709–736, 1986.

[35] A. E. M. van de Ven. Two loop quantum gravity. *Nucl. Phys. B*, 378:309–366, 1992.

[36] M Yu Kalmykov. Gauge and parametrization dependencies of the one-loop counterterms in einstein gravity. *Classical and Quantum Gravity*, 12(6):1401–1411, Jun 1995.

[37] M Yu Kalmykov, K A Kazakov, P I Pronin, and K V Stepanyantz. Detailed analysis of the dependence of 1-loop counter-terms on gauge and parametrization in Einstein gravity with a cosmological constant. *Classical and Quantum Gravity*, 15(12):3777–3794, Dec 1998.

[38] C. Becchi, A. Rouet, and R. Stora. Renormalization of Gauge Theories. *Annals Phys.*, 98:287–321, 1976.

[39] Mir Faizal. BRST and anti-BRST symmetries in perturbative quantum gravity. *Foundations of Physics*, 41(2):270–277, oct 2010.

[40] John F. Donoghue. Introduction to the effective field theory description of gravity. In *Advanced School on Effective Theories*, 6 1995.

[41] John F. Donoghue. Leading quantum correction to the newtonian potential. *Physical Review Letters*, 72(19):2996–2999, May 1994.

[42] N. Bjerrum-Bohr, John Donoghue, and B. Holstein. Erratum: Quantum corrections to the schwarzschild and kerr metrics [phys. rev. d 68, 084005 (2003)]. *Phys. Rev. D*, 71, 03 2005.

[43] Richard Arnowitt, Stanley Deser, and Charles W. Misner. Republication of: The dynamics of general relativity. *General Relativity and Gravitation*, 40(9):1997–2027, aug 2008.

[44] Robert M Wald. *General relativity*. Chicago Univ. Press, Chicago, IL, 1984.

[45] Renate Loll. Quantum gravity (review) - lecture 8, feb 2012. PIRSA:12020000 see, https://pirsa.org.

[46] S. A. Hojman, K. Kuchar, and C. Teitelboim. Geometrodynamics Regained. *Annals Phys.*, 96:88–135, 1976.

[47] J. A. Wheeler. SUPERSPACE AND THE NATURE OF QUANTUM GEOMETRODYNAMICS. *Adv. Ser. Astrophys. Cosmol.*, 3:27–92, 1987.

[48] P.A.M. Dirac. *Lectures on Quantum Mechanics*. Belfer Graduate School of Science, monograph series. Dover Publications, 2001.

[49] Claus Kiefer. Wave packets in minisuperspace. *Phys. Rev. D*, 38:1761–1772, Sep 1988.

[50] Abhay Ashtekar, Tomasz Pawlowski, and Parampreet Singh. Quantum nature of the big bang: An analytical and numerical investigation. *Physical Review D*, 73(12), jun 2006.

[51] K. V. Kuchar. Time and interpretations of quantum gravity. *Int. J. Mod. Phys. D*, 20:3–86, 2011.

[52] C. J. Isham. Canonical quantum gravity and the problem of time. *NATO Sci. Ser. C*, 409:157–287, 1993.

[53] Edward Anderson. Problem of time in quantum gravity. *Annalen der Physik*, 524, 2010.

[54] Abhay Ashtekar. New variables for classical and quantum gravity. *Phys. Rev. Lett.*, 57:2244–2247, Nov 1986.

[55] Carlo Rovelli and Lee Smolin. Loop space representation of quantum general relativity. *Nuclear Physics B*, 331(1):80–152, 1990.

[56] Carlo Rovelli. *Quantum gravity*. Cambridge Monographs on Mathematical Physics. Univ. Pr., Cambridge, UK, 2004.

[57] Abhay Ashtekar and Eugenio Bianchi. A short review of loop quantum gravity. *Reports on Progress in Physics*, 84(4):042001, mar 2021.

[58] Steven Weinberg. *Ultraviolet divergences in quantum theories of gravitation*, pages 790–831. 1980.

[59] Daniel F. Litim. Fixed points of quantum gravity. *Physical Review Letters*, 92(20), may 2004.

[60] M Niedermaier. The asymptotic safety scenario in quantum gravity: an introduction. *Classical and Quantum Gravity*, 24(18):R171–R230, aug 2007.

[61] Martin Reuter and Frank Saueressig. Functional Renormalization Group Equations, Asymptotic Safety, and Quantum Einstein Gravity. In *First Quantum Geometry and Quantum Gravity School*, pages 288–329, 2010.

[62] Jacques Distler and Hikaru Kawai. Conformal field theory and 2d quantum gravity. *Nuclear Physics B*, 321(2):509–527, 1989.

[63] Yu Nakayama. Liouville field theory: A decade after the revolution. *International Journal of Modern Physics A*, 19(17n18):2771–2930, jul 2004.

[64] E D'Hoker and P S Kurzepa. 2-d quantum gravity and liouville theory. *Modern Physics Letters A; (USA)*, 5.

[65] N. E. Mavromatos and J. L. Miramontes. Regularizing the Functional Integral in 2D Quantum Gravity. *Mod. Phys. Lett. A*, 4:1847, 1989.

[66] Joseph Polchinski. A Two-Dimensional Model for Quantum Gravity. *Nucl. Phys. B*, 324:123–140, 1989.

[67] F. David. Conformal Field Theories Coupled to 2D Gravity in the Conformal Gauge. *Mod. Phys. Lett. A*, 3:1651, 1988.

[68] P.Di Francesco, P. Ginsparg, and J. Zinn-Justin. 2d gravity and random matrices. *Physics Reports*, 254(1-2):1–133, mar 1995.

[69] I.K. Kostov and M.L. Mehta. Random surfaces of arbitrary genus: Exact results for d=0 and 2 dimensions. *Physics Letters B*, 189(1):118–124, 1987.

[70] V.A. Kazakov. Ising model on a dynamical planar random lattice: Exact solution. *Physics Letters A*, 119(3):140–144, 1986.

[71] D.V. Boulatov, V.A. Kazakov, I.K. Kostov, and A.A. Migdal. Analytical and numerical study of a model of dynamically triangulated random surfaces. *Nuclear Physics B*, 275(4):641–686, 1986.

[72] A. Billoire and F. David. Scaling Properties of Randomly Triangulated Planar Random Surfaces: A Numerical Study. *Nucl. Phys. B*, 275:617–640, 1986.

[73] Tom Levy and Yaron Oz. Liouville conformal field theories in higher dimensions. *Journal of High Energy Physics*, 2018(6), jun 2018.

[74] F. David. Simplicial quantum gravity and random lattices. In *Les Houches Summer School on Gravitation and Quantizations, Session 57*, pages 0679–750, 7 1992.

[75] A. Zvonkin. Matrix integrals and map enumeration: An accessible introduction. *Mathematical and Computer Modelling*, 26(8):281–304, 1997.

[76] Jérémie Bouttier. Matrix integrals and enumeration of maps. *arXiv: Mathematical Physics*, 2011.

[77] E. Fradkin. *Quantum Field Theory: An Integrated Approach.* Princeton University Press, 2021.

[78] Gerard 't Hooft. A Planar Diagram Theory for Strong Interactions. *Nucl. Phys. B*, 72:461, 1974.

[79] D. Bessis, C. Itzykson, and J. B. Zuber. Quantum field theory techniques in graphical enumeration. *Adv. Appl. Math.*, 1:109–157, 1980.

[80] E. Brezin, C. Itzykson, G. Parisi, and J. B. Zuber. Planar Diagrams. *Commun. Math. Phys.*, 59:35, 1978.

[81] T. Regge. General Relativity Without Coordinates. *Nuovo Cim.*, 19:558–571, 1961.

[82] Renate Loll. Quantum gravity (review) - lecture 13, feb 2012. PIRSA:12020007 see, https://pirsa.org.

[83] Michael R. Douglas and Stephen H. Shenker. Strings in Less Than One-Dimension. *Nucl. Phys. B*, 335:635, 1990.

[84] E. Brezin and V. A. Kazakov. Exactly Solvable Field Theories of Closed Strings. *Phys. Lett. B*, 236:144–150, 1990.

[85] David J. Gross and Vipul Periwal. String perturbation theory diverges. *Phys. Rev. Lett.*, 60:2105–2108, May 1988.

[86] David J. Gross and Alexander A. Migdal. Nonperturbative two-dimensional quantum gravity. *Phys. Rev. Lett.*, 64:127–130, Jan 1990.

[87] Raghav Govind Jha. Introduction to Monte Carlo for matrix models. *SciPost Phys. Lect. Notes*, 46:1, 2022.

[88] M. Gell-Mann and F. E. Low. Quantum electrodynamics at small distances. *Phys. Rev.*, 95:1300–1312, Sep 1954.

[89] Leo P. Kadanoff. Scaling laws for ising models near T_c. *Physics Physique Fizika*, 2:263–272, Jun 1966.

[90] Alessandro Codello. *A novel functional renormalization group framework for gauge theories and gravity*. PhD thesis, Mainz U., Inst. Phys., 2010.

[91] Jürgen Berges, Nikolaos Tetradis, and Christof Wetterich. Non-perturbative renormalization flow in quantum field theory and statistical physics. *Physics Reports*, 363(4-6):223–386, jun 2002.

[92] Antonio D. Pereira. Quantum spacetime and the renormalization group: Progress and visions. In *Progress and Visions in Quantum Theory in View of Gravity: Bridging foundations of physics and mathematics*, 4 2019.

[93] R. Percacci. *Asymptotic safety*, page 111–128. Cambridge University Press, 2009.

[94] Alessandro Codello, Roberto Percacci, and Christoph Rahmede. Investigating the ultraviolet properties of gravity with a wilsonian renormalization group equation. *Annals of Physics*, 324(2):414–469, feb 2009.

[95] Astrid Eichhorn. Asymptotically safe gravity. In *57th International School of Subnuclear Physics: In Search for the Unexpected*, 2 2020.

[96] Edouard Brézin and Jean Zinn-Justin. Renormalization group approach to matrix models. *Physics Letters B*, 288(1-2):54–58, aug 1992.

[97] Carles Ayala. Renormalization group approach to matrix models in two-dimensional quantum gravity. *Physics Letters B*, 311(1-4):55–63, jul 1993.

[98] Dario Benedetti and Joe Henson. Imposing causality on a matrix model. *Physics Letters B*, 678(2):222–226, jul 2009.

[99] R Loll. Quantum gravity from causal dynamical triangulations: a review. *Classical and Quantum Gravity*, 37(1):013002, dec 2019.

[100] Alicia Castro and Tim Koslowski. Renormalization Group Approach to the Continuum Limit of Matrix Models of Quantum Gravity with Preferred Foliation. *Front. in Phys.*, 9:114, 2021.

[101] J. Ambjørn and R. Loll. Non-perturbative lorentzian quantum gravity, causality and topology change. *Nuclear Physics B*, 536(1-2):407–434, dec 1998.

[102] Jaume Gomis. Conformal field theory - lecture 3, nov 2011. PIRSA:11110052 see, https://pirsa.org.

[103] P. Di Francesco, P. Mathieu, and D. Senechal. *Conformal Field Theory*. Graduate Texts in Contemporary Physics. Springer-Verlag, New York, 1997.

[104] Emmy Noether. Invariant variation problems. *Transport Theory and Statistical Physics*, 1(3):186–207, jan 1971.

[105] Jaume Gomis. Conformal field theory - lecture 4, nov 2011. PIRSA:11110053 see, https://pirsa.org.

[106] Jaume Gomis. Conformal field theory - lecture 5, nov 2011. PIRSA:11110054 see, https://pirsa.org.

[107] Eric W. Weisstein. Cauchy-riemann equations. From MathWorld–A Wolfram Web Resource. https://mathworld.wolfram.com/Cauchy-RiemannEquations.html.

[108] Jaume Gomis. Conformal field theory - lecture 6, nov 2011. PIRSA:11110057 see, https://pirsa.org.

[109] J. Polchinski. *String theory. Vol. 1: An introduction to the bosonic string*. Cambridge Monographs on Mathematical Physics. Cambridge University Press, 12 2007.